

---

Theses and Dissertations

---

Spring 2016

## Determination of effective riser sleeve thermophysical properties for simulation and analysis of riser sleeve performance

Thomas John Williams  
*University of Iowa*

Follow this and additional works at: <https://ir.uiowa.edu/etd>



Part of the [Mechanical Engineering Commons](#)

Copyright 2016 Thomas John Williams

This thesis is available at Iowa Research Online: <https://ir.uiowa.edu/etd/3217>

---

### Recommended Citation

Williams, Thomas John. "Determination of effective riser sleeve thermophysical properties for simulation and analysis of riser sleeve performance." MS (Master of Science) thesis, University of Iowa, 2016.  
<https://doi.org/10.17077/etd.9u5zhtg0>

---

Follow this and additional works at: <https://ir.uiowa.edu/etd>



Part of the [Mechanical Engineering Commons](#)

DETERMINATION OF EFFECTIVE RISER SLEEVE THERMOPHYSICAL PROPERTIES  
FOR SIMULATION AND ANALYSIS OF RISER SLEEVE PERFORMANCE

by  
Thomas John Williams

A thesis submitted in partial fulfillment  
of the requirements for the Master of  
Science degree in Mechanical Engineering  
in the Graduate College of  
The University of Iowa

May 2016

Thesis Supervisor: Professor Christoph Beckermann

Graduate College  
The University of Iowa  
Iowa City, Iowa

CERTIFICATE OF APPROVAL

---

MASTER'S THESIS

---

This is to certify that the Master's thesis of

Thomas John Williams

has been approved by the Examining Committee  
for the thesis requirement for the Master of Science  
degree in Mechanical Engineering at the May 2016 graduation.

Thesis Committee: \_\_\_\_\_  
Christoph Beckermann, Thesis Supervisor

\_\_\_\_\_  
H. S. Udaykumar

\_\_\_\_\_  
Albert Ratner

## ACKNOWLEDGEMENTS

This work would not have been possible without support and guidance from many people. I would like to thank my advisor, Professor Christoph Beckermann, for providing the opportunity to accomplish this work and also for his advice and direction for the project. I want to express my gratitude to my thesis committee, Professors Albert Ratner and H.S. Udaykumar for giving me their time even when it was requested in the eleventh hour and during a busy time. I want to acknowledge all of the members of the Solidification Laboratory for their support and encouragement, especially Richard Hardin and Daniel Galles who provided immense experimental, computational, and editorial support. I also want to thank Jerry Thiel, Sairam Ravi, and all the staff and students at the University of Northern Iowa Metal Casting Center for their assistance with the casting experiments. I would like to acknowledge the members of the Steel Founders' Society of America for their advice and support for the project. Special thanks to my parents Ray and Eileen who taught me to work hard and pursue my goals and who have always provided their encouragement. Finally, I want to thank my partner Melissa Kessler who has supported me throughout this process.

## ABSTRACT

Riser sleeve thermophysical properties for simulation are developed using an inverse modeling technique. Casting experiments using riser sleeves are performed in order to measure temperatures in the liquid steel, the riser sleeve, and the sand mold. Simulations are created and designed to replicate the casting experiments. Riser sleeve material thermophysical properties are iteratively modified until agreement is achieved between the simulation and the measured data. Analyses of sleeve material performance are carried out using the developed thermophysical properties. The modulus extension factor (MEF) is used to quantify sleeve performance and is determined for all riser sleeve materials studied here. Values are found to range from 1.07 to 1.27. A sleeve material's effects on casting yield are shown to depend only on the MEF and therefore a sleeve's exothermic or insulating properties serve only to increase the overall quality of the sleeve, expressed by the MEF, and do not independently affect the casting yield at any casting size studied here. The use of riser sleeves is shown to increase the maximum yield up to 40% for chunky castings, however increases of only 8% are observed for very rangy castings. Riser sleeve thickness is shown to be extremely influential on casting yield. Scaling the sleeve thickness by the riser diameter shows that, for a typical sleeve, an optimum riser sleeve thickness is 0.2 times the riser diameter for chunky castings. A scaled sleeve thickness of 0.1 is found to be an optimum sleeve thickness for very rangy castings. Below a scaled sleeve thickness of 0.1 sleeve performance is found to be highly sub-optimal.

## PUBLIC ABSTRACT

The usage of riser sleeves is ubiquitous within the metal casting industry. Despite the heavy usage of sleeves, there is little literature discussing their thermophysical properties. In this study, riser sleeve thermophysical properties for simulation are developed using an inverse modeling technique. Casting experiments using riser sleeves are performed in order to measure temperatures. Simulations are performed to replicate the experiments. Riser sleeve thermophysical properties are iteratively modified until agreement is achieved between the simulation and the measured data. These finalized properties can be used to effectively predict and therefore optimize the solidification behavior of a given casting. Analyses of sleeve performance are carried out using the developed properties. The modulus extension factor (MEF) is used to quantify sleeve performance and is determined for all riser sleeve materials studied here. A sleeve material's effects on casting yield are shown to depend only on the MEF and therefore a sleeve's exothermic or insulating properties serve only to increase the overall quality of the sleeve, expressed by the MEF, and do not independently affect the casting yield at any casting size studied here. Riser sleeves are found to substantially increase the maximum achievable yield for chunky castings but rangy castings only experience small increases in yield due to sleeve usage. Riser sleeve thickness is shown to be extremely influential on casting yield. By observing sleeve thickness effects on the casting yield, optimum sleeve thicknesses for chunky and rangy castings are discerned. An effective lower threshold sleeve thickness is also described.

## TABLE OF CONTENTS

LIST OF TABLES .....	vi
LIST OF FIGURES .....	vii
LIST OF NOMENCLATURE.....	xii
LIST OF SYMBOLS .....	xiii
CHAPTER 1: INTRODUCTION .....	1
1.1 Motivation .....	1
1.2 Objective of the Present Study .....	2
CHAPTER 2: LITERATURE REVIEW .....	4
2.1 Introduction .....	4
2.2 Previous Evaluations of Riser Sleeve Performance .....	4
2.3 Previous Determinations of Sleeve Thermophysical Properties .....	6
CHAPTER 3: CASTING EXPERIMENTS .....	9
3.1 Introduction .....	9
3.2 Casting Experiment Process .....	9
CHAPTER 4: THERMAL SIMULATIONS OF CASTING EXPERIMENTS .....	16
4.1 Introduction .....	16
4.2 Simulations of Castings Without Sleeves .....	16
4.3 Simulations of Castings With Sleeves .....	19
CHAPTER 5: ANALYSES OF RISER SLEEVE MATERIAL PERFORMANCE.....	60
5.1 Introduction .....	60
5.2 The Modulus Extension Factor .....	60
5.2.1 Derivation of the Modulus Extension Factor .....	60
5.2.2 Determination of the Modulus Extension Factor .....	61
5.2.3 Analysis of the Modulus Extension Factor.....	62
5.3 The Effects of Riser Sleeves on Casting Yield .....	64
CHAPTER 7: CONCLUSIONS AND RECOMMENDATIONS FOR FUTURE STUDIES ....	77
7.1 Conclusions .....	77
7.2 Recommendations for Future Studies .....	78
REFERENCES .....	80

## LIST OF TABLES

### Table

- 3.1. Riser sleeves tested and the dimensions of the corresponding sleeve and no sleeve control castings. Sleeves are indicated to be insulating or exothermic using “-I” or “-E” respectively after their product name. .... 15
- 4.1. Riser sleeve exothermic properties used for simulation, ordered by heat generation. .. 45



## LIST OF FIGURES

### Figure

2.1. Experimental setup used by Wlodawer to test the performance of several exothermic riser lining materials. Adapted from [7].	8
2.2. Resulting riser pipe shape depending on the thickness of the riser lining material and exothermic hot topping. Riser lining thickness of 0.15 or greater results in a flat feeding riser pipe (far right). Adapted from [7].	8
3.1. Schematic diagrams of experimental casting setups for (a) castings without a sleeve and (b) castings with a sleeve.	13
3.2. Photographs of casting experiments. (a) A sand mold without cope that has been instrumented with thermocouples. (b) Liquid steel being poured directly into casting cavities via crane hoisted ladle.	14
4.1. Temperature dependent interfacial heat transfer coefficient applied at the steel-sand and steel-sleeve interfaces in simulations performed in this study.	25
4.2. Sand mold thermophysical properties. (a) The sand density curve used for all simulations. (b) The sand specific heat curve used for all simulations. (c) Sand thermal conductivity curves.	26
4.3. Example curves for effective steel thermophysical properties for simulation. (a) The thermal conductivity. (b) The density. (c) The specific heat.	27
4.4. (a) Two solid fraction curves. The black curve corresponds to solid fraction curve 3 in Figure 4.5. (b) Temperature results in the steel showing how solid fraction affects the agreement between measured and simulated temperatures.	28
4.5. Solid fraction curves developed for all no sleeve control cases and applied to the corresponding sleeve casting simulations.	29
4.6. Measured and simulated temperatures for the control casting corresponding to FOSECO Kalminex 2000 and ASK Exactcast EX sleeve castings. Data for thermocouples placed in (a) the steel and (b) the sand mold. Sand thermal conductivity RH1 and solid fraction curve 5 are applied to this simulation.	30
4.7. Measured and simulated temperatures for the control casting corresponding to the FOSECO Kalmin 70 sleeve castings. Data for thermocouples placed in (a) the steel and (b) the sand mold. Sand thermal conductivity RH1 and solid fraction curve 8 are applied to this simulation. In (b) the line type denotes position at 10 mm (dashed line) and 20 mm (solid line) from steel-mold interface.	31

4.8. Measured and simulated temperatures for the control casting corresponding to the FOSECO Kalminex 21 sleeve casting. Data for thermocouples placed in (a) the steel and (b) the sand mold. Sand thermal conductivity RH1 and solid fraction curve 1 are applied to this simulation. In (b) the line type denotes position at 10 mm (dashed line) and 20 mm (solid line) from steel-mold interface. ....	32
4.9. Measured and simulated temperatures for the control casting corresponding to FOSECO Kalfax 100 and Exochem ES sleeve castings. Data for thermocouples placed in (a) the steel and (b) the sand mold. Sand thermal conductivity TW25 and solid fraction curve 4 are applied to this simulation. In (b) the line type denotes position at 10 mm (dashed line) and 20 mm (solid line) from steel-mold interface. ....	33
4.10. Measured and simulated temperatures for the control casting corresponding to Joymark CFX 700 and ASK Exactcast IN sleeve castings. Data for thermocouples placed in (a) the steel and (b) the sand mold. Sand thermal conductivity TW6 and solid fraction curve 3 are applied to this simulation. In (b) the line type denotes position at 10 mm (dashed line) and 20 mm (solid line) from steel-mold interface. ....	34
4.11. Measured and simulated temperatures for the control casting corresponding to Joymark CFX 760 and Joymark CFX 800 sleeve castings. Data for thermocouples placed in (a) the steel and (b) the sand mold. Sand thermal conductivity RH1 and solid fraction curve 2 are applied to this simulation. ....	35
4.12. Measured and simulated temperatures for the control casting corresponding to the Exochem SNA sleeve casting. Data for thermocouples placed in (a) the steel. Sand mold thermocouples were burnt out. Sand thermal conductivity RH1 and solid fraction curve 7. ....	36
4.13. Measured and simulated temperatures for the control casting corresponding to Exochem ESPX. Data for thermocouples placed in (a) the steel and (b) the lid. Sand mold thermocouples were burnt out. Sand thermal conductivity TW6 and solid fraction curve 6. ....	37
4.14. The difference in solidification time percentage for a sleeved cylinder casting, as predicted by casting simulation, for all permutations of cases where the sleeve material thermophysical properties $k$ and product $\rho c_p$ are multiplied by factors of 0.5 and 2. Differences are relative to results for the unmodified properties. Cases are grouped according to multiplier of $k$ , and individual bars correspond to cases of $\rho c_p$ . ....	38
4.15. Specific heat curve used for all sleeves in this work. ....	39

4.16. (a) Temperature dependent riser sleeve thermal conductivity curve determined for the ASK Exactcast IN sleeve material properties with base curve and curves multiplied by factors of 0.5 and 2. Measured cooling curves (red curves) are compared to predicted curves in the (b) steel, (c) sleeve, and (d) sand mold. Effect of multiplying the sleeve thermal conductivity by factors of 0.5 and 2 is shown by the blue and green curves, respectively. Note in (d) there are two measured mold TCs in the plot at 10 mm and 20 mm from the sleeve-metal interface corresponding to the solid and dashed curves, respectively. ....	40
4.17. Riser sleeve temperature dependent thermal conductivity curves for sleeve materials sorted by sleeve manufacturer. (a) FOSECO (b) Exochem (c) Joymark (d) AMCOR and ASK Chemical. ....	41
4.18. Temperature vs. time results in the <b>steel</b> for the Foseco Kalminex 21 sleeve showing in (a) and (b) the effect of modifying the heat generation on agreement between measured and predicted temperatures on long and short time scales, respectively. Figures (c) and (d) show the effect of modifying the burn time on agreement between measured and predicted temperatures. Black curves are simulation results using the final determined properties for the sleeve. ....	42
4.19. Temperature curves in the <b>sleeve</b> for the Foseco Kalminex 21 sleeve showing in (a) and (b) the effect of modifying the heat generation on agreement between measured and predicted temperatures on long and short time scales, respectively. Figures (c) and (d) show the effect of modifying the burn time on agreement between measured and predicted temperatures. Black curves are simulation results using the final determined properties for the sleeve. ....	43
4.20. Temperature curves in the steel and sleeve for the Joymark CFX 760 sleeve showing in (a), (b) and (c) the effect of modifying the heat generation on agreement between measured and predicted temperatures on long times scales in (a) and (b) and a short time scale for the sleeve in (c). Analogous temperature curves showing effect of modifying the burn time on agreement between measured and predicted temperatures are shown in (d) for the steel and (e) and (f) for the sleeve. ....	44
4.21. FOSECO Kalminex 2000 sleeve casting measured and simulated temperatures. Thermocouples placed in (a) the steel, (b) the sleeve, and (c) the sand mold. Line types denote different nominal positions of the TC. ....	46
4.22. ASK Exactcast EX sleeve casting measured and simulated temperatures. Thermocouples placed in (a) the steel, (b) the sleeve, and (c) the sand mold. Line types denote different nominal positions of the TC. ....	47
4.23. FOSECO Kalmin 70 sleeve casting measured and simulated temperatures. Thermocouples placed in (a) the steel, (b) the sleeve, and (c) the sand mold. Line types denote different nominal positions of the TC. ....	48
4.24. FOSECO Kalminex 21 sleeve casting measured and simulated temperatures. Thermocouples placed in (a) the steel, (b) the sleeve, and (c) the sand mold. ....	49

4.25. FOSECO Kalfax 100 sleeve casting measured and simulated temperatures. Thermocouples placed in (a) the steel, (b) the sleeve, and (c) the sand mold. Line types denote different nominal locations for the TC.....	50
4.26. Exochem ES sleeve casting measured and simulated temperatures. Thermocouples placed in (a) the steel, (b) the sleeve, and (c) the sand mold. Line types denote different nominal locations of the TC. ....	51
4.27. Joymark CFX 700 sleeve casting measured and simulated temperatures. Thermocouples placed in (a) the steel, (b) the sleeve, and (c) the sand mold. Line types denote different nominal locations of the TC.....	52
4.28. ASK Exactcast IN sleeve casting measured and simulated temperatures. Thermocouples placed in (a) the steel, (b) the sleeve, and (c) the sand mold. Line types denote different nominal positions of the TC.....	53
4.29. Joymark CFX 760 sleeve casting measured and simulated temperatures. Thermocouples placed in (a) the steel, (b) the sleeve, and (c) the sand mold. Line types denote different nominal locations for the TC.....	54
4.30. Joymark CFX 800 sleeve casting measured and simulated temperatures. Thermocouples placed in (a) the steel and (b) the sand mold. Sleeve TCs were burnt out. Line types denote different nominal positions of the TC. ....	55
4.31. Exochem SNA sleeve casting measured and simulated temperatures. Thermocouples placed in (a) the steel, (b) the sleeve, and (c) the sand mold. Line types denote different nominal locations of the TC. ....	56
4.32. Exochem ESPX sleeve casting measured and simulated temperatures. Thermocouples placed in (a) the steel, (b) the sleeve, and (c) the sand mold. ....	57
4.33. A second group of ASK Exactcast IN sleeve casting measured and simulated temperatures used to confirm sand and steel properties for the AMCOR Rosstherm K sleeve case. Thermocouples in the control casting, poured with these sleeve castings, failed. ASK Exactcast IN sleeve properties were previously developed. Thermocouples placed in (a) the steel, (b) the sleeve, and (c) the sand mold.....	58
4.34. AMCOR Rosstherm K sleeve casting measured and simulated temperatures. Thermocouples placed in (a) the steel, (b) the sleeve, and (c) the sand mold. Line type denotes different nominal location of the TC.....	59
5.1. Simulation geometry used to determine the apparent modulus and modulus extension factor for a given riser sleeve. The riser without sleeve has a variable diameter. Riser aspect ratio is always 1. ....	68
5.2. Sensitivity of the modulus extension factor $f$ to three casting parameters; superheat, casting size and alloy. Base case is an 8” cube casting with 6” riser, 0.5” sleeve, and WCB alloy steel with 30 °C superheat. ....	69

5.3. Modulus extension factors for the 13 sleeve materials investigated. Factors were determined via simulation for identical 0.5” thick sleeves insulating a 6” diameter x 6” tall cylindrical top riser on an 8” cube casting.....	70
5.4. General schematics of the simulation geometries used to study achievable casting yield. (a) Schematic geometry for a cube of side length $c_s$ . Side lengths of 3, 6, 9, 12, 18, and 24 inches were used. (b) Schematic geometry for a square plate of thickness $t_{plate}$ and aspect ratio 15. The six plate castings studied have volumes equivalent to the six cube volumes.....	71
5.5. Plot of riser sleeve dimensions as listed in manufacturer’s product data. The red line is a linear approximation of the data. The fit indicates that the riser sleeve thickness in inches, $t_{sleeve}$ , increases with the riser sleeve inner diameter in inches, $D$ , according to the equation $t_{sleeve} = 0.08D + 0.126$ .....	72
5.6. Examples of simulated shrinkage porosity used to determine maximum achievable casting yield. A 0.7% porosity threshold was used to determine the extent of the riser pipe. The minimum margin of safety goal was 10% of the riser height.....	73
5.7. Maximum achievable casting yield for (a) cube castings and (b) square plate castings without sleeve, castings with insulating riser sleeves, and castings with exothermic sleeves. Insulating and exothermic sleeves behave similarly at all sizes. $f$ values are those from Figure 5.3.....	74
5.8. Absolute increase in maximum achievable casting yield for the exothermic riser sleeved casting over the casting with no sleeve case versus the scaled sleeve thickness ( $t_{sleeve}/D$ ) used. Results are shown for cube castings (squares) and square plate castings (triangles) with an aspect ratio 15 having volumes equal to those of the cube castings. ....	75
5.9. Scaled sleeve thickness of commercially available riser sleeves as determined from manufacturer product information and approximate predicted increases in casting yield for high moduli castings. Predicted increases in yield correspond to the absolute increase in yield over chunky castings with no sleeve. The red curve is the approximation of commercially available sleeve thicknesses derived from Figure 5.5 .....	76

## LIST OF NOMENCLATURE

### Acronyms

DSC	Differential Scanning Calorimetry
DTA	Differential Thermal Analysis
IHTC	Interfacial Heat Transfer Coefficient
MEF	Modulus Extension Factor
PUNB	Polyurethane No Bake
TC	Thermocouple
UNIMCC	University of Northern Iowa Metal Casting Center

## LIST OF SYMBOLS

$A$	heat loss surface area ( $m^2$ )
$c_p$	specific heat (kJ/kg-K)
$c_s$	cube side length (inches)
$D$	riser diameter (inches)
$f$	modulus extension factor
$H$	riser height (inches)
$k$	thermal conductivity (W/m-K)
$K$	solidification constant (s/m <sup>2</sup> )
$M_A$	apparent modulus (m)
$M_G$	geometric modulus (m)
$\rho$	density (kg/m <sup>3</sup> )
$t$	time (s)
$t_{plate}$	plate thickness (inches)
$t_s$	time to solidification (s)
$t_{sleeve}$	sleeve thickness (inches)
$T$	temperature (°C)
$T_{solidus}$	solidus temperature (°C)
$V$	volume (m <sup>3</sup> )

## CHAPTER 1: INTRODUCTION

### 1.1 Motivation

Contraction during the solidification and cooling of steel castings results in the need for excess liquid metal to “feed” the casting. This excess liquid metal is held in cavities called risers that are generally placed above the casting. In order for a riser to function properly, the liquid metal inside of it must take longer to solidify than the liquid metal in the casting below the riser. Riser sleeves are prefabricated material used to line and insulate the inside of riser cavities, increasing the time it takes the riser to solidify. Riser sleeves are generally divided into insulating and exothermic categories. Insulating sleeves are those which are composed of purely insulating material, generally a fibrous ceramic, and contain no material designed to ignite and burn. Exothermic sleeves, in addition to being constructed from insulating materials, contain materials which undergo an exothermic reaction, particularly the thermite reaction. Riser sleeves have been used for decades as feeding aids in the metal casting industry. Despite their ubiquitous application throughout the industry, there is almost no literature discussing the thermophysical properties of riser sleeves. Additionally, there is no consensus regarding the optimal usage of riser sleeves or even whether exothermic or insulating sleeves are preferable [1]. Most foundries use sleeves according to guesswork, trial-and-error testing, the recommendations of the manufacturer, or some combination thereof.

The best method available to properly design a casting is through the use of simulation software. Because there is little to no information available regarding sleeve thermophysical properties, accurate simulations using riser sleeves are difficult to create. The only available sleeve properties for simulation are those of some select sleeves from a few manufacturers. These properties are provided in the form of a separate black box module that can be added on to casting software. Because the module is a black box, the properties can be neither viewed nor edited. The properties can only be blindly applied to a material designated as a sleeve within the simulation geometry. In order for foundries to accurately model their castings using simulation software,



thermophysical properties for riser sleeves must be developed. Once these properties are developed, the performance of different sleeve materials can be compared. Additionally, parametric and other analyses can be performed to investigate riser sleeve performance under different casting conditions. These analyses can answer outstanding questions about the optimal application of riser sleeves.

### 1.2 Objective of the Present Study

The objective of this work is to develop effective thermophysical properties of several commonly used riser sleeves. These properties are intended to be used in simulation software to effectively and accurately model the effects a riser sleeve has in a sand casting. After these properties are developed, analyses of sleeve performance can be performed in order to provide guidance to foundries regarding riser sleeve usage. With this guidance, foundries can create accurate simulations using riser sleeves, increase process efficiency, and make informed riser sleeve purchasing decisions. Because of the large number of riser sleeves available for purchase, only commonly used sleeves were studied. These sleeves are described in Chapter 3. The most commonly used sleeves were identified via a survey of member foundries of the Steel Founders' Society of America (SFSA) [2].

In the present study, casting experiments are performed to obtain temperature data for castings with and without sleeve. Thermocouples are placed in the steel, sand mold, and directly into the riser sleeve in order to provide the most accurate data. These experiments are replicated via the metal casting simulation software *MAGMAsoft* [3]. By modeling these casting experiments, the developed sleeve properties capture and account for all sleeve effects and interactions in a real casting. These effects, such as evolution of hot gasses due to material decomposition, may go undetected in laboratory tests of sleeve thermophysical properties. As such, the properties developed here are considered effective properties. Simulations modeling castings without sleeves, also called control castings, are used to develop thermophysical properties for sand and steel. Simulations modeling castings with sleeves focus on developing thermophysical properties

for the sleeves only. Properties are developed in an iterative fashion. The thermophysical properties are modified many times until temperature data from the simulation matches experimentally measured temperature data.

Once the thermophysical properties have been developed, analyses are carried out on sleeve material performance. The modulus extension factor (MEF) is determined for all sleeves studied here and used to quantify sleeve material performance. A standard method to calculate this factor is detailed. The method is designed such that factors can be developed using either experimental or simulated castings. Sleeve effects on casting yield are analyzed as well. One study discerns the advantages of using sleeves for different casting shapes and sizes as well as the importance of the exothermic effect on casting yield. Another investigation describes the effect of sleeve thickness on casting yield over a range of casting sizes.

## CHAPTER 2: LITERATURE REVIEW

### 2.1 Introduction

Riser sleeves have been heavily used as feeding aids in foundries for several decades. Despite the longevity and extent of their use, very little open or verified information exists regarding their application. Literature regarding the determination of riser sleeve properties is scarcer yet. This chapter will review 1) previous evaluations and analyses of riser sleeve performance and recommendations of application and 2) previous attempts at developing thermophysical properties of riser sleeves.

### 2.2 Previous Evaluations of Riser Sleeve Performance

Foundries have always placed importance on the proper application of riser sleeves. Mair [4] lists general assessments regarding their application. In particular he prompts the need to understand sleeve thermal properties in order to maximize casting yield and cost efficiency in foundries. Perhaps the most practical advice regarding feeding castings and the application of riser sleeves is given in the Foundryman's Handbook [5, 6]. Although these chapters discuss only a few sleeves, they provide simple practical methods of sizing risers with sleeves. Tables list the volume and weight of the riser based on the sleeve diameter and height. Recommendations regarding sleeve thickness are given. Simple graphs are used to relate appropriate riser sleeve dimensions with the weight of the casting section being fed. Additionally, modulus concepts are discussed and the modulus extension factor (MEF) is introduced. Unfortunately, the methods by which these recommendations were developed are not transparent.

Wlodawer [7] tested several exothermic riser lining materials packed in different thicknesses around a spherical casting with a thermocouple in the middle as shown in Figure 2.1. In Figure 2.1 the spherical castings are shown to be filled via a small pouring gate. The thermocouple is inserted from the bottom, and a small vent through the exothermic material and sand mold is located at the top of the casting. Wlodawer found that exothermic materials varied strongly from one another in their extension of the sphere's solidification time. More importantly

he found that thickness of the exothermic material played an important role in the materials elongation of the solidification time. He also investigated riser pipe formation in cylindrical risers using exothermic riser linings. He found that a lining thickness of 0.15 times the diameter of the cylinder was sufficient to result in a desired flat shrinkage cavity rather than the typical conic shape. These findings are illustrated in Figure 2.2. Figure 2.2 illustrates the riser pipe shapes found to result from different thicknesses of riser lining and hot topping. The rightmost riser shows the desired flat shrinkage cavity for a lining thickness of 0.15. Exothermic hot topping was applied to the open top of the cylinder in these tests which must be accounted for when applying these findings solely to the riser lining material. Many of Wlodawer's other findings are useful for specific geometries and materials but cannot be generalized.

Sully, Wren, and Bates [8] reviewed several publications regarding the evaluation of riser sleeve or lining materials. However they concluded that most of the evaluations were flawed for one or more of the following reasons: risers were not placed above a casting, the riser size was not based on traditional casting principles, or hot topping materials were not used in conjunction with sleeve materials. Riser sleeve tests reviewed in this work were concerned with riser pipe formation, riser cooling histories, and modulus principles so the lack of a casting or an incorrectly sized riser was important. Additionally, the inclusion of hot topping materials was significant since these analyses were designed to guide best practices at the time which included the use of hot topping for risers. Subsequently Bates et al. [9] attempted to develop a test casting to evaluate different riser sleeves and provide the results of initial evaluations. They tested sensitivities of the riser pipe size for several different casting sizes combined with several different sleeves. They found that cube castings of 6" side length or greater resulted a suitable amount of variability between the performance of different sleeve products. The positive of this test is that foundries can compare results for specific sleeve products that they are interested in. Unfortunately, the results cannot be generally applied to a given sleeve material or to the general application of sleeves because this procedure suffered from many of the same deficiencies common to other evaluations. The riser pipe size, used as the measure of performance here, is sensitive to the

specific casting setup and so any results here can only be applied to these castings. Additionally, there was no control for the dimensions of the riser sleeve and therefore the riser. Thickness, height, and diameter all varied between sleeves atop identical castings. Therefore any results here can only be applied to that specific sleeve formulation and geometry.

Foseco [10] published methods of determining the MEF and the apparent surface alteration factor (ASAF). These factors can be used to determine the relative performance of several sleeve materials. However their exact values vary based on sleeve thickness, casting parameters, and the shape of the casting underneath. The article asserts that ASAF evaluations are superior to MEF evaluations because ASAF evaluations are accomplished under strictly controlled and isolated conditions. However there is no reason these conditions cannot be applied to MEF evaluations. The one benefit the ASAF has that the MEF does not is an easy way to combine the effects of riser sleeve and hot topping. Additionally it is mentioned within that a sleeve thickness of 0.2 times the riser diameter is considered to be effectively infinite.

### 2.3 Previous Determinations of Sleeve Thermophysical Properties

Most of the evaluations listed in the preceding section are specific in their scope and cannot be generalized to assess sleeve performance. For this reason, sleeve thermophysical properties must be known so that simulation can predict sleeve performance for any casting situation. In the following section, attempts to determine sleeve thermophysical properties are detailed.

Midea et al. [11] discussed the need for sleeve properties to be developed in *in situ* casting tests rather than laboratory tests due to the vast differences in conditions for the two types of tests. Temperature dependent plots of riser sleeve thermophysical properties are displayed, however no values are given on the axes. While the absence of values is not ideal, having these plots to guide thermophysical property development is significant. Additionally, simulation software is used to determine the sensitivity of sleeve performance to different thermophysical properties as well as the heat transfer coefficient between sleeve and steel. It was found that thermal conductivity is by far the most influential property. Sleeve performance was more sensitive to differences in the

thermal conductivity than the exothermic heat release by a factor of two. Thermal conductivity was about 4 times more influential than the heat capacity of the sleeve. Modifications to the heat transfer coefficient between steel and sleeve were found to be less influential than modifications to the thermal conductivity by an order of magnitude. This is important in simplifying the process for developing riser sleeve properties. It implies that the heat transfer coefficient and heat capacity can be predetermined or assigned average values while property development focuses on the thermal conductivity and heat release properties.

Ignaszak et al. [12, 13] used an inverse modelling approach in order to develop average values for sleeve thermophysical properties. Experiments were performed in order to obtain temperature data in the sand mold and steel. A computer program was then used to conduct simulations of the castings where all thermophysical properties were iteratively modified until the error between simulation results and measured data is minimized. Their final results agree quite well on a large time scale however the results on the solidification time scale appear inconsistent. Specifically, the time to solidification is incorrect by up to a few hundred seconds by inspection. As sleeves are only important in the casting process while the riser is liquid, it is most important to match the curves over this time scale. The properties they obtain are average non-temperature-dependent properties for two unidentified sleeves. Additionally temperatures are not measured in the sleeve. Still, this represents the most advanced published work regarding the development of thermophysical properties of riser sleeves.

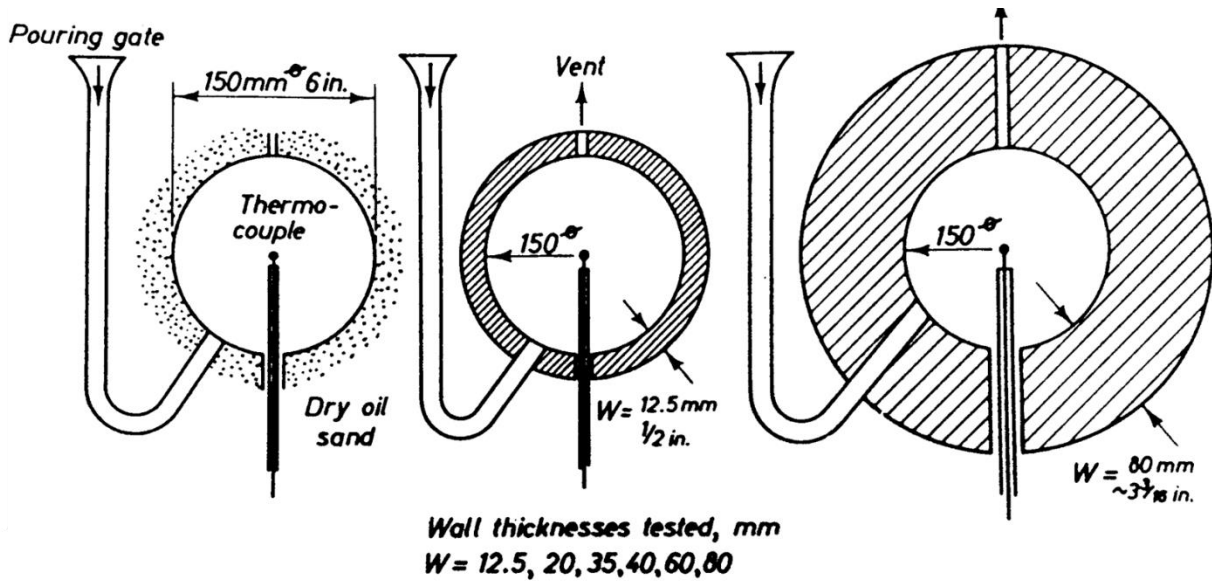


Figure 2.1. Experimental setup used by Wlodawer to test the performance of several exothermic riser lining materials. Adapted from [7].

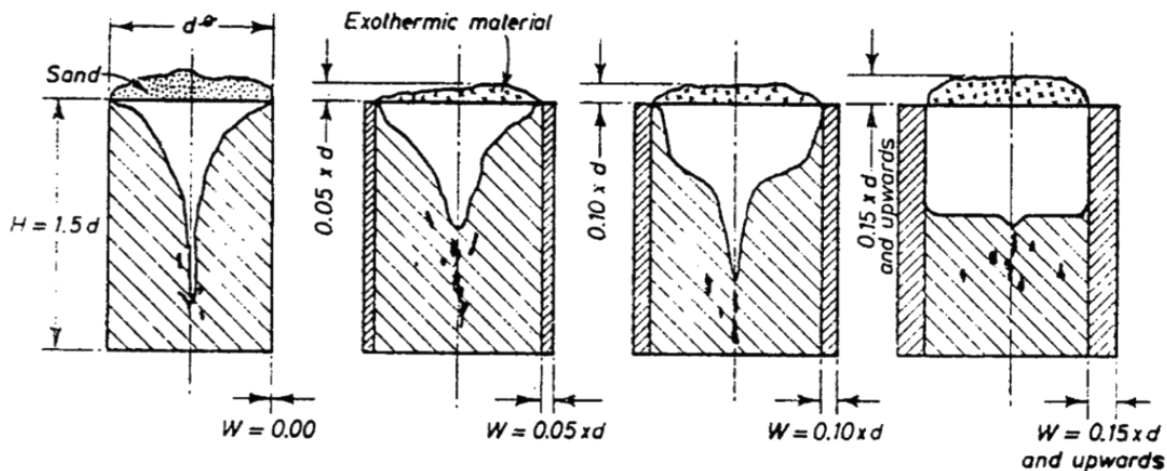


Figure 2.2. Resulting riser pipe shape depending on the thickness of the riser lining material and exothermic hot topping. Riser lining thickness of 0.15 or greater results in a flat feeding riser pipe (far right). Adapted from [7].

## CHAPTER 3: CASTING EXPERIMENTS

### 3.1 Introduction

In application, riser sleeves experience high heating rates, large temperature gradients, large pressures, exposure to hot gasses and other effects which are impossible to account for in laboratory tests such as DTA or DSC. Therefore, data from casting experiments must be used to inversely model and develop accurate, effective thermophysical properties for simulations using riser sleeves. Section 3.2 details the casting experiments used to acquire temperature data for this work. Many sets of casting experiments were carried out over the course of approximately 2 years. All experiments were performed at the University of Northern Iowa Metal Casting Center (UNIMCC).

### 3.2 Casting Experiment Process

The experimental setup was chosen in order to isolate the effect of the riser sleeve. In order to do this, two types of castings must be created. The first casting type is a casting without sleeve, also called a control casting. This casting allows for the development of sand and steel thermophysical properties without the effect of the riser sleeve. The second casting type is a casting with sleeve. Since sand and steel properties are developed separately, simulations of these castings are able to focus on developing accurate sleeve properties. Each set of casting experiments contains at least one casting without sleeve so that sand and steel properties unique to that set of experiments can be developed. Illustrations of castings without and with sleeves are shown in Figure 3.1 (a) and (b) respectively. Both types of castings are shown to be completely encased inside a sand mold and are instrumented with thermocouples in order to measure temperatures in the sand, steel, and any included riser sleeve. Liquid steel is poured into the casting cavity via a conical pouring cup and small down sprue running through the top of the mold.

A previous experimental casting design left the top of the casting exposed to the atmosphere and liquid steel was poured directly into the open casting cavity as shown in Figure 3.2. Figure 3.2 (a) shows the sand mold of a casting with sleeve that has been instrumented with



thermocouples. Figure 3.2 (b) shows the same sand mold and an additional sleeve casting sand mold being filled with liquid steel. Due to the open casting cavity, the thermocouples are in danger of being destroyed due to the splashing of liquid metal during pouring. The liquid metal is also losing a large amount of heat via radiation to the atmosphere, apparent in the bright orange-white color of the metal. This radiant heat loss is difficult to account for in casting simulations. The desire to control this heat loss and to contain splashing in the mold cavity, led to the development of the finalized casting design from Figure 3.1.

The sleeves used in these casting experiments are shown in Table 3.1. Table 3.1 indicates whether the sleeve is insulating or exothermic and lists the measured room temperature density of the sleeve used in simulations in Chapter 4. Table 3.1 also includes the dimensions of the riser sleeve and the corresponding castings with and without sleeve. The sleeves in Table 3.1 are indicated to be heavily used in a survey of steel casting foundries [2] and are estimated to account for 70% of riser sleeve usage in this industry. In order to account for potential variation between individual sleeves of the same product line and to provide a failsafe, two castings with sleeve per sleeve are created.

Sand molds are created using silica sand bound with a phenolic urethane no-bake (PUNB) binder system. The amount of binder is equivalent to 1.25% of the total sand weight. The binder is created by chemical reaction of 2 reactants called Part 1 and Part 2, and a catalyst. Parts 1 and 2 are mixed in a 55:45 weight ratio and the catalyst accounts for 6% of the total binder weight. The mold is comprised of a lower portion, called the drag, which surrounds the main casting and an upper portion called the cope. The cope and drag are formed using separate wooden mold boxes. Two mold sizes are used in this work depending on the size of the casting which must be created. For the first mold size, the drag has dimensions of 9" x 10" x 9" (W x L x H) and the cope has dimensions of 9" x 10" x 2". For the second mold size, the drag has dimensions of 11" x 11" x 14" and the cope has dimensions of 11" x 11" x 2". Riser sleeves are placed inside the mold box for the drag prior to adding the binder coated sand. Care was taken to ensure that the sand was packed tightly around the riser sleeve in order to ensure unimpeded heat transfer from

the sleeve to the sand. In this experimental design the cope functions as a lid to control heat loss. A 1" diameter down sprue is drilled by hand through the cope. This down sprue allows liquid metal to flow into the main casting cavity. Pouring cups for the sand mold are made from the same material and formed using a pattern provided by the UNIMCC. After the molds have been instrumented with thermocouples but before pouring, the cope is fixed to the drag using standard mold glue. The pouring cup is then centered over the down sprue and fixed to the cope using mold glue.

The setup shown in Figure 3.1 is instrumented with several thermocouples in order to measure temperatures in the steel, sleeve, and sand mold. All thermocouples are intended to be vertically located at the half height of the steel cylinder. Due to issues with instrumenting molds with thermocouples in a foundry setting, the final vertical position varied by up to 25 mm from the intended location. Temperatures in the steel and riser sleeve are measured using Type-B thermocouples encased in thin quartz tubing in order to protect them from the molten steel or any exothermic behavior of the riser sleeve. Thermocouples in the steel are intended to be located 50 mm radially from the metal interface with either the mold or sleeve. Radial placement of the thermocouples in the metal varied by up to 15 mm. Thermocouples in the sleeve are located 6 mm radially from the metal-sleeve interface. Radial placement of the thermocouples in the sleeve varied by about 2mm. Thermocouples placed in the sand mold were Type-K thermocouples. Generally thermocouples are placed at 10 mm and 20 mm radially from the sand mold interface with either the metal or sleeve. Exact placement varied by about 5 mm. Exact locations for all thermocouples are recorded to ensure accurate simulations. Temperature data was recorded using multiple data-logging devices connected to a laptop running the DASyLab [14] data acquisition software.

The steel used in this work was melted and prepared by the staff at the UNIMCC. The target steel composition was ASTM A216 grade WCB carbon steel. Due to issues with the spectrometer on the premises, there are no official steel chemistries available. However an unofficial device, used to check the chemistries during preparation of the molten steel, indicated

that final chemistries would be within the target specification. Steel heats of 250-300 pounds were prepared in an induction furnace at a temperature of approximately 1700 °C. This temperature is about 200 °C higher than the common liquidus temperature for the target steel grade. In order to develop accurate thermophysical properties for the steel, riser sleeve, and sand mold, the thermocouples must record the steel cooling down to the liquidus temperature. A high preparation temperature is used to ensure this. In order to pour the castings, the molten steel was transferred from the furnace to a crane-hoisted pouring ladle. Immediately before pouring the metal into the castings, slag was removed from the surface of the ladle. Ambient temperatures for casting heats ranged from approximately 0 to 40 °C. As a result the steel temperature is generally only 50 °C above the liquidus temperature at the time of pouring.

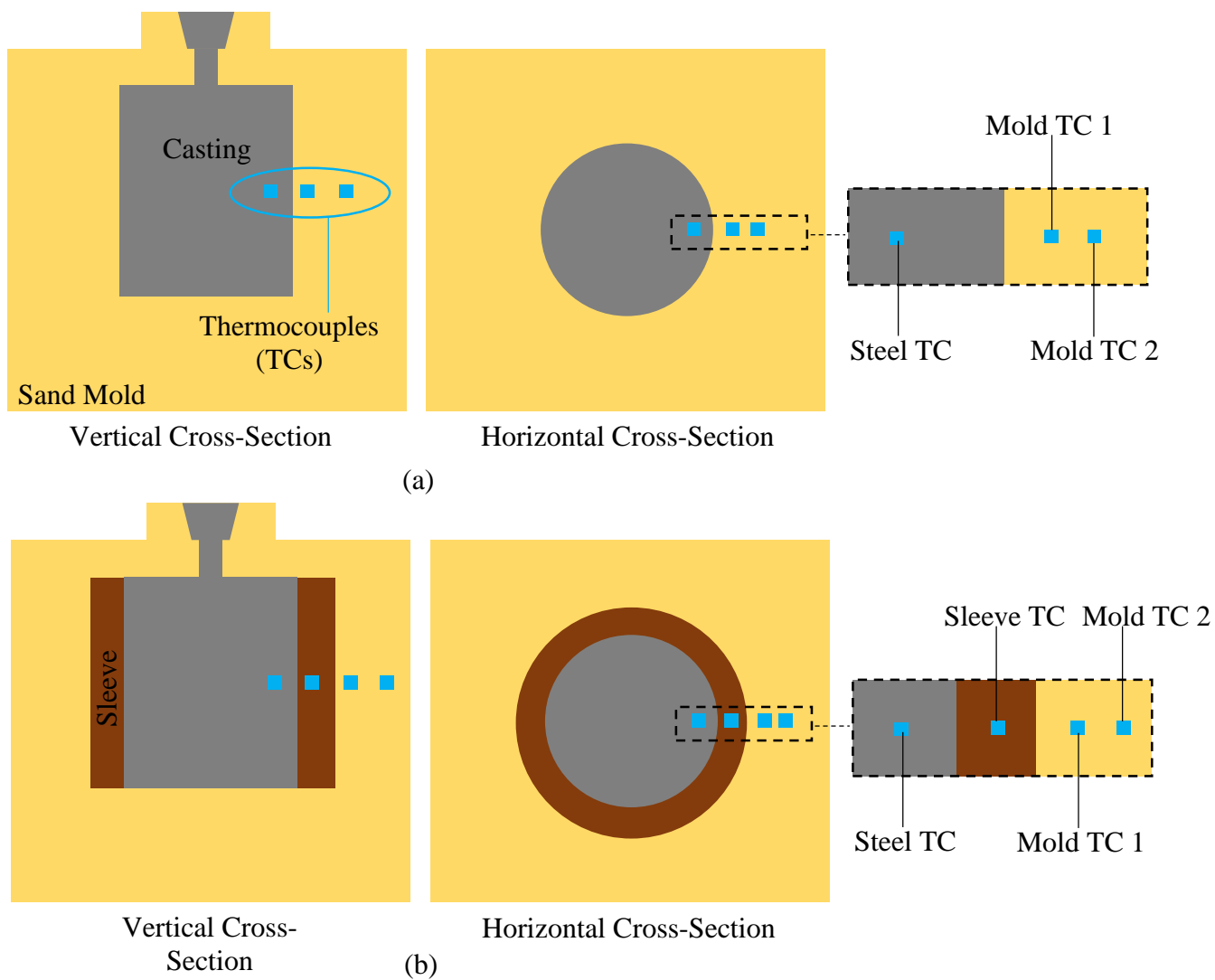
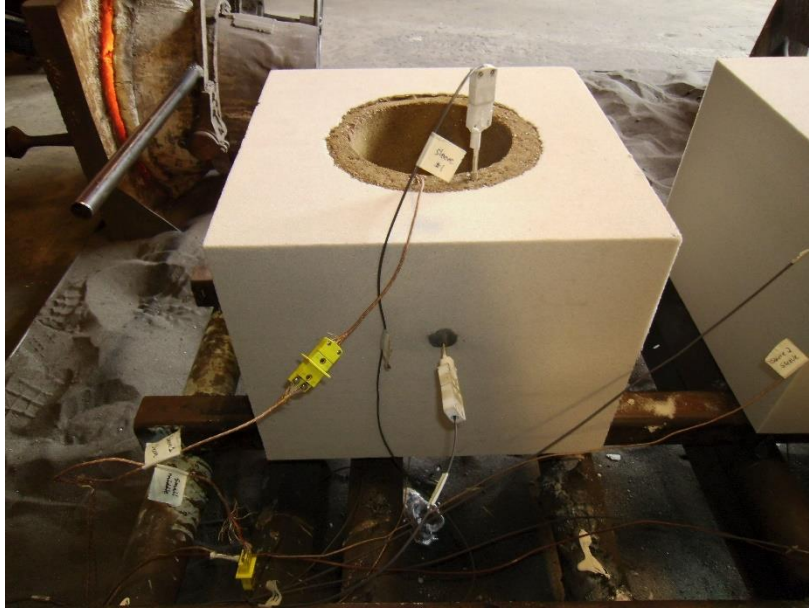


Figure 3.1. Schematic diagrams of experimental casting setups for (a) castings without a sleeve and (b) castings with a sleeve.



(a)



(b)

Figure 3.2. Photographs of casting experiments. (a) A sand mold without cope that has been instrumented with thermocouples. (b) Liquid steel being poured directly into casting cavities via crane hoisted ladle.

Table 3.1. Riser sleeves tested and the dimensions of the corresponding sleeve and no sleeve control castings. Sleeves are indicated to be insulating or exothermic using “-I” or “-E” respectively after their product name.

Manufacturer	Sleeve-Insulating/ Exothermic	Density (kg/m <sup>3</sup> )	Sleeve Inner Diameter (inches)	Casting Height (inches)	Sleeve Thickness (inches)	Control Casting Diameter (inches)	Control Casting Height (inches)
FOSECO	Kalminex 2000-E	422	3.5	6	0.5	4.5	6
	Kalminex 21-E	621	8	8	1	6	6
	Kalfax 100-E	534	3	6	0.625	3	5
	Kalmin 70-I	422	2.5	6	0.375	6	8
Joymark	CFX 700-E	451	5	5	0.5	5	8
	CFX 760-E	451	4.5	6	0.75	4.5	6
	CFX 800-E	451	6	6	1	4.5	6
Exochem	ES-E	676	3	6	1.25	3	5
	ESPX-E	531	3	5	0.5	3	5
	SNA-I	479	6	6	0.5	6	6
ASK	Exactcast EX-E	529	4.5	6	0.5	4.5	6
	Exactcast IN-I	395	4.25	6	0.375	4.5	6
AMCOR	Rosstherm K-I	256	4	4	0.5	3	5

## CHAPTER 4: THERMAL SIMULATIONS OF CASTING EXPERIMENTS

### 4.1 Introduction

In the present study, an inverse modeling method is used to develop riser sleeve thermophysical properties. Sleeve thermophysical properties are iteratively adjusted until temperature data from simulations agrees with temperature data from the casting experiments in Chapter 3. Before simulations with sleeves can be created, steel and sand properties must be determined by simulating castings without sleeve. The simulation software *MAGMASoft* [3] is used for all simulations performed here.

### 4.2 Simulations of Castings Without Sleeves

In order to determine sand and steel thermophysical properties independent of the effects of a riser sleeve, each set of casting experiments contained one casting without a sleeve. Specific sand and steel properties were determined for each set of experiments. The mold, lid, pouring cup, steel, and any air pockets are all included in simulations of the control casting. Due to the casting geometry, a vertical symmetry plane is applied, allowing for a finer mesh by reducing the volume of casting and mold that needed to be simulated. For all simulations an interfacial heat transfer coefficient (IHTC) between the steel and sand mold is required. This IHTC is shown below in Figure 4.1. The values of the IHTC approximate perfect contact ( $\sim 1000 \text{ W/m}^2\text{-K}$ ) at higher temperatures and a growing air gap impeding heat transfer, or decreasing the IHTC value, as the liquid metal solidifies and shrinks.

Sand and steel thermophysical properties necessary for casting simulation are the temperature dependent density, thermal conductivity, and specific heat. Additionally, the latent heat of fusion and temperature dependent solid fraction are needed for a steel thermophysical property dataset

As a result of familiarity with PUNB silica sand, a thermophysical property dataset already existed prior to this work. This dataset adequately simulated the sand mold for most of the casting trials. Modifications to the thermal conductivity of this dataset were made for some experiments.

The density and specific heat of the sand were never modified. Sand thermophysical properties used in this work can be seen in Figure 4.2. Figure 4.2 (a) plots the temperature dependent specific heat which increases with temperature and has a spike at low temperatures to model the burn-off of mold binder. Figure 4.2 (b) plots the temperature dependent density of the sand mold which decreases by about 7% with between 0 and 2000 °C. Figure 4.2 (c) plots the temperature depend sand mold thermal conductivities used in this work labeled RH1, TW6, and TW25. RH1 and TW6 are similar with increased thermal conductivity at low temperatures in order to model hot gasses flowing through the mold initially. This thermal conductivity decreases as the gas forming binder is burned away before increasing again with temperature. TW25 has a much different profile, with a low initial value of thermal conductivity which increases as temperature increases. While both RH1 and TW 6 were used for several experiments, TW25 was only applied to simulations of one set of experimental castings.

The latent heat of fusion is set to 192 kJ/kg for all steel property datasets used in this work. Due to variations in chemistry, other steel thermophysical properties are more variable, even with the same target chemistry. The software IDS [15] calculates thermophysical properties based on a steel composition input. A composition for ASTM A216 grade WCB steel is entered into the software and the calculated temperature dependent thermal conductivity, density, and specific heat are obtained. However, from experience, these steel properties require some modification to create accurate simulations in *MAGMASoft*. Examples of the modified curves for the temperature dependent thermal conductivity, density, and specific heat can be seen in Figure 4.3 (a), (b), and (c) respectively.

In order to create specific properties for each set of castings, the following procedure was used. For every set of experiments, the liquidus and solidus temperatures were determined. In order to model the increased heat transfer of convection in the liquid metal, rather than explicitly simulating it, the temperature dependent thermal conductivity of the steel was increased to 150 W/m-K at 1°C above the liquidus temperature and higher. At 1°C below the liquidus temperature the thermal conductivity is set at 33 W/m-K. This value was chosen to approximate the value of



the unmodified thermal conductivity at this temperature. At lower temperatures the thermal conductivity was unmodified. This modification is captured in Figure 4.3 (a) where the steep increase in thermal conductivity is shown to begin at 1499 °C and end at 1501 °C indicating a liquidus temperature of 1500 °C.

The temperature dependent curve for density shows a steep increase in the steel density as the steel cools between the liquidus and solidus temperatures. This increase reflects the density increase from the solidification of the liquid metal. In order to adapt this density curve for different casting experiments, the entire curve is shifted along the temperature axis so that the onset of the increase begins at the liquidus temperature determined for a given set of experiments. No other modifications are made to the density curve. The increase in density in Figure 4.3 (b) begins at 1500 °C which is the liquidus temperature determined for most of the experimental WCB steel heats.

The specific heat curve of the steel is left unmodified. A spike at approximately 700 °C, visible in Figure 4.3 (c), is used to emulate the release of latent heat that occurs due to a solid state transformation from  $\gamma$ -austenite to  $\alpha$ -ferrite and pearlite. This spike can be shifted or modified in magnitude but no shifting or modification is necessary in this work. This leaves the solid fraction curve to be determined.

The solid fraction curve is determined using an inverse modeling method, i.e. the curve is modified iteratively until the simulation results match the experimental temperature data. Figure 4.4 shows that modifying the solid fraction curve drastically alters the shape of the temperature curve. The blue curve labeled “B” in Figure 4.4 (a) exhibits increases an increase from 0.0 solid fraction to 0.9 solid fraction over a smaller temperature range than the black curve “A”. This results in a much longer time spent near liquidus temperature for the corresponding blue curve “B”, relative to the black curve “A”, in Figure 4.4 (b). Solid fraction curves for this work are shown in Figure 4.5 labeled using arbitrarily assigned numbers. The ends of the solid fraction curve are anchored at the liquidus temperature (solid fraction = 0) and the solidus temperature (solid fraction = 1) that are determined for a given heat of steel. For this reason, the curves in

Figure 4.5 begin an end at different temperatures. Liquidus temperatures ranged from 1466-1500 °C and solidus temperatures ranged from 1350-1410 °C. Between these two temperatures the curve should have a general shape, apparent in Figure 4.5, where the solid fraction reaches 0.9 within an approximate 50 °C range of the liquidus temperature and the increase in solid fraction from 0.9 to 1 occurs within an approximate 50°C range of the solidus temperature. The final shape of the curve will depend upon achieving agreement between the measured and simulated temperatures for the casting.

Agreement between measured (red curves) and simulated (black curves) temperatures for all control cases can be seen in Figures 4.6-4.13. These figures show temperature data plotted on the time scale of solidification, i.e. the time it takes for the steel to reach the solidus temperature. Because riser sleeves are designed to keep the metal in the liquid state, they are only effective before the steel solidifies. Thus it is most important to achieve good agreement over the solidification time scale and to correctly predict the time to solidification i.e. the time to reach solidus temperature. The solidus temperature is indicated on all steel temperature plots. The liquidus temperature is not indicated because it is apparent from the temperature arrest after the initial cool down. These figures show excellent agreement on the whole between the measured and simulated temperatures. Some cases show good agreement at multiple thermocouple locations, indicated by different line types, within the same material. Although not shown, most control cases exhibited excellent long term agreement as well. With the thermophysical properties for sand and steel determined, riser sleeve properties can be developed.

#### 4.3 Simulations of Castings With Sleeves

Steel and sand thermophysical properties for each set of casting experiments were set by simulating the castings without sleeve. These properties are applied to simulations for the corresponding castings with sleeve. Three IHTCs are required for a sleeve casting simulation, one between steel and sleeve, one between steel and sand, and one between sleeve and sand. The IHTCs between steel and sleeve or sand are equivalent to the IHTC in Figure 4.1. The IHTC

between sleeve and sand mold is set to a constant  $1000 \text{ W/m}^2\text{-K}$ , approximating perfect contact. This value is also sufficiently large that modifications to it do not affect the simulated temperature results and therefore the developed properties can be considered insensitive to this condition. This leaves the sleeve properties to be adjusted independently. The main riser sleeve thermophysical properties necessary for simulation are the density  $\rho$ , thermal conductivity  $k$ , and specific heat  $c_p$ . Some riser sleeves have exothermic properties which are modeled using a heat generation per unit mass, a burn time for a discrete element of the sleeve, and an ignition temperature for the exothermic reaction. With three temperature dependent properties for all sleeves, it can be extremely tedious to develop unique temperature dependent properties for each sleeve. Therefore, pre-determining two of the properties or setting them to constant or average values would be extremely beneficial. However, this is only possible if one of the properties has a larger effect on a riser sleeve's performance.

In order to determine which property has the largest effect on a sleeve performance, a simple cylinder lined with a riser sleeve is simulated. The riser sleeve has base thermophysical properties  $k$ ,  $\rho$ , and  $c_p$  equivalent to the properties of the Rosstherm K sleeve presented later. The sensitivity to each property is determined by modifying one or both of the thermal conductivity  $k$  and  $\rho c_p$ , the heat capacity, by factors of 0.5, and 2 and recording the solidification time of the cylinder. The solidification time of the cylinder is considered to be a measure of sleeve performance. The results of all permutations of these modifications are shown in Figure 4.14 and presented as the percent difference in solidification time relative to the unmodified case. Cases are grouped by modifications of  $k$  and individual bars represent modifications of  $\rho c_p$ . It is clear from Figure 4.14 that sleeve performance is about 3 times more sensitive to modifications made to the thermal conductivity than to changes in the heat capacity. This finding is supported by Midea et al. who found that solidification time near the interface between a riser and a casting was much more sensitive to changes in the thermal conductivity than to differences in the specific heat or density [11]. As such, the density and specific heat are set to predetermined values for each sleeve while the thermal conductivity is determined using inverse modeling.

It is estimated that the density for a sleeve will not change by more than 10% during its heating and cooling. Figure 4.14 shows that much larger differences in density will be needed to meaningfully affect the solidification time. As a result, the density was set as a constant equal to the measured room temperature density of the sleeve for this work. Densities are listed in Table 3.1. The densities have a large range from 250-670 kg/m<sup>3</sup>. Given the results in Figure 4.14, this range of densities does not significantly distinguish the performance of different sleeves.

In this work, one specific heat curve was applied to all sleeve property datasets. Midea et al. present a temperature dependent curve for specific heat, however no values are given on the axes [11]. The curve used in this work can be seen in Figure 4.15 and is similar in shape to the curve presented by Midea et al. The value of the specific heat begins at 400 J/kg-K at 0 °C increasing to and ranging from 600-740 J/kg-K at temperatures of 380-2000 °C.

With the specific heat and density predetermined, the thermal conductivity is left to be developed. The thermal conductivity is developed using the inverse modeling method where it is iteratively modified until agreement is achieved between simulation results and measured temperature data. Figure 4.16 illustrates how modifications of the final determined thermal conductivity of the ASK Exactcast IN sleeve material affect the simulation results in the steel, sleeve, and sand mold and the agreement of these results with the measured data. In Figure 4.16 (a) the base thermal conductivity curve  $k$  is plotted along with curves modified by factors of 0.5 and 2. The simulated temperature curves resulting from these modifications, plotted in Figure 4.16 (b), (c), and (d) show large sensitivities to the thermal conductivity. Particularly, the steel and sand mold temperatures, plotted in Figure 4.15 (b) and (d) respectively, experience large variance depending on the value of the thermal conductivity. Although modifications made to the thermal conductivity curves in this work were much smaller, these curves illustrate the difficulty and compromises that must be made in order to minimize the error between the simulated results and the measured data. Thermal conductivities developed for all sleeves studied here are shown in Figures 4.17. All thermal conductivity curves begin at low values, typically around 0.15 W/m-K,

and increase to higher values which are generally between 0.5 and 1.0 W/m-K. The increase occurs across a range of temperatures, roughly around 1000 °C.

Exothermic properties must be developed for those sleeves which have an exothermic nature. The thermocouple placed inside the riser sleeve allows for precise development of the exothermic properties which produce a distinct spike on the temperature-time curve. The characteristics of this spike are controlled by the heat generation and the burn time. Figures 4.18 and 4.19 illustrate the effects of modifying the final determined exothermic properties of the FOSECO Kalminex 21 sleeve material. Figure 4.18(a) and (b) illustrate how modifying the exothermic heat generation effects the agreement between simulated and measured temperatures in the steel. The heat generation has small effects on the long term time scale shown in Figure 4.18(a) and also in the initial cooldown to liquidus shown in Figure 4.18(b). Figure 4.18(c) and (d) illustrate that modifying the exothermic burn time does not affect steel temperatures. Figure 4.19(a) and (b) illustrate that the heat generation does not influence the long term temperature of the sleeve but does affect the height of the exothermic spike. Figure 4.19(c) and (d) show that burn time does not affect the long term temperature in the sleeve but does influence the width of the exothermic spike. Figure 4.20 supports these same conclusions by modifying the final exothermic properties of the Joymark CFX 760 sleeve material. Figures 4.18-4.20 illustrate that modifications to the heat generation and burn time have independent effects. As a result, developing these properties is relatively trivial if one has experimental temperature data from the sleeve. An appropriate ignition temperature for sleeves using a thermite reaction, as all sleeves in this work are believed to do, is in the range of 400-800 °C. In this range, modifications to the ignition temperature have little effect on the agreement between measured and simulated temperatures so the ignition temperature was set to 600 °C for all sleeves.

Exothermic properties for all sleeves are listed in Table 4.1. The exothermic heat release ranges from 250-850 kJ/kg and the burn time ranges from 15-60 seconds. All exothermic sleeves in this work are believed to utilize the thermite reaction to produce heat. According to the chemistry of this reaction [17], the heat release should be 825 kJ per mole of reactant or 3981 kJ

per kilogram of reactant. Based on this, a sleeve with a heat release in the range of 250-850 kJ/kg would be composed of about 6-21% thermite reactants per total mass. Compositions of sleeves, including exothermic content, are understandably proprietary and not provided by manufacturers, however a 6-21% by mass composition seems reasonable by author estimation.

In some cases after the exothermic properties were determined, the sleeve thermal conductivity required some extra iterations in order to rectify discrepancies in the agreement between simulation results and measured data. The temperature dependent thermal conductivities shown in Figure 4.17, however, are the final thermal conductivities and take this secondary modification into account.

Agreement between measured and simulated temperatures for all castings with sleeve are shown in Figures 4.21-4.34. Again the cases show excellent agreement on the whole. The most important targets for matching were the time to reach solidus temperature in the steel and the whole of the sleeve temperature curves.

A few cases display temperature results for multiple thermocouples at the same nominal locations, indicated by use of the same line type in the plot, in the same material. A good example of this is the sleeve temperature in Figure 4.29 (b) which shows two thermocouples at the same nominal location reading a 200 °C difference in temperature. This difference between measured temperatures at the same nominal location illustrates a theoretical tolerance for error between the measured and simulated temperature. This difference can be due to a variety of factors such as small errors in radial placement of the thermocouple or even differences in composition of individual products of the same line.

One case of special mention is the Rosstherm K case (results in Figure 4.34). The thermocouples in the steel for the control casting failed in this case. Luckily, this sleeve was tested alongside the ASK Exactcast IN sleeve (results in Figure 4.33) which had sleeve properties developed previously. Measured and simulated temperatures from the previous experiment are shown in Figure 4.28. In this case the sand, steel, and sleeve properties from the previous experiment (results in Figure 4.28) were applied to the ASK Exactcast IN casting in the newer

experiment (results in Figure 4.33) and found to exhibit the same level agreement. Therefore it is reasonable to apply these same sand and steel properties to the AMCOR Rosstherm K case. The sleeve properties for AMCOR Rosstherm K were then iteratively modified. The measured and simulated temperatures for the AMCOR Rosstherm K sleeve casting, shown in Figure 4.34, exhibit the same level of agreement as the ASK Exactcast IN. While not ideal, this indicates that the developed properties for the AMCOR Rosstherm K are sufficiently effective for simulating the effects of the sleeve.

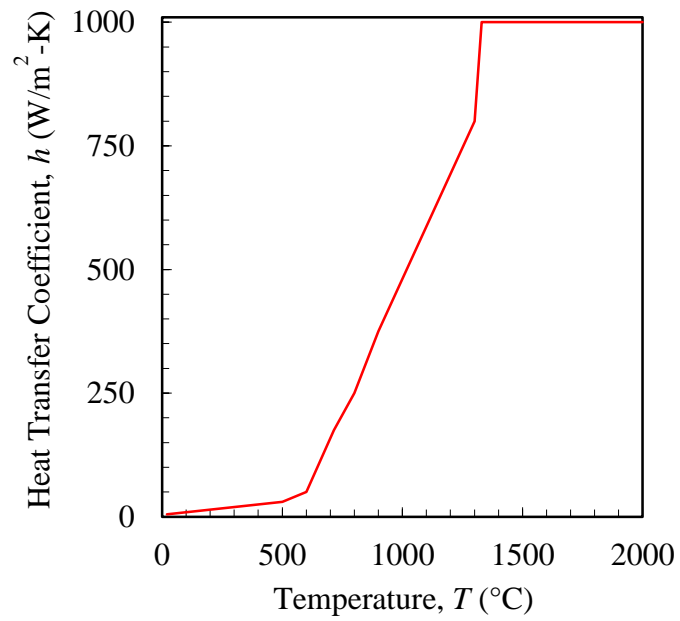


Figure 4.1. Temperature dependent interfacial heat transfer coefficient applied at the steel-sand and steel-sleeve interfaces in simulations performed in this study.



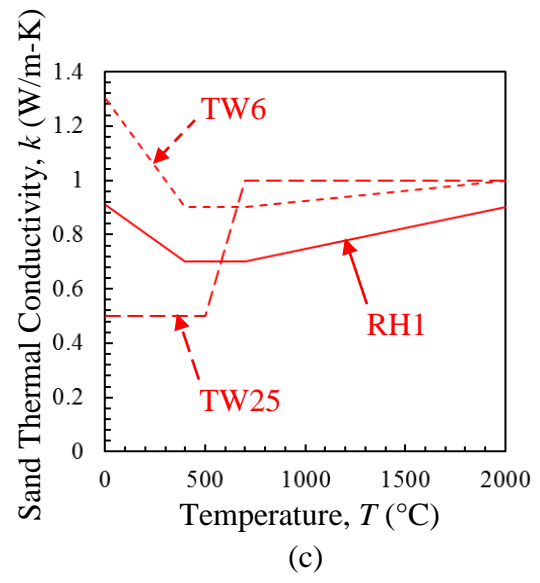
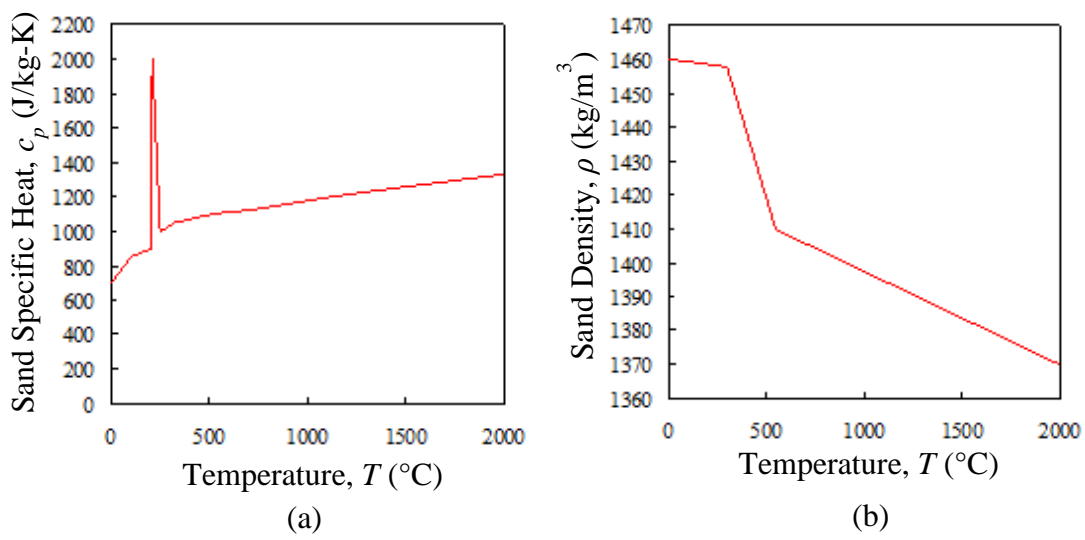


Figure 4.2. Sand mold thermophysical properties. (a) The sand density curve used for all simulations. (b) The sand specific heat curve used for all simulations. (c) Sand thermal conductivity curves.

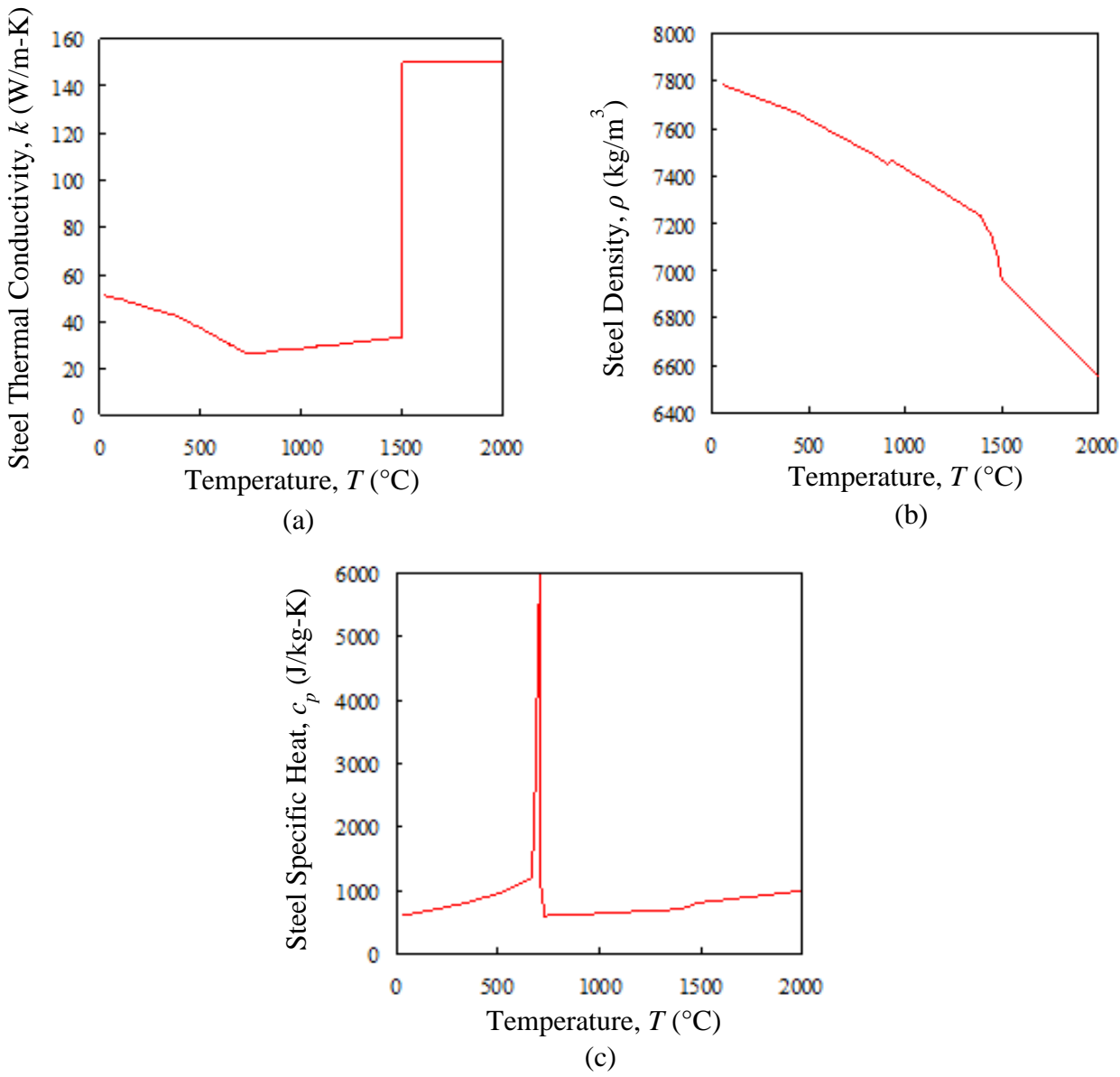


Figure 4.3. Example curves for effective steel thermophysical properties for simulation. (a) The thermal conductivity. (b) The density. (c) The specific heat.

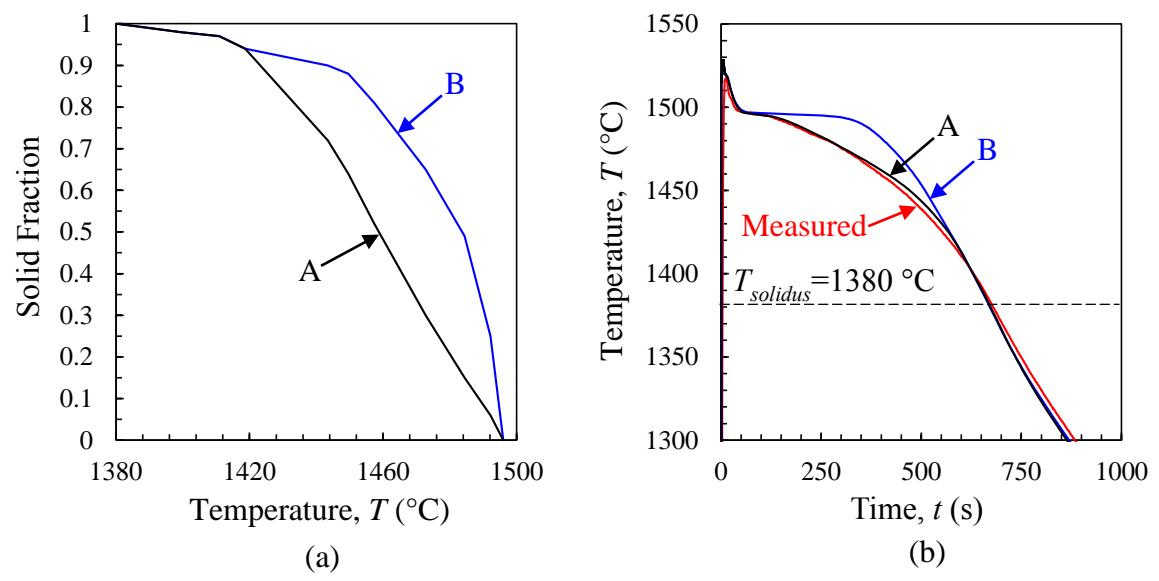


Figure 4.4. (a) Two solid fraction curves. The black curve corresponds to solid fraction curve 3 in Figure 4.5. (b) Temperature results in the steel showing how solid fraction affects the agreement between measured and simulated temperatures.

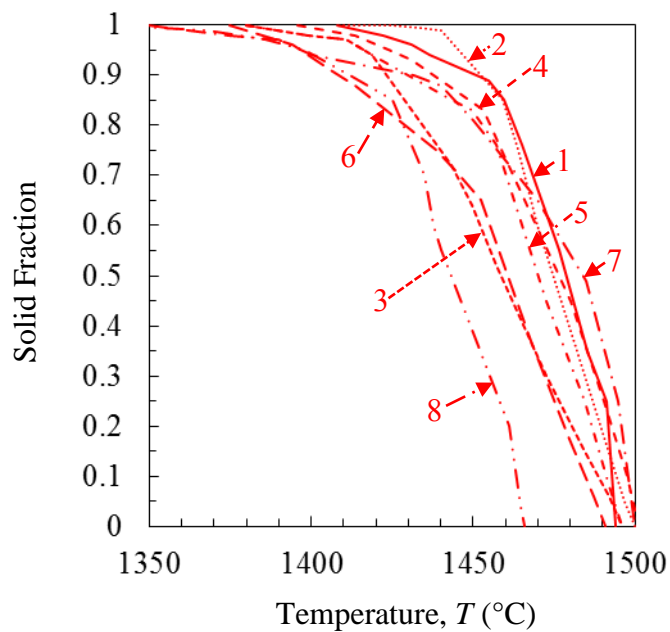


Figure 4.5. Solid fraction curves developed for all no sleeve control cases and applied to the corresponding sleeve casting simulations.

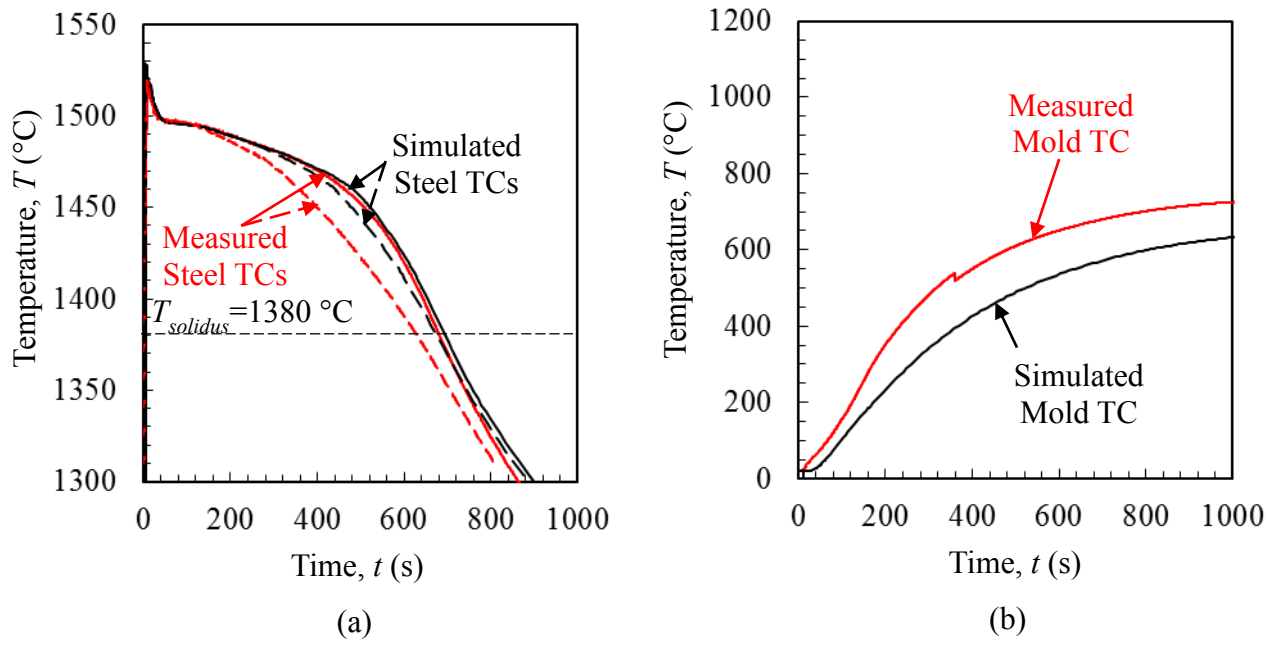


Figure 4.6. Measured and simulated temperatures for the control casting corresponding to FOSECO Kalminex 2000 and ASK Exactcast EX sleeve castings. Data for thermocouples placed in (a) the steel and (b) the sand mold. Sand thermal conductivity RH1 and solid fraction curve 5 are applied to this simulation.

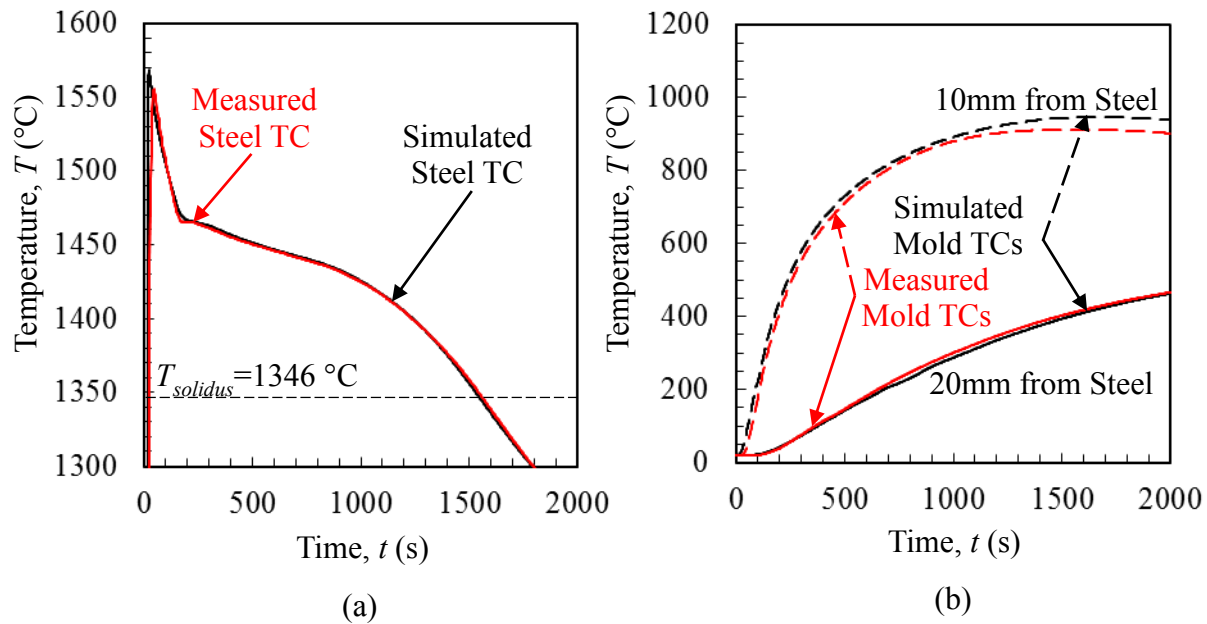


Figure 4.7. Measured and simulated temperatures for the control casting corresponding to the FOSECO Kalmin 70 sleeve castings. Data for thermocouples placed in (a) the steel and (b) the sand mold. Sand thermal conductivity RH1 and solid fraction curve 8 are applied to this simulation. In (b) the line type denotes position at 10 mm (dashed line) and 20 mm (solid line) from steel-mold interface.

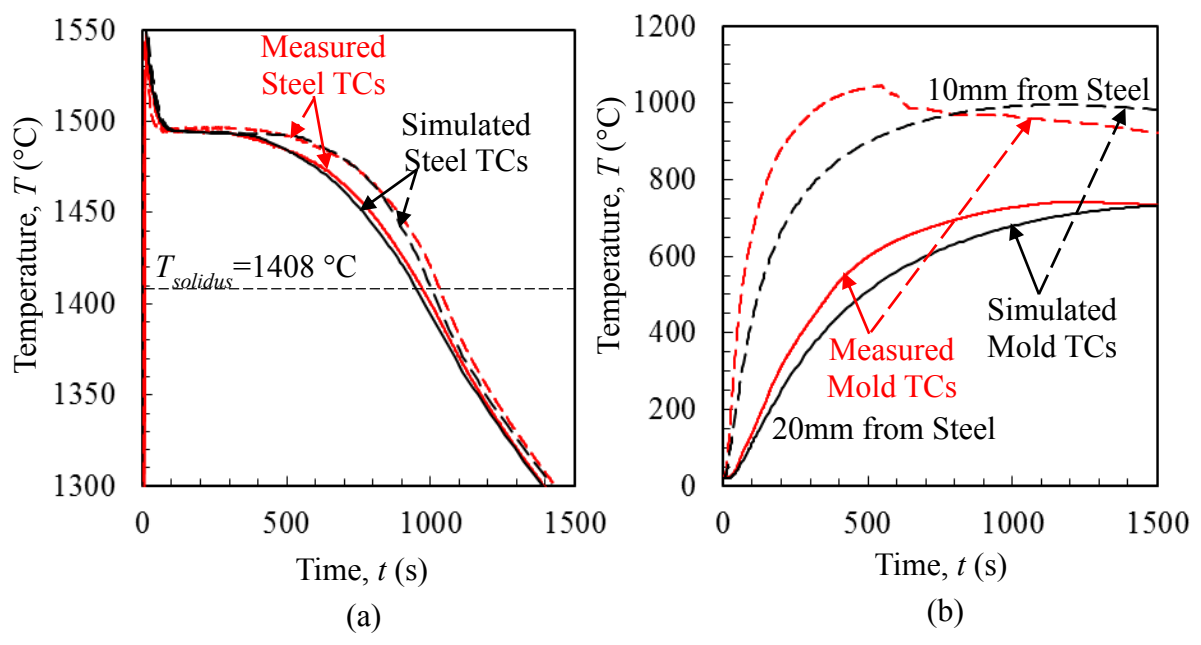


Figure 4.8. Measured and simulated temperatures for the control casting corresponding to the FOSECO Kalminex 21 sleeve casting. Data for thermocouples placed in (a) the steel and (b) the sand mold. Sand thermal conductivity RH1 and solid fraction curve 1 are applied to this simulation. In (b) the line type denotes position at 10 mm (dashed line) and 20 mm (solid line) from steel-mold interface.

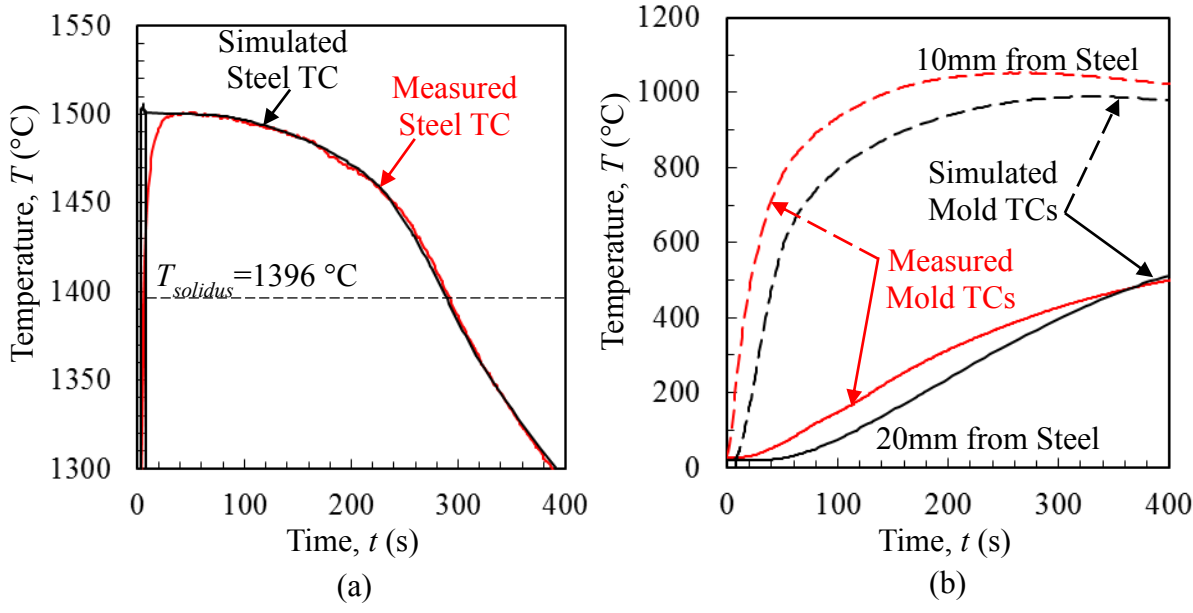


Figure 4.9. Measured and simulated temperatures for the control casting corresponding to FOSECO Kalfax 100 and Exochem ES sleeve castings. Data for thermocouples placed in (a) the steel and (b) the sand mold. Sand thermal conductivity TW25 and solid fraction curve 4 are applied to this simulation. In (b) the line type denotes position at 10 mm (dashed line) and 20 mm (solid line) from steel-mold interface.



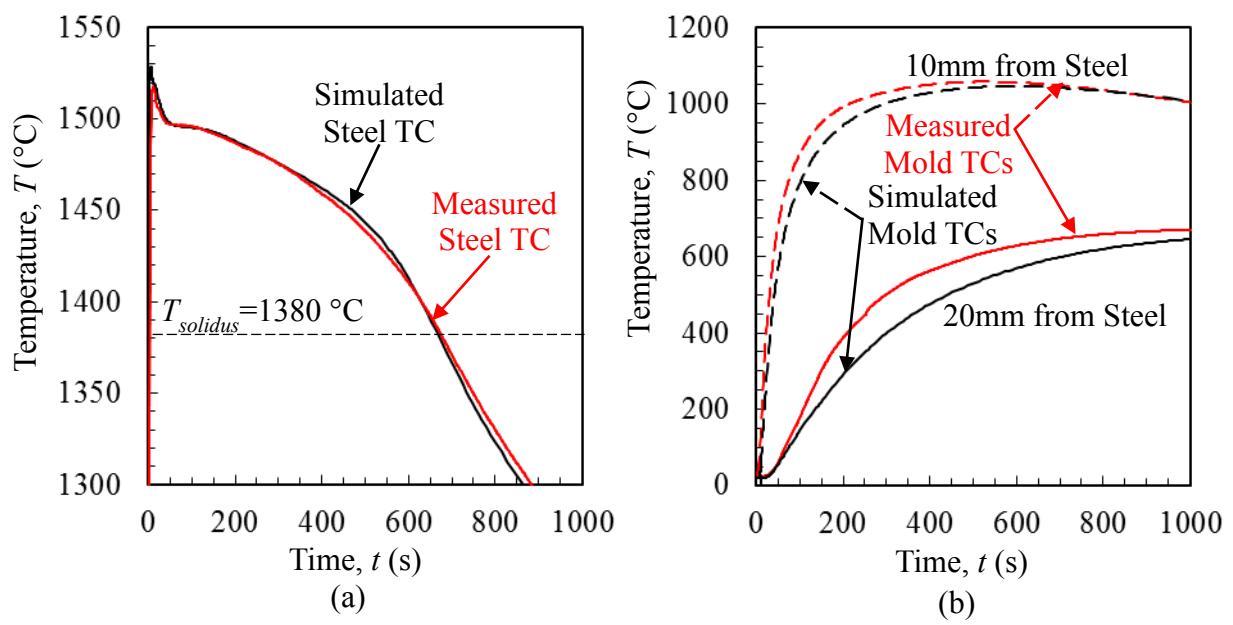


Figure 4.10. Measured and simulated temperatures for the control casting corresponding to Joymark CFX 700 and ASK Exactcast IN sleeve castings. Data for thermocouples placed in (a) the steel and (b) the sand mold. Sand thermal conductivity TW6 and solid fraction curve 3 are applied to this simulation. In (b) the line type denotes position at 10 mm (dashed line) and 20 mm (solid line) from steel-mold interface.

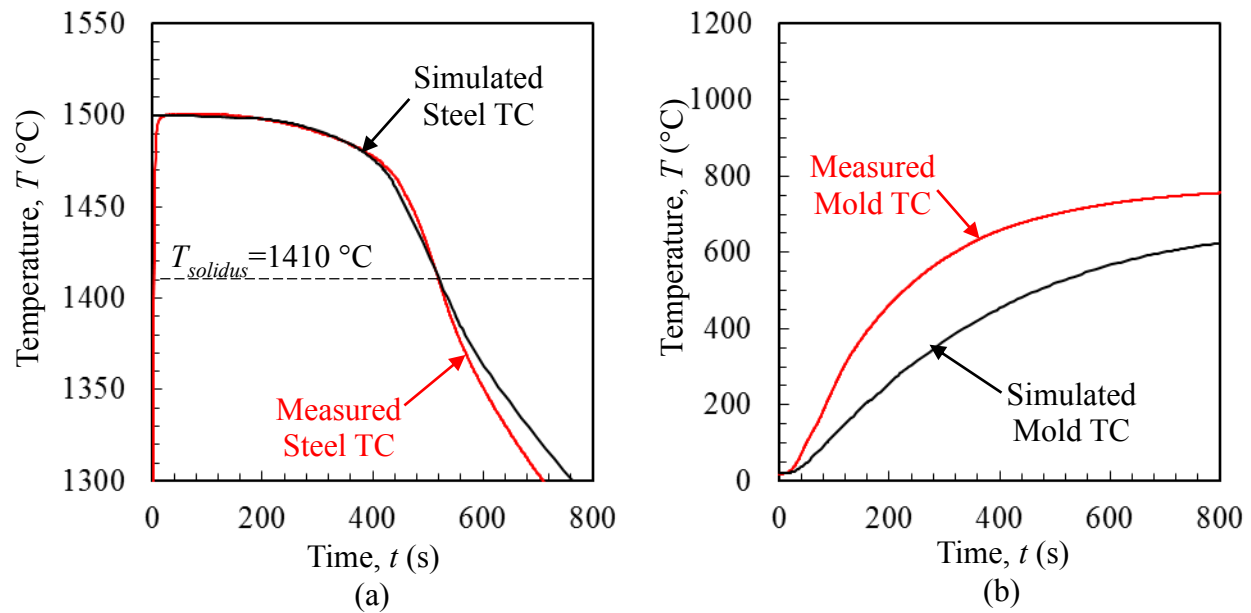


Figure 4.11. Measured and simulated temperatures for the control casting corresponding to Joymark CFX 760 and Joymark CFX 800 sleeve castings. Data for thermocouples placed in (a) the steel and (b) the sand mold. Sand thermal conductivity RH1 and solid fraction curve 2 are applied to this simulation.

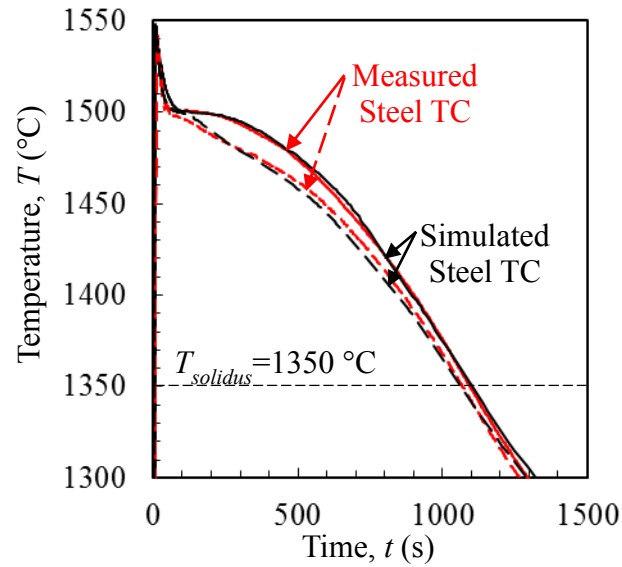


Figure 4.12. Measured and simulated temperatures for the control casting corresponding to the Exochem SNA sleeve casting. Data for thermocouples placed in (a) the steel. Sand mold thermocouples were burnt out. Sand thermal conductivity RH1 and solid fraction curve 7.

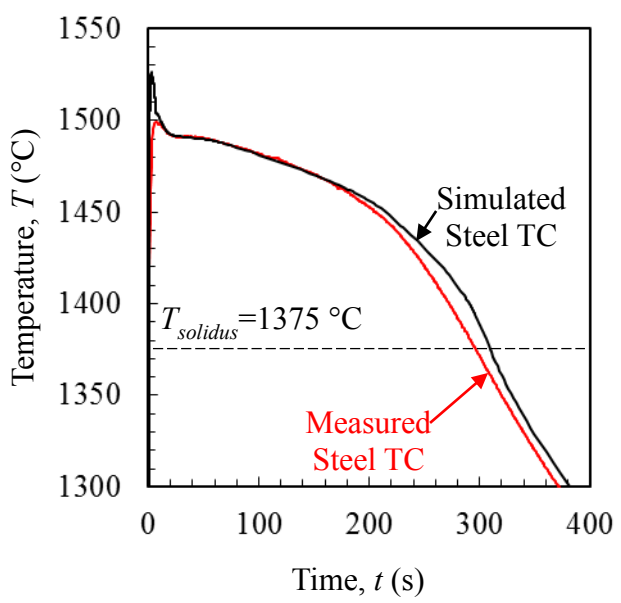


Figure 4.13. Measured and simulated temperatures for the control casting corresponding to Exochem ESPX. Data for thermocouples placed in (a) the steel and (b) the lid. Sand mold thermocouples were burnt out. Sand thermal conductivity TW6 and solid fraction curve 6.

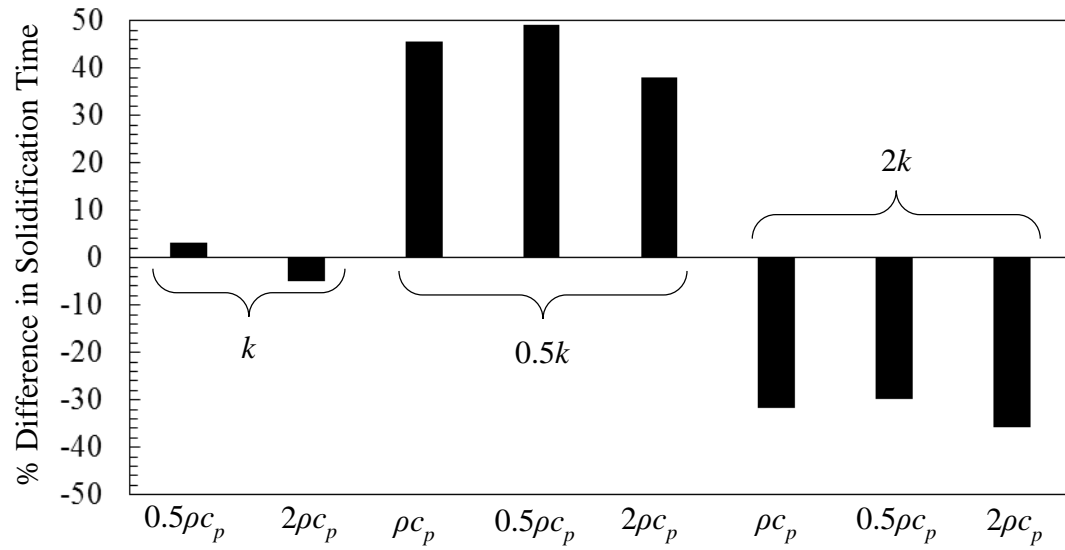


Figure 4.14. The difference in solidification time percentage for a sleeved cylinder casting, as predicted by casting simulation, for all permutations of cases where the sleeve material thermophysical properties  $k$  and product  $\rho c_p$  are multiplied by factors of 0.5 and 2. Differences are relative to results for the unmodified properties. Cases are grouped according to multiplier of  $k$ , and individual bars correspond to cases of  $\rho c_p$ .

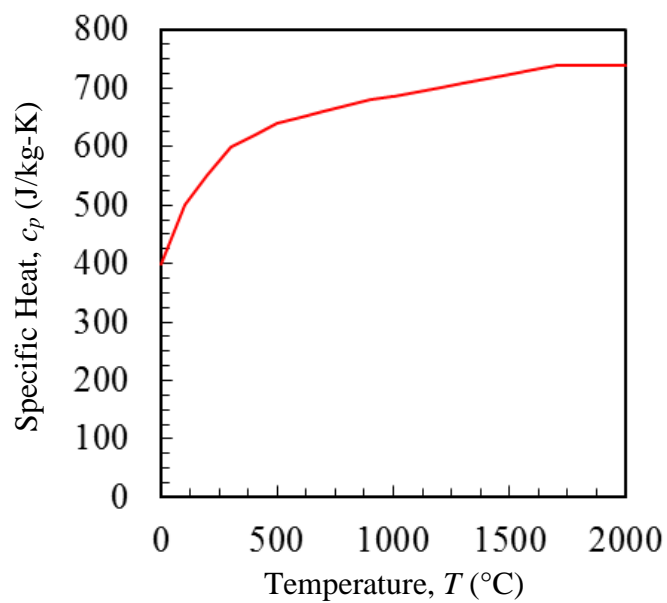


Figure 4.15. Specific heat curve used for all sleeves in this work.

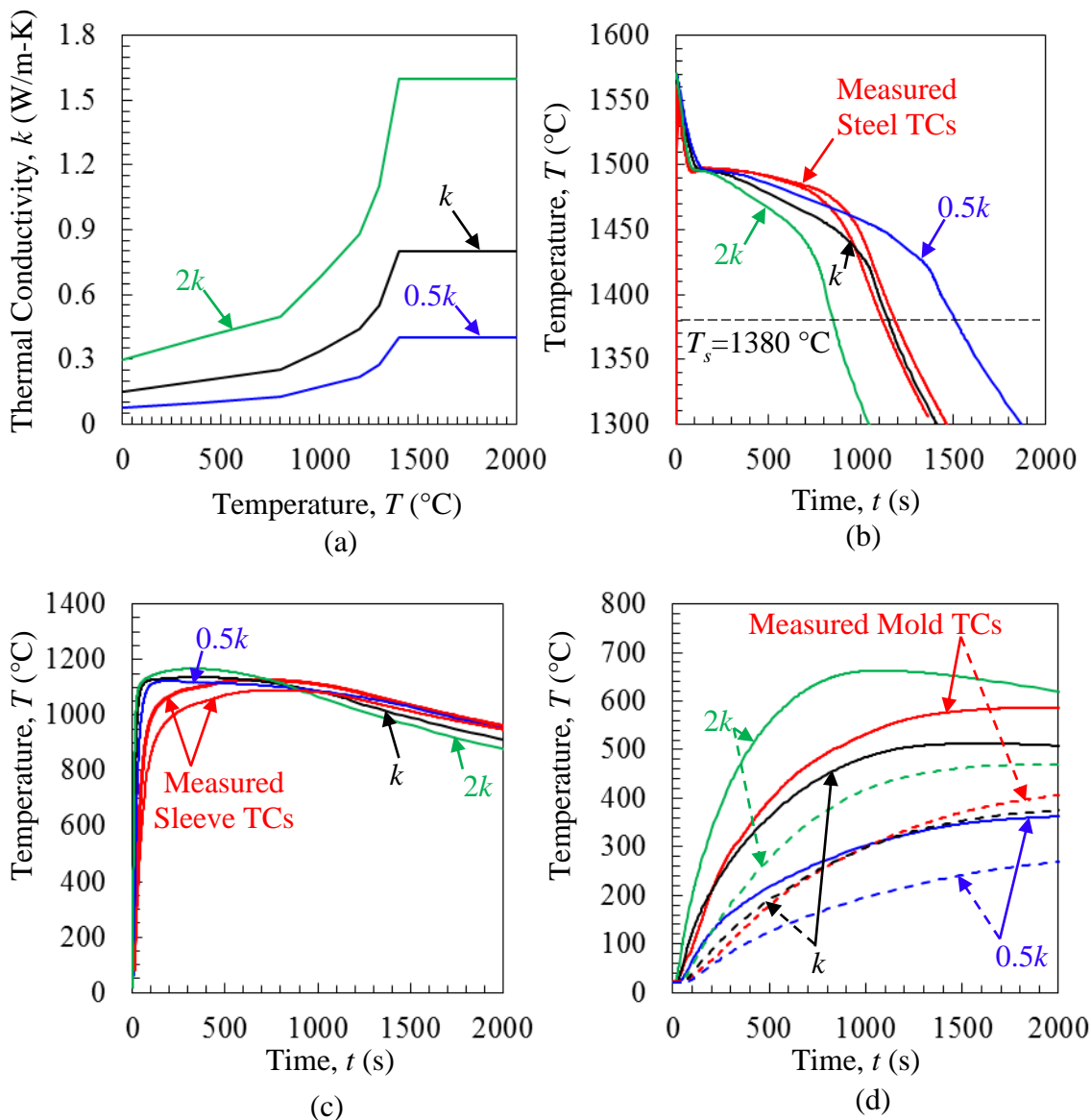


Figure 4.16. (a) Temperature dependent riser sleeve thermal conductivity curve determined for the ASK Exactcast IN sleeve material properties with base curve and curves multiplied by factors of 0.5 and 2. Measured cooling curves (red curves) are compared to predicted curves in the (b) steel, (c) sleeve, and (d) sand mold. Effect of multiplying the sleeve thermal conductivity by factors of 0.5 and 2 is shown by the blue and green curves, respectively. Note in (d) there are two measured mold TCs in the plot at 10 mm and 20 mm from the sleeve-metal interface corresponding to the solid and dashed curves, respectively.

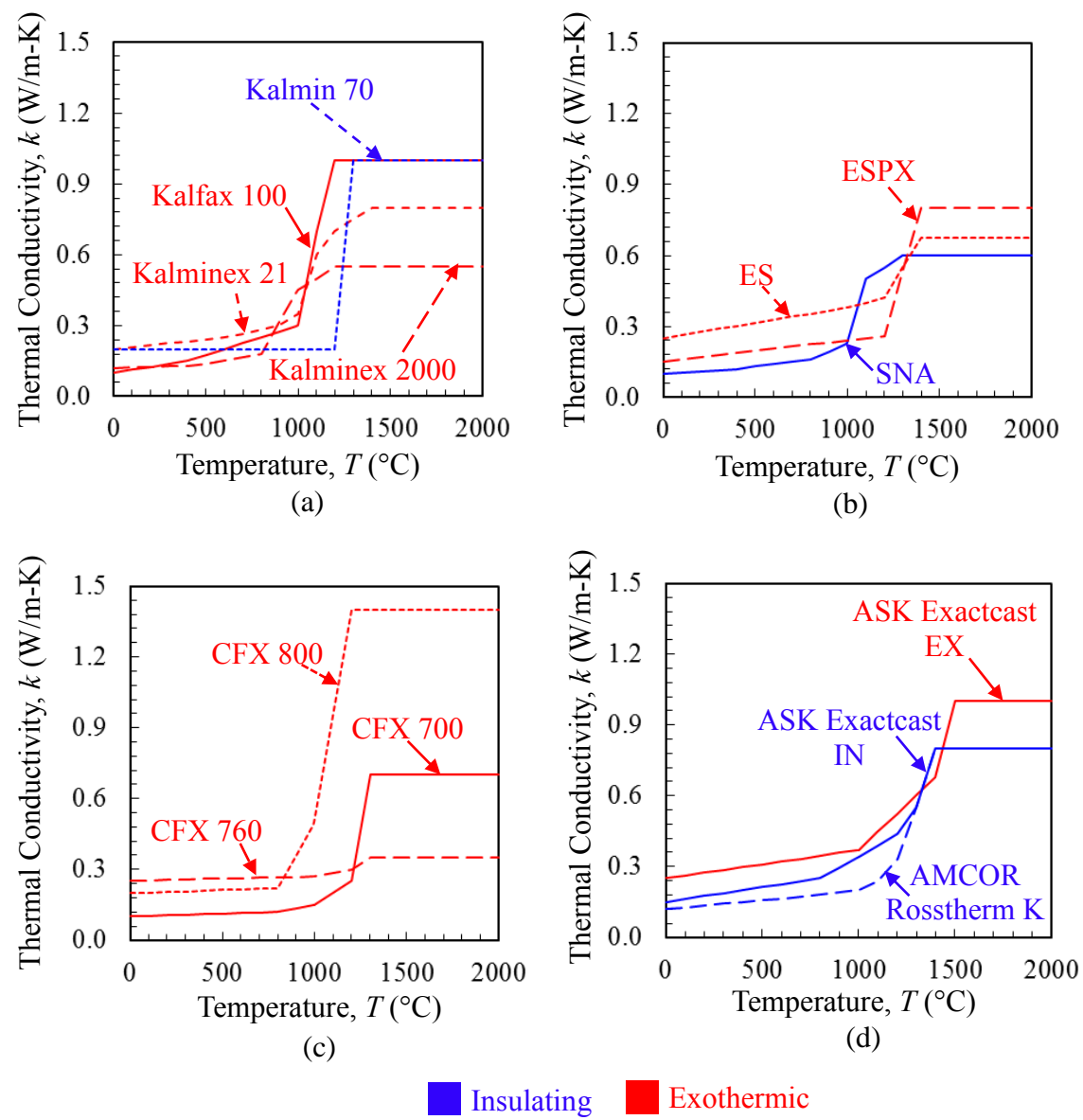


Figure 4.17. Riser sleeve temperature dependent thermal conductivity curves for sleeve materials sorted by sleeve manufacturer. (a) FOSECO (b) Exochem (c) Joymark (d) AMCOR and ASK Chemical.



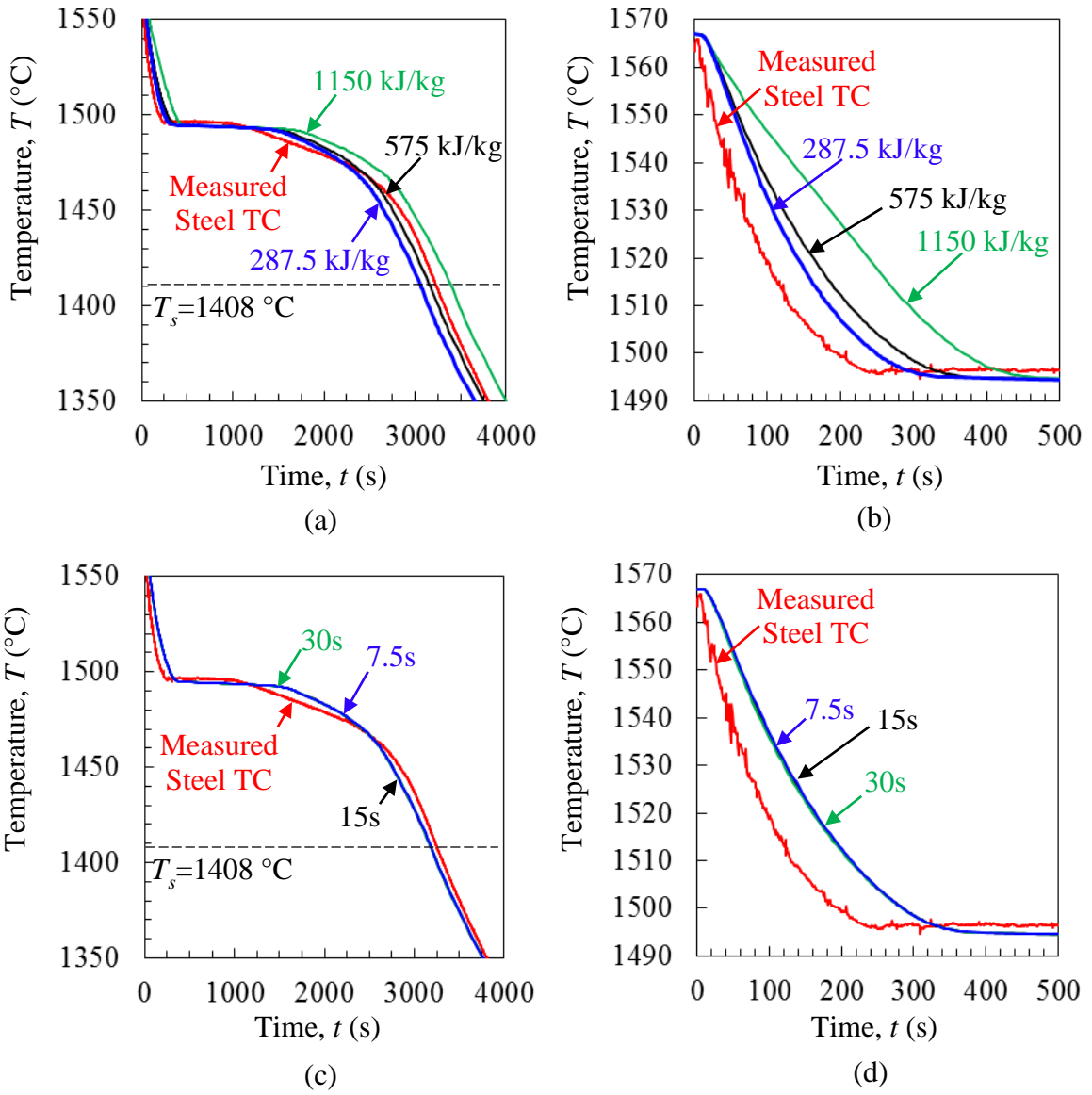


Figure 4.18. Temperature vs. time results in the **steel** for the Foseco Kalminex 21 sleeve showing in (a) and (b) the effect of modifying the heat generation on agreement between measured and predicted temperatures on long and short time scales, respectively. Figures (c) and (d) show the effect of modifying the burn time on agreement between measured and predicted temperatures. Black curves are simulation results using the final determined properties for the sleeve.

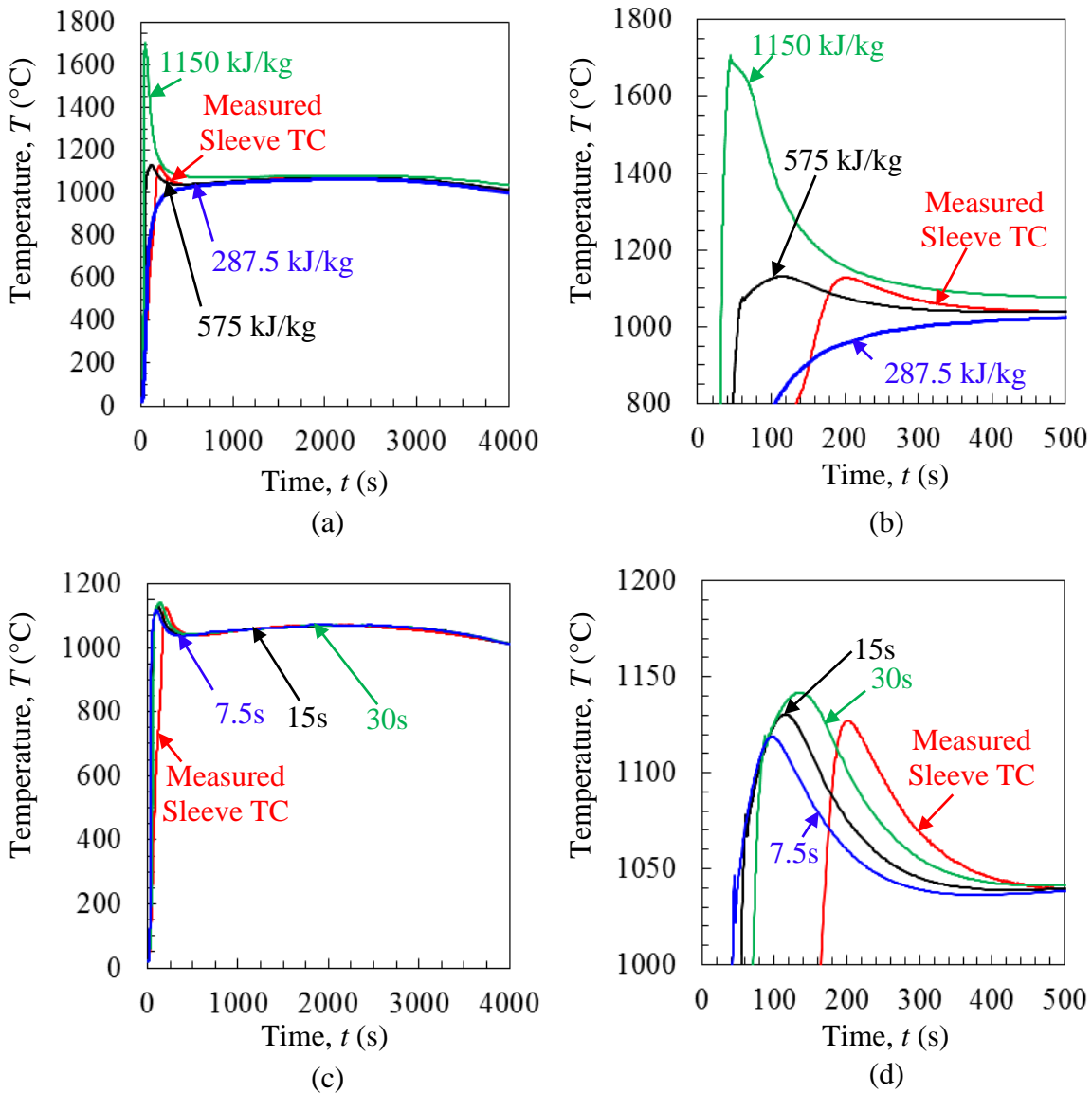


Figure 4.19. Temperature curves in the **sleeve** for the Foseco Kalminex 21 sleeve showing in (a) and (b) the effect of modifying the heat generation on agreement between measured and predicted temperatures on long and short time scales, respectively. Figures (c) and (d) show the effect of modifying the burn time on agreement between measured and predicted temperatures. Black curves are simulation results using the final determined properties for the sleeve.

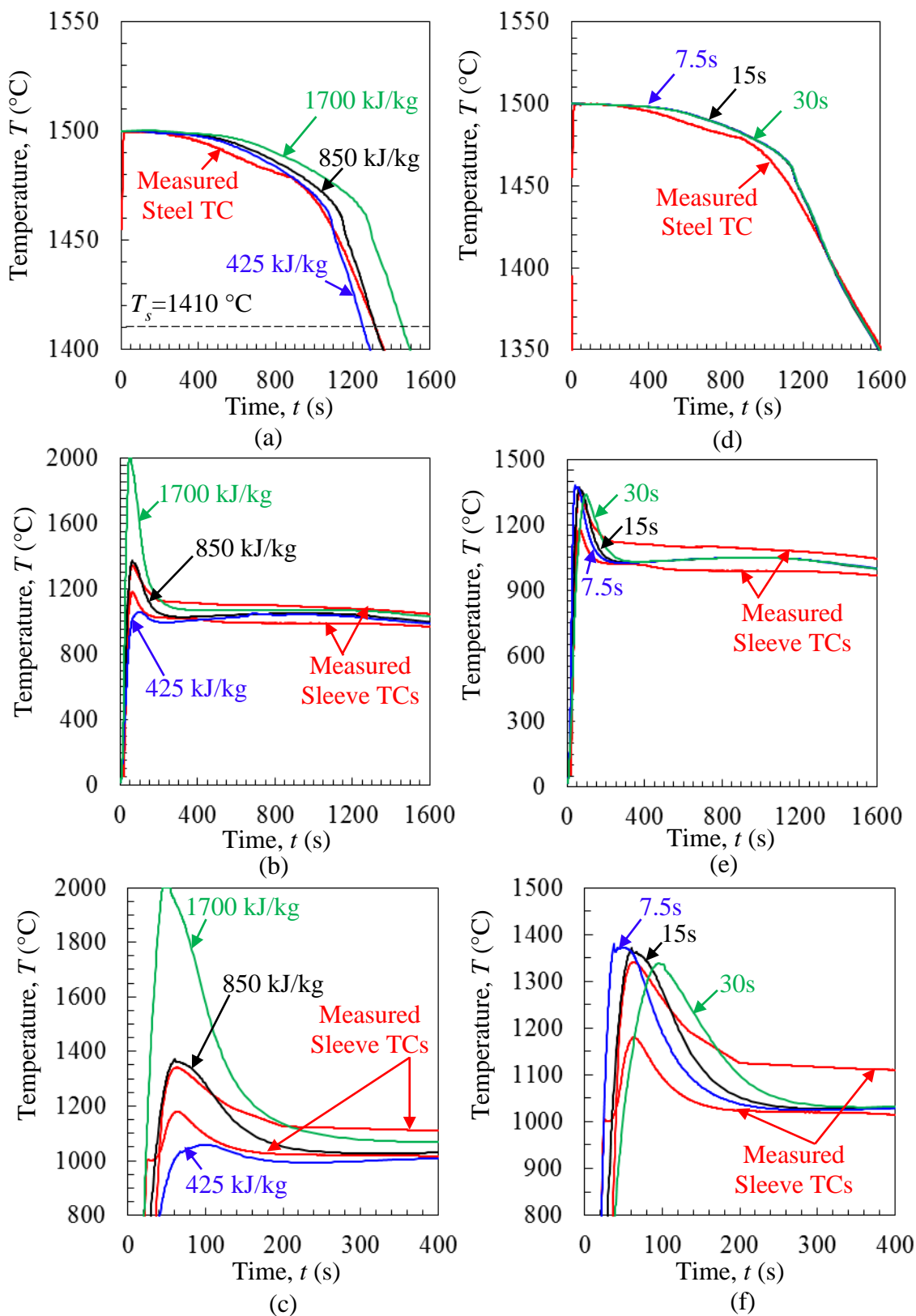


Figure 4.20. Temperature curves in the steel and sleeve for the Joymark CFX 760 sleeve showing in (a), (b) and (c) the effect of modifying the heat generation on agreement between measured and predicted temperatures on long times scales in (a) and (b) and a short time scale for the sleeve in (c). Analogous temperature curves showing effect of modifying the burn time on agreement between measured and predicted temperatures are shown in (d) for the steel and (e) and (f) for the sleeve.

Table 4.1. Riser sleeve exothermic properties used for simulation, ordered by heat generation.

Sleeve	Heat Generation (kJ/kg)	Burn Time (s)	Ignition Temperature (°C)
Joymark CFX 760	850	15	600
Joymark CFX 700	750	15	
FOSECO Kalminex 21	575	15	
Exochem ESPX	520	60	
Exochem ES	500	45	
ASK Exactcast EX	425	30	
Joymark CFX 800	425	18	
FOSECO Kalminex 2000	250	40	
FOSECO Kalfax 100	250	20	

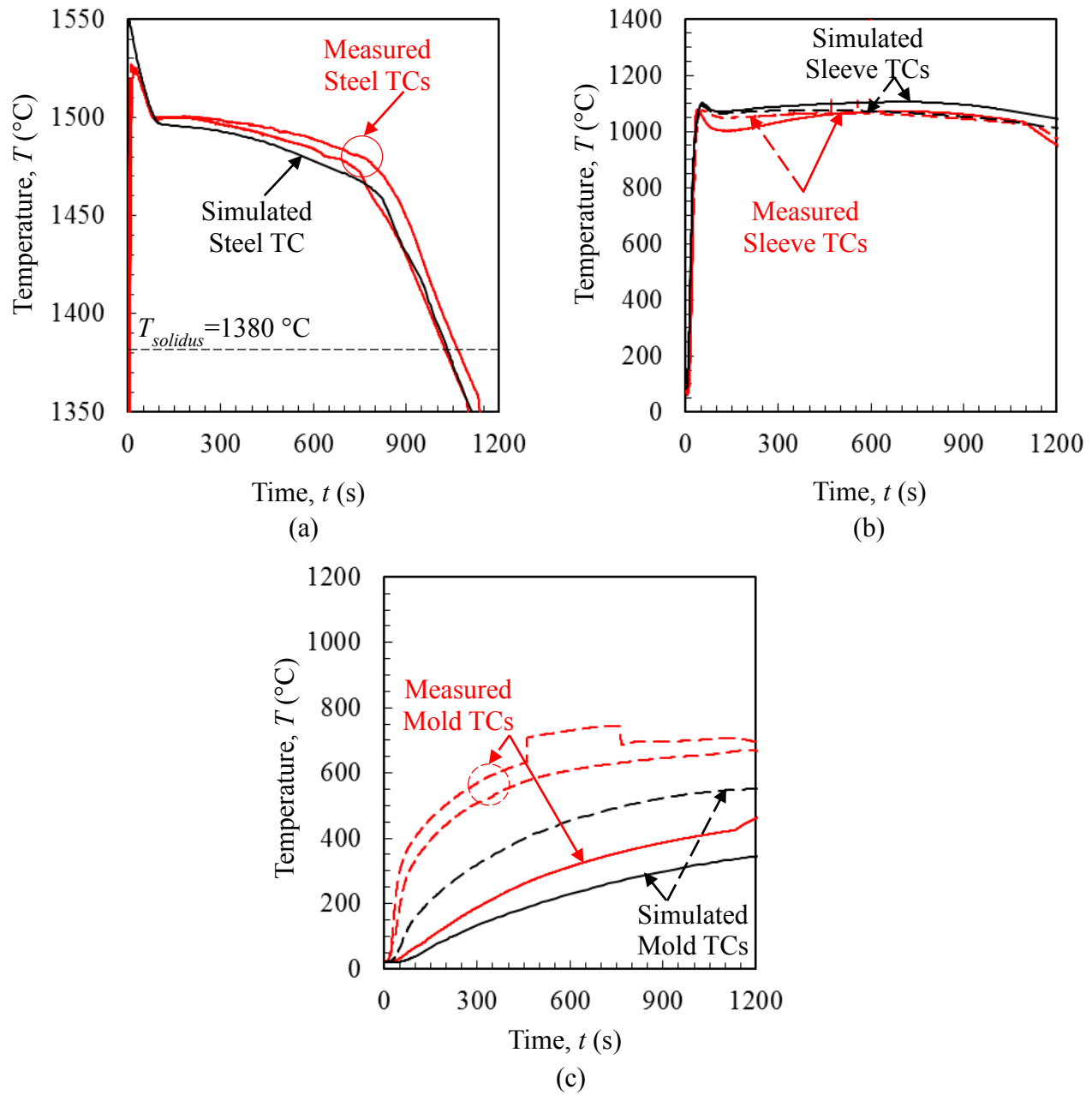


Figure 4.21. FOSECO Kalminex 2000 sleeve casting measured and simulated temperatures. Thermocouples placed in (a) the steel, (b) the sleeve, and (c) the sand mold. Line types denote different nominal positions of the TC.

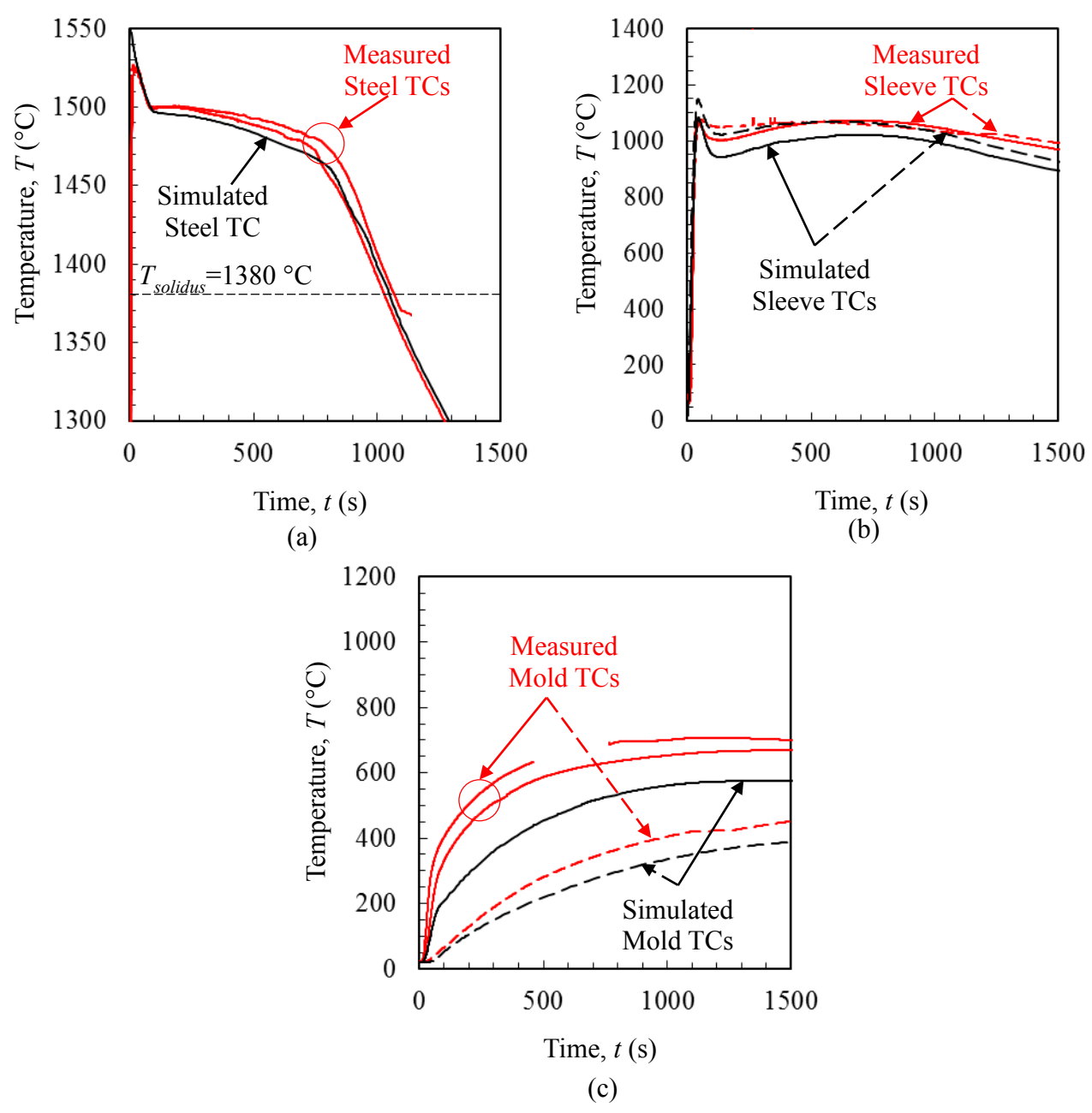


Figure 4.22. ASK Exactcast EX sleeve casting measured and simulated temperatures. Thermocouples placed in (a) the steel, (b) the sleeve, and (c) the sand mold. Line types denote different nominal positions of the TC.

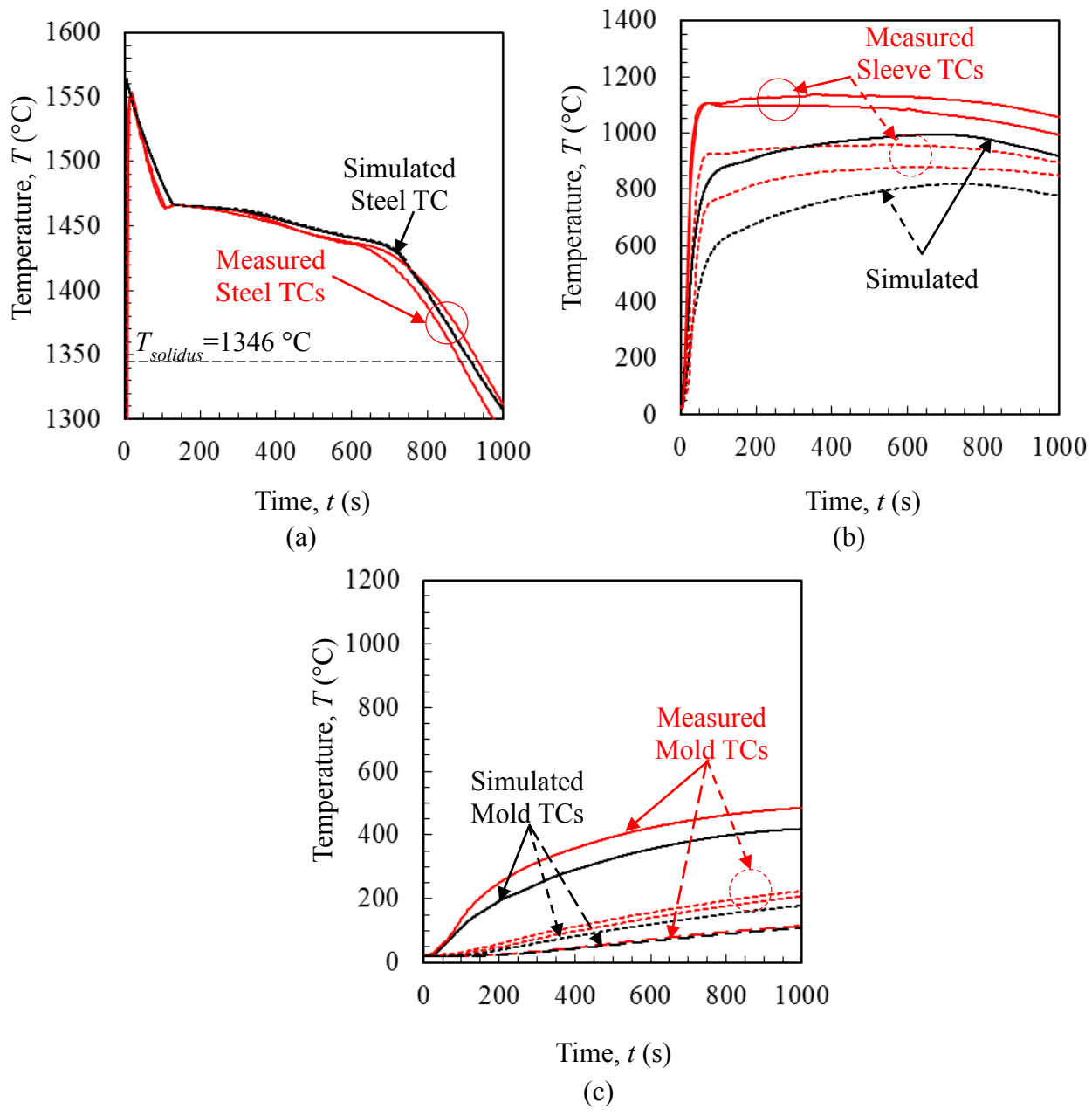


Figure 4.23. FOSECO Kalmin 70 sleeve casting measured and simulated temperatures. Thermocouples placed in (a) the steel, (b) the sleeve, and (c) the sand mold. Line types denote different nominal positions of the TC.

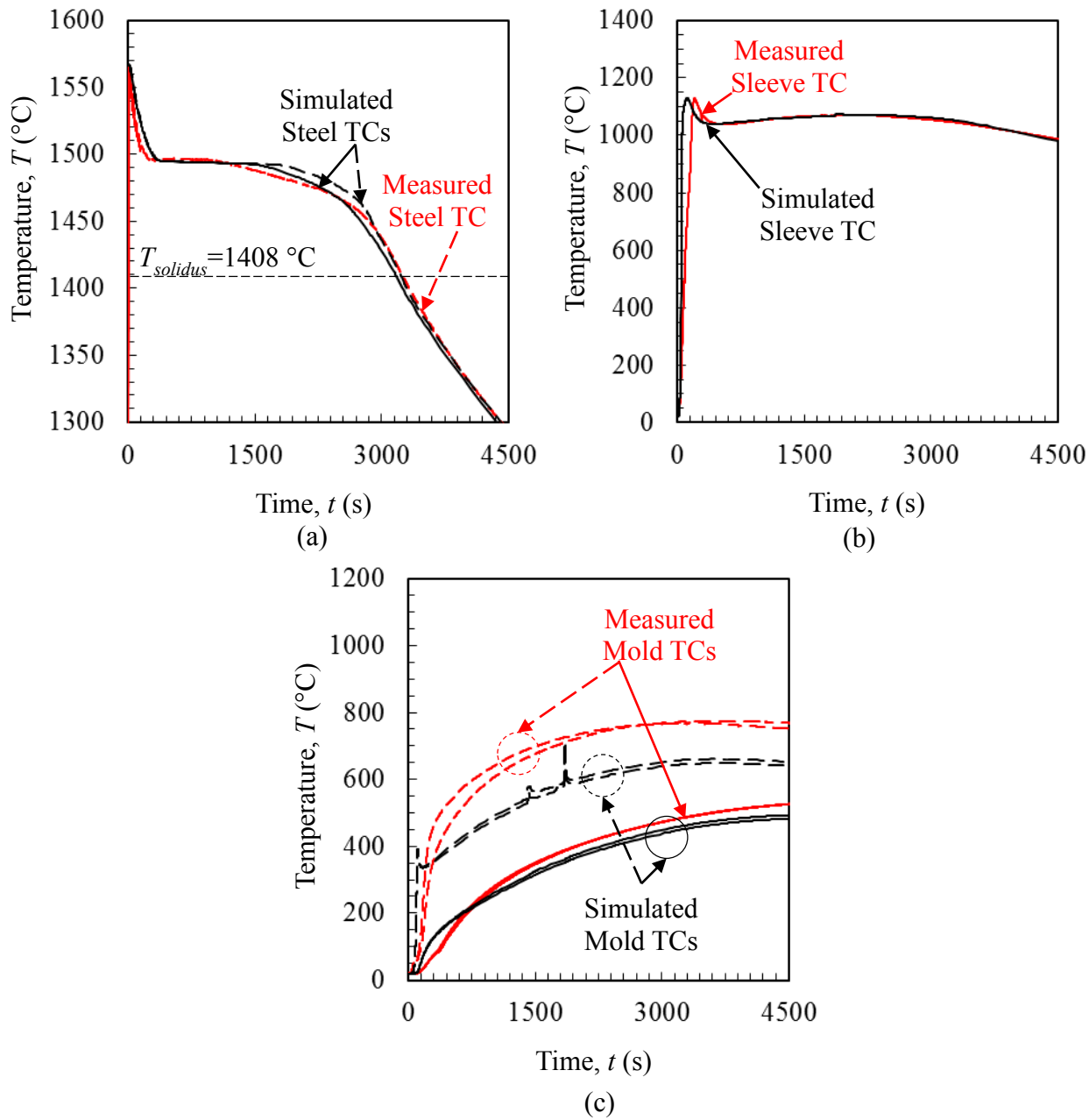


Figure 4.24. FOSECO Kalminex 21 sleeve casting measured and simulated temperatures. Thermocouples placed in (a) the steel, (b) the sleeve, and (c) the sand mold.



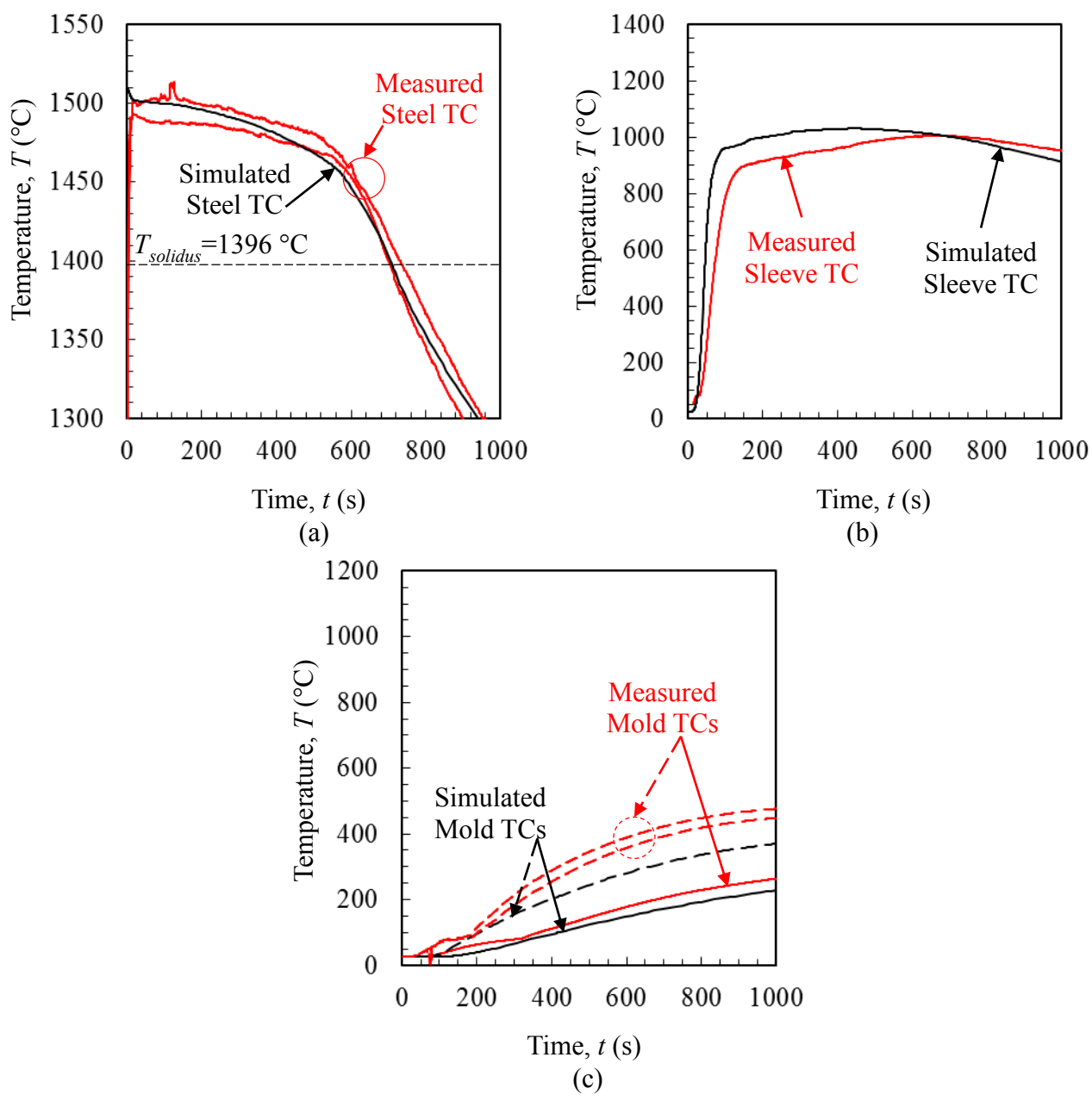


Figure 4.25. FOSECO Kalfax 100 sleeve casting measured and simulated temperatures. Thermocouples placed in (a) the steel, (b) the sleeve, and (c) the sand mold. Line types denote different nominal locations for the TC.

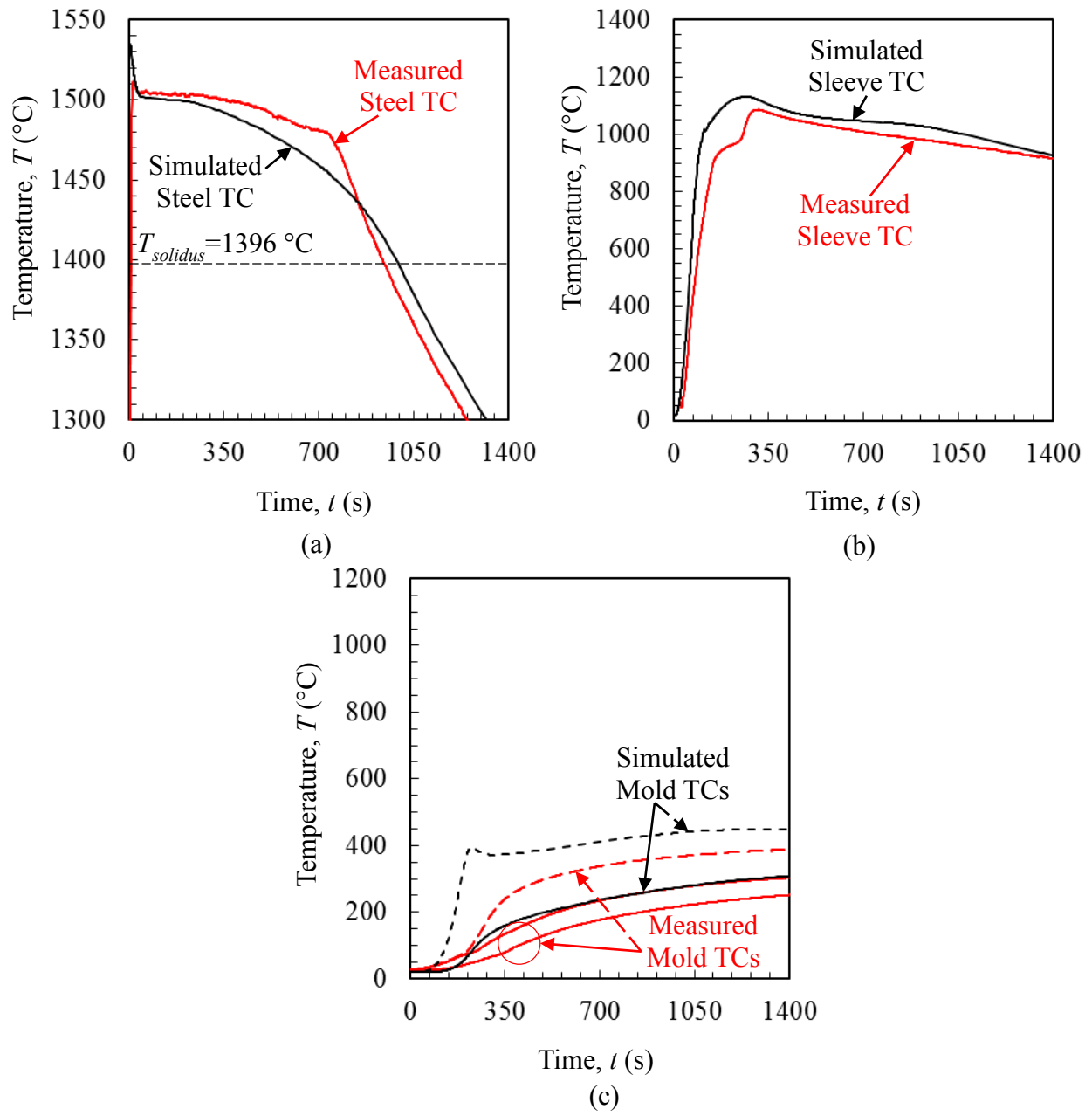


Figure 4.26. Exochem ES sleeve casting measured and simulated temperatures. Thermocouples placed in (a) the steel, (b) the sleeve, and (c) the sand mold. Line types denote different nominal locations of the TC.

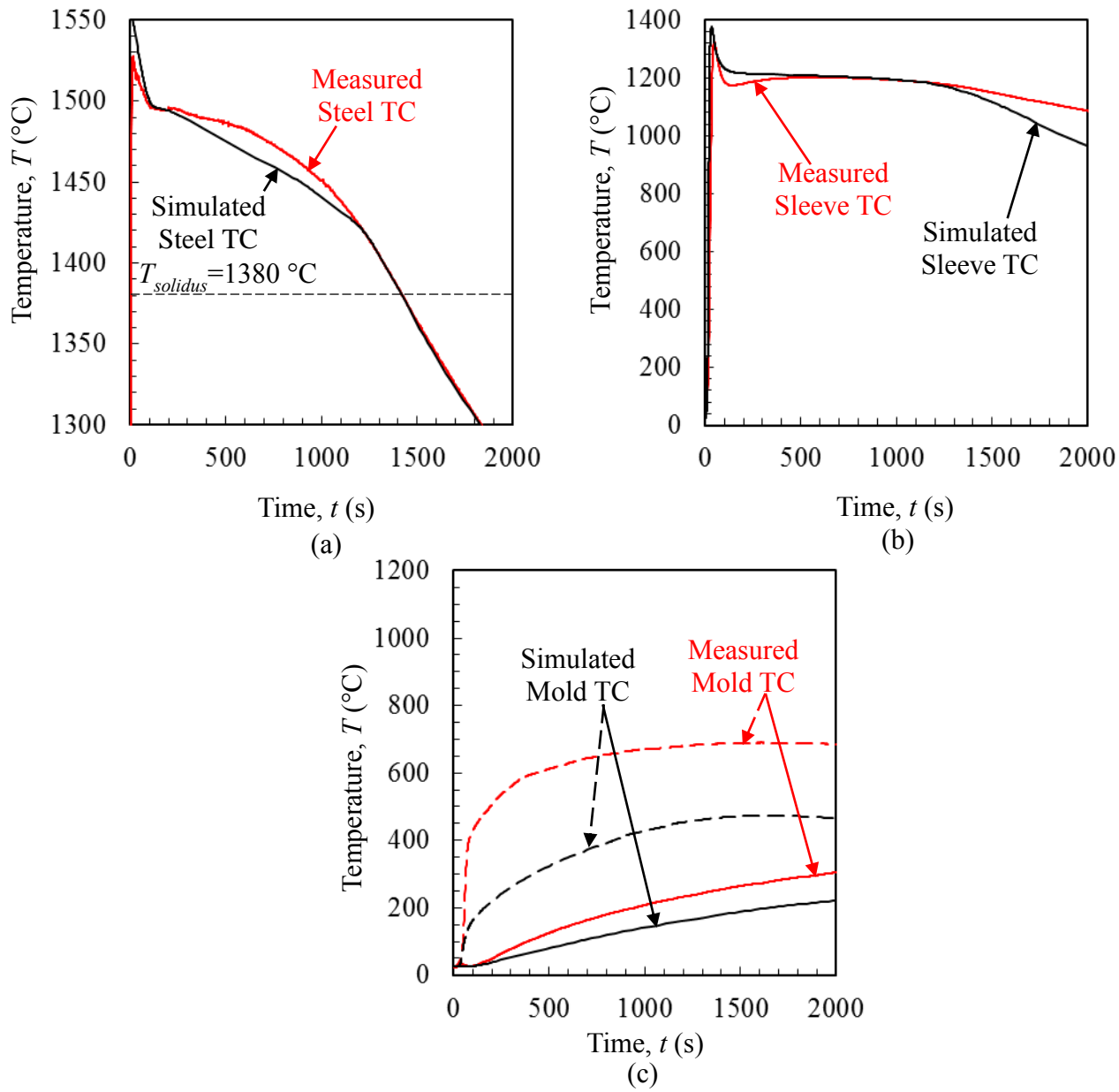


Figure 4.27. Joymark CFX 700 sleeve casting measured and simulated temperatures. Thermocouples placed in (a) the steel, (b) the sleeve, and (c) the sand mold. Line types denote different nominal locations of the TC.

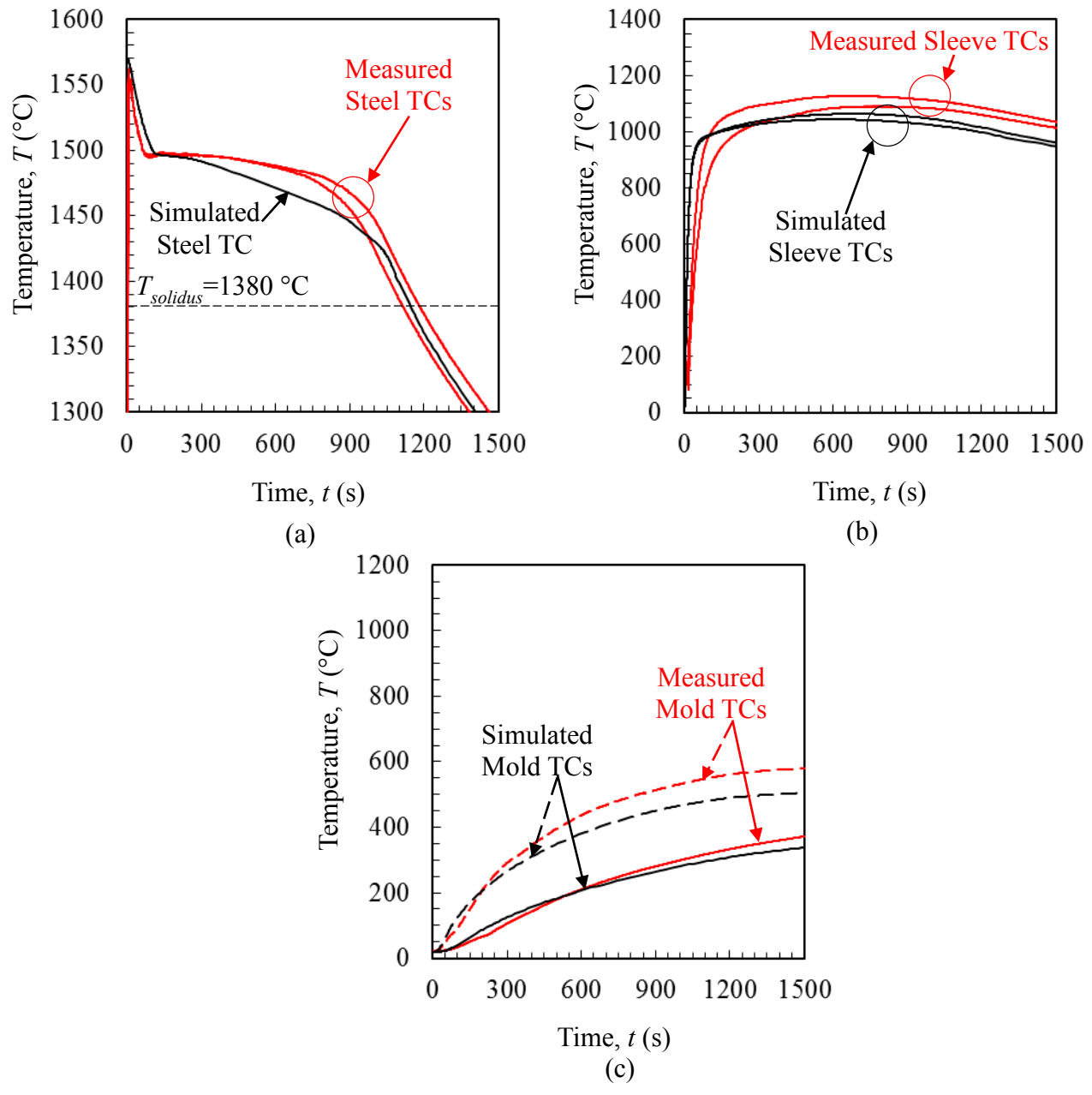


Figure 4.28. ASK Exactcast IN sleeve casting measured and simulated temperatures. Thermocouples placed in (a) the steel, (b) the sleeve, and (c) the sand mold. Line types denote different nominal positions of the TC.

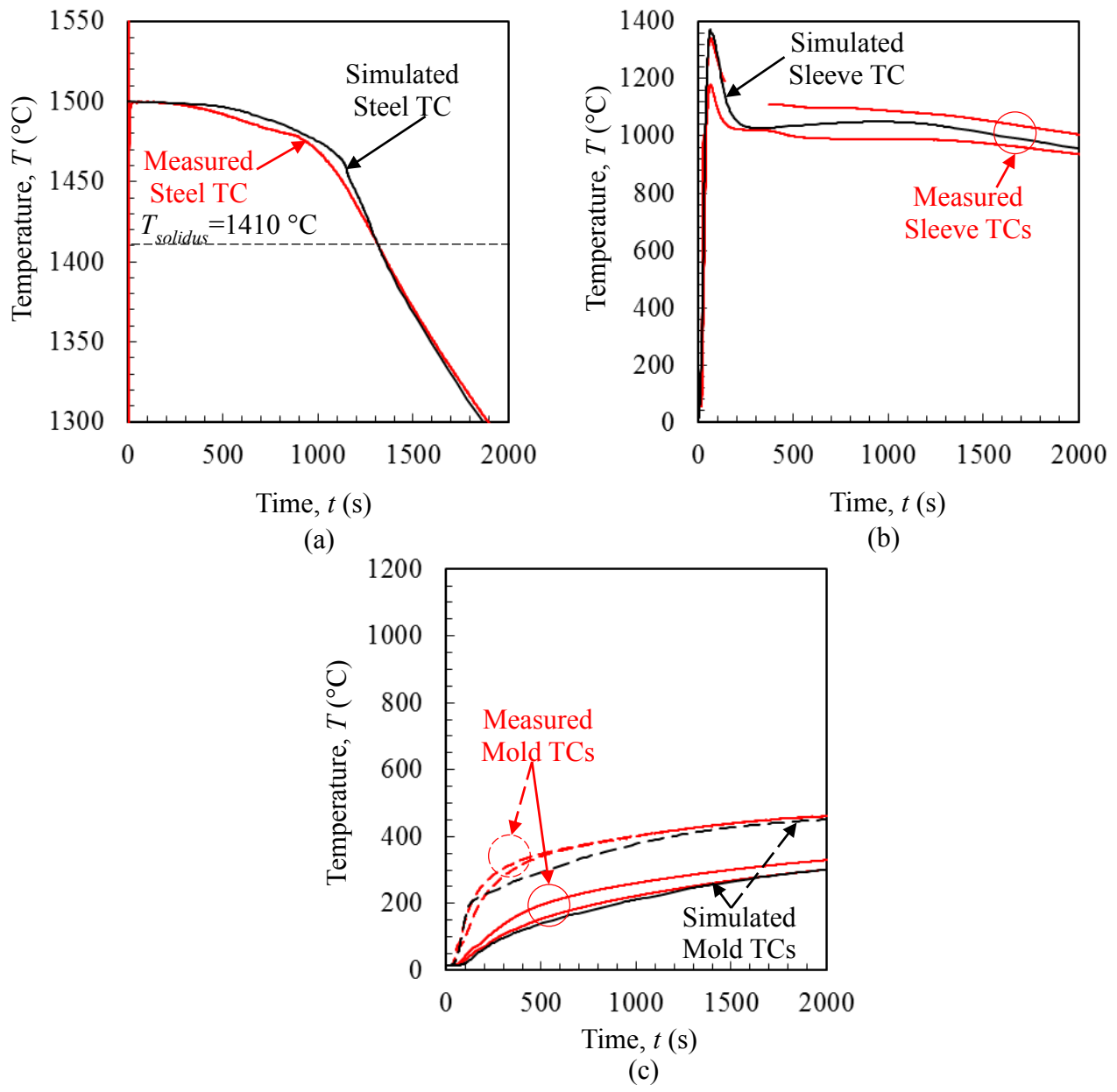


Figure 4.29. Joymark CFX 760 sleeve casting measured and simulated temperatures. Thermocouples placed in (a) the steel, (b) the sleeve, and (c) the sand mold. Line types denote different nominal locations for the TC.

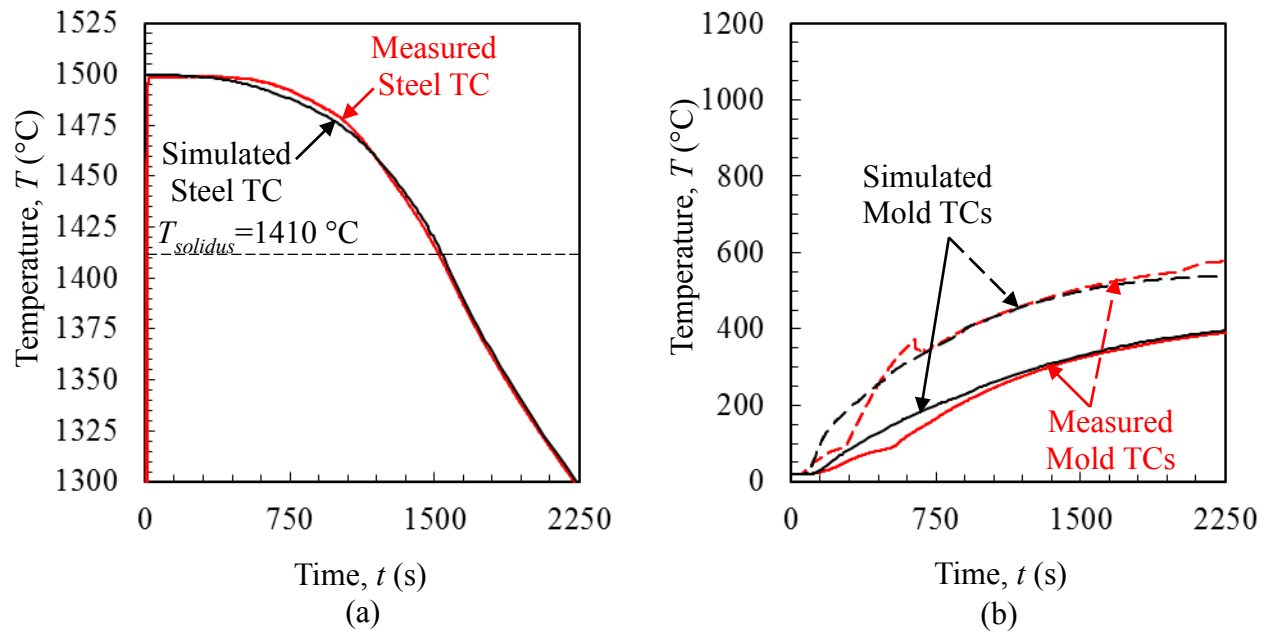


Figure 4.30. Joymark CFX 800 sleeve casting measured and simulated temperatures. Thermocouples placed in (a) the steel and (b) the sand mold. Sleeve TCs were burnt out. Line types denote different nominal positions of the TC.

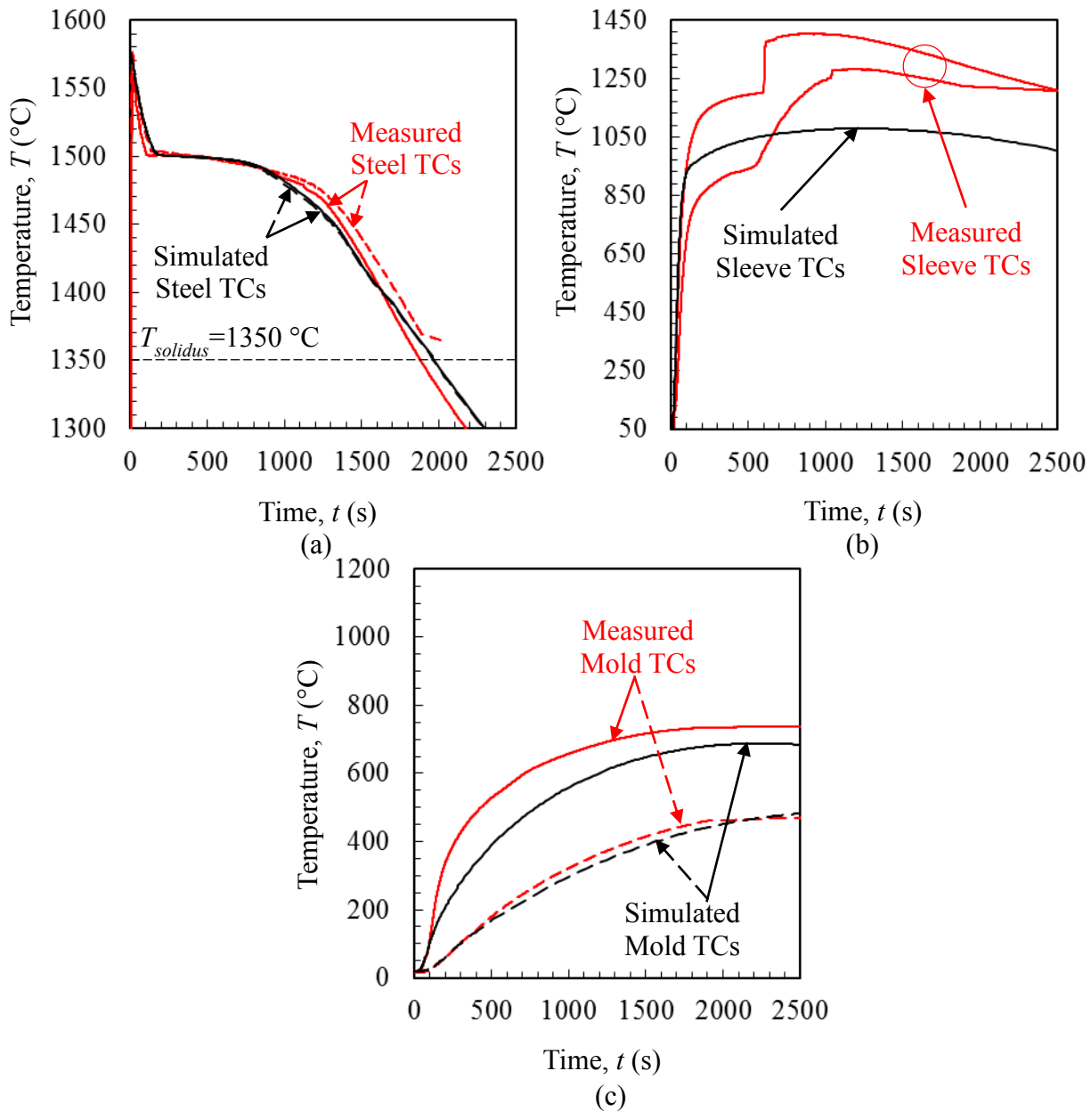


Figure 4.31. Exochem SNA sleeve casting measured and simulated temperatures. Thermocouples placed in (a) the steel, (b) the sleeve, and (c) the sand mold. Line types denote different nominal locations of the TC.

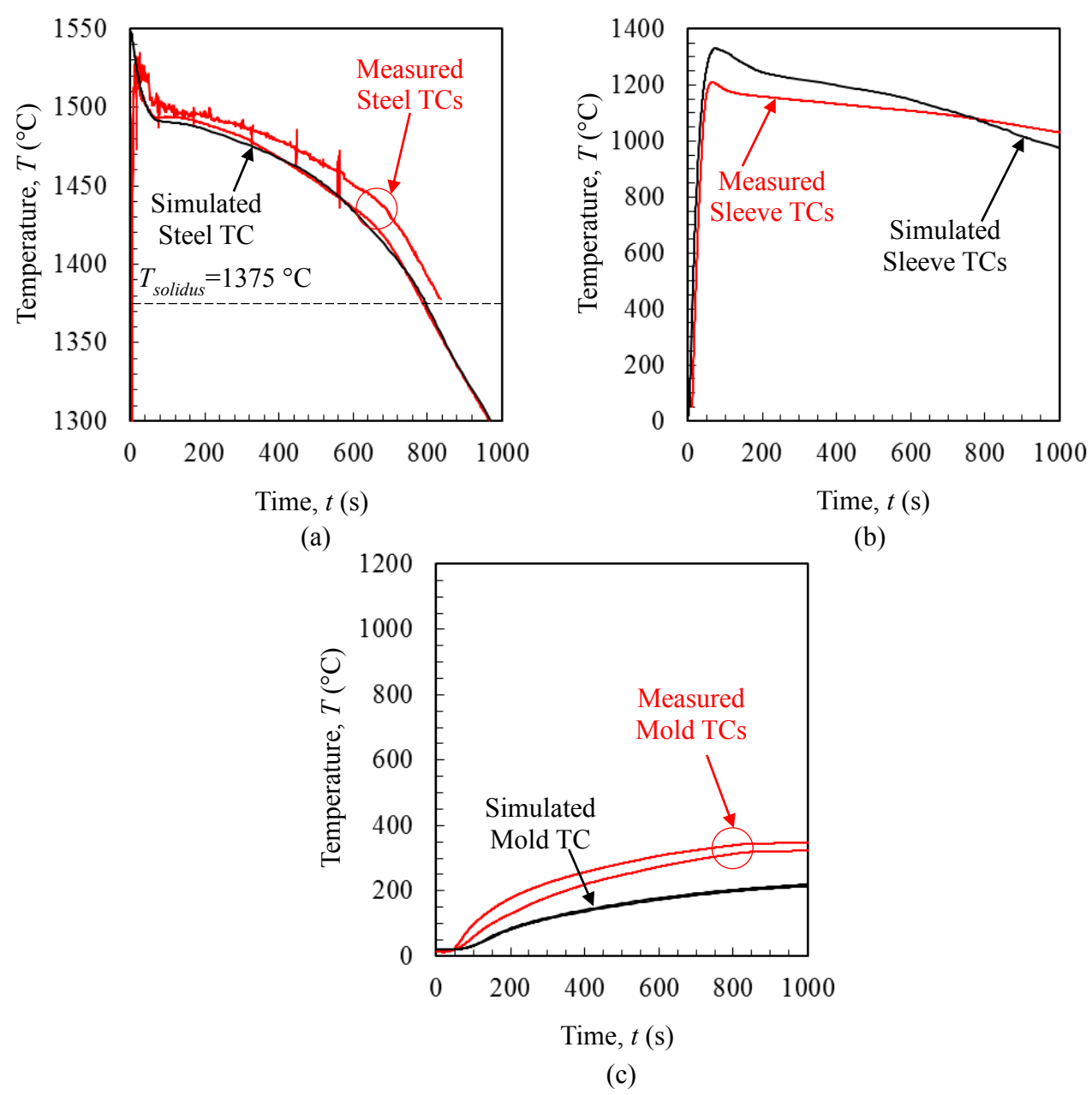


Figure 4.32. Exochem ESPX sleeve casting measured and simulated temperatures. Thermocouples placed in (a) the steel, (b) the sleeve, and (c) the sand mold.



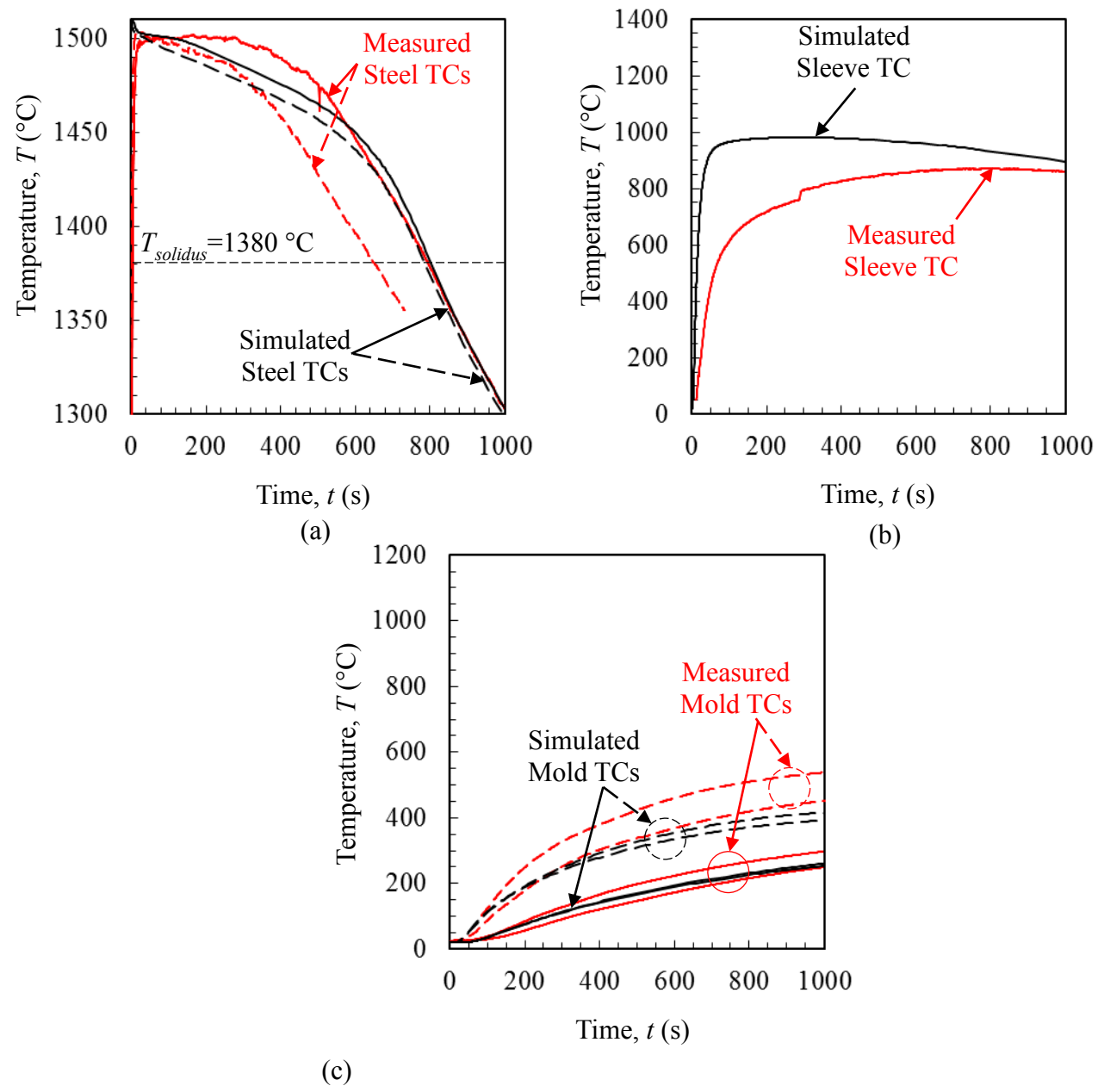


Figure 4.33. A second group of ASK Exactcast IN sleeve casting measured and simulated temperatures used to confirm sand and steel properties for the AMCOR Rosstherm K sleeve case. Thermocouples in the control casting, poured with these sleeve castings, failed. ASK Exactcast IN sleeve properties were previously developed. Thermocouples placed in (a) the steel, (b) the sleeve, and (c) the sand mold.

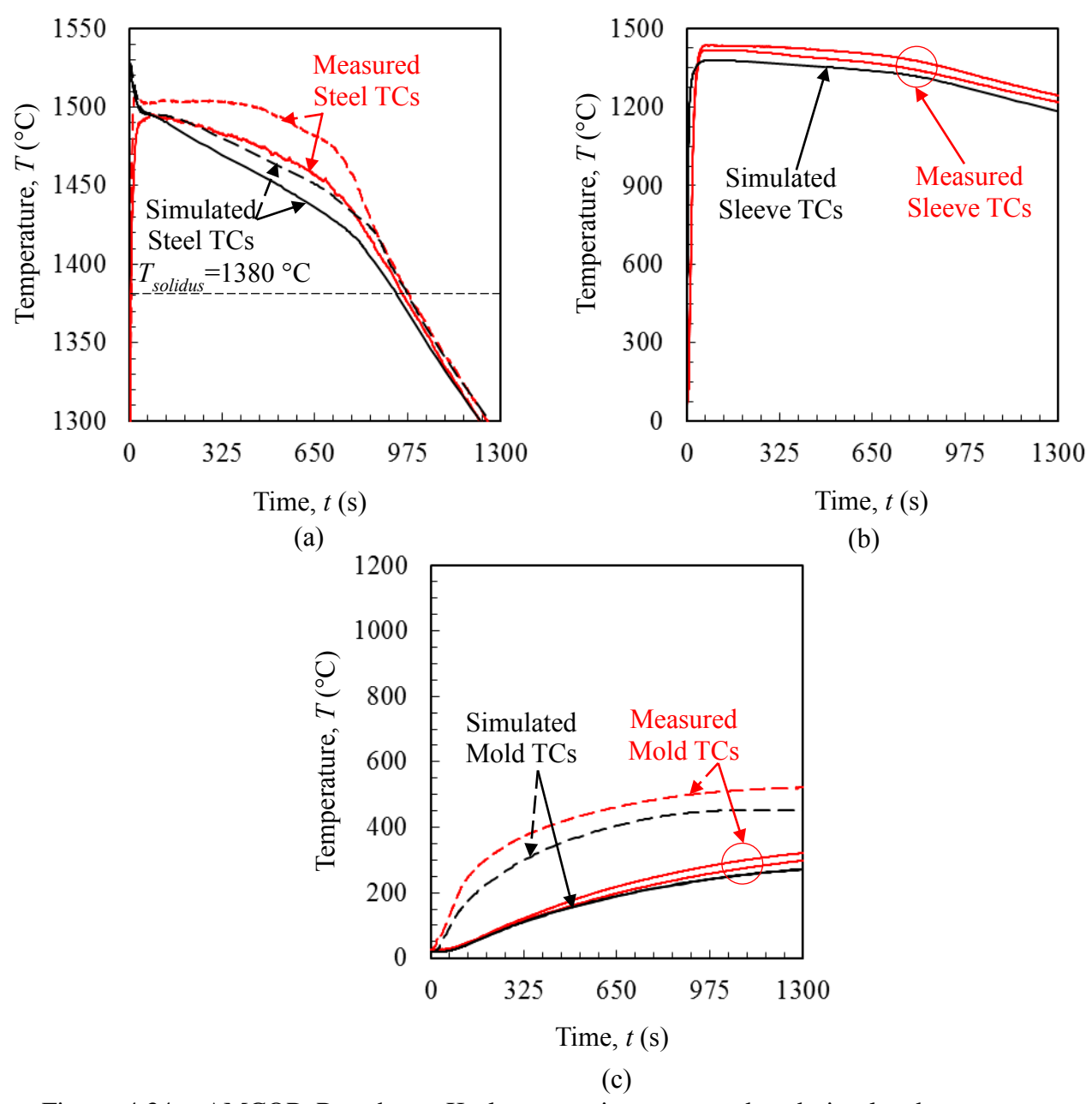


Figure 4.34. AMCOR Rosstherm K sleeve casting measured and simulated temperatures. Thermocouples placed in (a) the steel, (b) the sleeve, and (c) the sand mold. Line type denotes different nominal location of the TC.

## CHAPTER 5: ANALYSES OF RISER SLEEVE MATERIAL PERFORMANCE

### 5.1 Introduction

Analyses of riser sleeve material performance are carried out using the riser sleeve properties developed in Chapter 4. A method of determining a quantitative description of sleeve material performance called the modulus extension factor is presented. The sensitivity of the modulus extension factor to several casting parameters is determined. Subsequently the modulus extension factor is calculated for all sleeves investigated in this work. The effects of different riser sleeves on casting yield are determined for different casting shapes. Particularly, the significance of the exothermic attributes is ascertained. Finally, the influence of sleeve thickness is described, including the suggestion of an optimum riser sleeve thickness.

### 5.2 The Modulus Extension Factor

#### *5.2.1 Derivation of the Modulus Extension Factor*

Currently, riser sleeves are sold using non-specific, unquantified language or unverified size dependent quantities. In order for foundries to understand the advantages of using a particular sleeve material, a quantitative, size independent description of riser sleeves must be developed. Sleeve performance is most easily quantified by a sleeve's effect on the modulus of the riser. The modulus is a quantity used by foundries to estimate the minimum size of a riser necessary to feed a casting section based on Chvorinov's rule [15]:

$$t_s = K \left( \frac{V}{A} \right)^2 \quad (5.1)$$

where  $t_s$  is the time to solidification of a casting section, for example a riser,  $K$  is a grouping of sand mold and steel properties, and the quotient  $V/A$  is the *geometric* modulus of the riser defined by the ratio of  $V$  the volume of the riser, and  $A$  the *heat loss* surface area of the riser, i.e., the surface area that is not in contact with other sections of liquid metal. Equation 5.1, predicts the time to solidification of the riser when no riser sleeve is used. However, when a riser sleeve is used the time to solidification increases despite no change in the geometry of the riser. The increase in

solidification time is explained by saying that the riser has an *apparent modulus* larger than its geometric modulus. The apparent modulus is related to the geometric modulus as follows [10]:

$$M_A = fM_G \quad (5.2)$$

Where  $M_A$  is the apparent modulus,  $M_G$  is the geometric modulus, and  $f$  is the modulus extension factor. The value of  $f$  will vary based on the quality of the sleeve, however  $f$  is not itself a material property as it will depend on the geometry of the sleeve, particularly including the thickness. It will be shown that  $f$  is size independent. The modulus extension factor cannot be directly measured so a standard method must be employed in order to calculate it.

### 5.2.2 Determination of the Modulus Extension Factor

Currently there is no standard method for determining the modulus extension factor. According to its derivation, the modulus extension factor is calculated by dividing the apparent modulus of a sleeved riser by its geometric modulus. While the geometric modulus is readily calculated, the apparent modulus is not. The rationale of a method for determining the apparent modulus is provided by Equation 5.1 which states that castings with the same modulus have the same solidification time if steel and mold properties are assumed constant. Therefore a sleeved riser and a sand riser with the same solidification time have the same modulus. If a sleeved riser's solidification time is matched to the solidification time of a sand riser, the apparent modulus of the sleeved riser is assumed equal to the geometric modulus of that sand riser. Therefore, the apparent modulus and  $f$  are calculated by determining such a sand riser. Motivated by this reasoning, Foseco published a non-specific method for finding the apparent modulus [10]. This method utilizes a sleeved riser set atop a casting, several sand risers set atop identical castings, and thermocouples to measure the solidification time. These are used to match the solidification time of a sleeved and sand riser as explained above. Here a more specific standard method is proposed.

The proposed method for determining the modulus extension factor requires that a casting with a sleeved riser and several castings with sand risers be created. Both types of castings are 8" cubes with 4" of sand measured outwards from each face of the cube excluding the top face. A

thermocouple is placed at the center of the riser/casting junction, and the top of the riser is open. For simulations in *MAGMASoft*, the riser is declared as a feeder and the default external boundary condition is used. Sleeved risers are 6" tall with a 6" diameter and sleeves have 0.5" thickness. Sand risers have variable size but the aspect ratio is always 1. A schematic of this setup is shown in Figure 5.1. The sand is PUNB silica sand and the steel is a WCB alloy with 30 °C superheat. The solidification time of the risers is taken as the time to solidus temperature as measured by the thermocouple at the riser/casting junction. The location of final solidification of the riser can be difficult to pinpoint in a casting experiment so this static location is used instead. In simulations riser diameters for the larger sand riser are varied in 0.25" increments, while keeping the aspect ratio at 1. In real casting experiments, larger increments will likely need to be employed. Riser diameters of consecutive increments with times to solidus which bracket the sleeved riser solidification time are used to interpolate the proper sand riser size. This riser's geometric modulus is calculated and adopted as the apparent modulus of the sleeved riser. Finally, the modulus extension factor is calculated by dividing the apparent modulus by the geometric modulus of the sleeved riser. An important aspect of this method is that it can be accomplished through both simulations and experiments. For experiments, care must be taken in order to ensure steel and sand properties are consistent between castings.

### 5.2.3 Analysis of the Modulus Extension Factor

Using the method outlined above, the sensitivity of the modulus extension factor to various experimental parameters is determined. The  $f$  value for the AMCOR Rosstherm K sleeve is shown in Figure 5.2 as determined by the method established in section 5.3 and also for several modifications to this method. These modifications represent industrial parameters which vary widely within the industry including superheat, casting size, and the alloy poured. Pouring temperature, and therefore the superheat of the liquid metal, can be very difficult to control in a foundry. In the method established in section 5.3, a 30 °C superheat is used. Repeating the procedure but substituting a 150 °C superheat causes the value of  $f$  to drop from 1.26 to 1.21

indicating that  $f$  is sensitive to superheat. Foundries pour casting sections which range in thickness from a few inches to several feet. In order to establish the size dependency of  $f$ , the dimensions of the castings used to determine  $f$  are doubled so that the cube has 16" sides, the sleeved riser is 12" high by 12" diameter, there are 8" of sand measured out from the faces of the cube, and the riser sleeve thickness is increased to 1". It is important to note that sleeve thickness is scaled along with the casting as sleeve thickness strongly affects sleeve performance. The effects of sleeve thickness are discussed in depth later in this work. Increasing the casting size resulted in no change of the  $f$  value, confirming that  $f$  is size independent. Foundries pour a wide variety of steel alloys. To investigate the sensitivity of  $f$  to steel alloy, a CN3MN stainless steel alloy is substituted for the WCB alloy. CN3MN has a much lower liquidus temperature however the superheat, 30 °C, was kept the same. The change in alloy caused an increase in  $f$  from 1.26 to 1.28 which indicates a slight sensitivity. All sleeves should be affected similarly so the use of  $f$  as a comparative description of sleeve material performance is valid regardless of the exact parameters used. However, if a foundry engineer wishes to use these factors to estimate sleeve performance on a specific casting, these sensitivities should be kept in mind.

With sensitivities to casting parameters established,  $f$  is calculated for all 13 sleeves in this project using a constant 0.5" thickness and plotted in Figure 5.3. The factors calculated for these sleeves range from 1.28 to 1.07 indicating that performance is quite variable between different products. Additionally there is no consistent trend to establish whether exothermic or insulating sleeves are better with some exothermic sleeves having higher  $f$  values than insulating sleeves while other exothermic sleeves have lower values. Instead, these results imply that sleeve performance only depends on the overall quality of the material. This suggests that the mechanism, whether insulating, exothermic, or some combination thereof, by which the material quality is improved is unimportant. This finding will be further investigated in the next section. The  $f$  values calculated here can be applied to traditional modulus calculations to estimate the size of the riser needed to feed a casting section. Note that these values correspond to a 0.5" thick sleeve on a 6" x 6" riser and do not necessarily reflect commercially available products. It is recommended to

double check any modulus estimates by using simulation and the thermophysical properties developed in Chapter 4. These  $f$  values provide a simple guide to compare the performance of several popular sleeve products. However these values do not provide an idea of how sleeves improve the efficiency of the casting process. Additionally, these factors do not account for differences in sleeve thickness, which are highly variable among commercial products.

### 5.3 The Effects of Riser Sleeves on Casting Yield

Risers are cavities of extra metal which are removed before the final castings are shipped. In order to minimize this scrap, foundries wish to minimize the riser size. Efficiency in this endeavor is measured by the casting yield which is the ratio of the volume of the cast part to the total volume of metal poured. Typically foundries operate with yields around 50% for their castings. Employing the thermophysical properties developed in Chapter 4 in conjunction with simulation software should increase the operating yield for foundries. However it is important to establish how different sleeves affect the achievable casting yield.

In order to investigate the effect of sleeves on casting yield, the maximum achievable casting yield will be determined for two types of casting simulation geometries. These geometries are shown in Figure 5.4. The first geometry is a cube which is a simple approximation of a chunky casting which has high feeding demand on the riser. Cubes of side length ( $c_s$ ) 3, 6, 9, 12, 18, and 24 inches are simulated in this study. The second geometry is a square plate with thickness  $t_{plate}$  and aspect ratio 15. This geometry is extremely rangy and has a low feeding demand. Plate volumes are equivalent to those of the simulated cubes. This results in a range of plate thicknesses from about 0.5 to 4 inches. The maximum achievable yield for these castings is determined by minimizing the riser size. As a result the riser size is highly variable and unrealistically small increments between sizes are used. Therefore a continuous approximation for the sleeve thickness as a function of the riser diameter is required. This approximation, denoted by the red line in Figure 5.5, is a linear fit of product data provided by sleeve manufacturers which is marked by the black crosses. The approximation is defined by  $t_{sleeve} = 0.08D + 0.126$  and indicates that

commercially available sleeves have a minimum thickness of about 0.125” and increase in thickness with 8% of the riser diameter. This approximation constrains the sleeve thickness leaving the riser size as the only variable in finding the maximum achievable yield. The minimum riser size is determined by setting a 10% minimum margin of safety, based on the riser height, between the top of the casting and the bottom of the riser pipe. Because this investigation is performed using simulation software, a 0.7% porosity cutoff is used to define the edges of the riser pipe. For simplicity, risers have an aspect ratio of 1. For consistency, simulation properties for a WCB alloy are used with a superheat of 30°C and a feeding effectivity of 70%. Feeding effectivity is an important parameter used by the simulation software to predict porosity. Minimization of the riser size is illustrated in Figure 5.6 using plots of porosity at the mid-plane of the casting. In Figure 5.6 the casting on the left has a riser pipe which violates the 10% minimum safety margin requirement. The diameter and height of this riser are increased by 0.1 inches resulting in the casting on the right which has a 12% safety margin. Smaller increments in riser size are insignificant so the riser size on the right is taken as the minimum riser size. This minimization process is carried out for 3 riser sleeve materials: FOSECO Kalminex 2000 and Kalmin 70 and Joymark CFX 760. The FOSECO sleeve materials have approximately the same  $f$  value ( $f \sim 1.2$ ) however the Kalminex 2000 is exothermic while the Kalmin 70 is insulating. The CFX 760 sleeve material has a significantly higher  $f$  value ( $f = 1.27$ ) and also a high exothermic output.

The results of this casting yield investigation are shown in Figure 5.7. Immediately noticeable is that the rangy plate castings have a much higher yield than chunky castings of the same volume. While including sleeves produces large increases in yield for chunky castings, rangy castings gain less than 10% yield. This indicates that sleeves may not be economical for very rangy castings from a casting yield perspective. Also noticeable is that the achievable casting yield for the FOSECO sleeve materials are entirely overlapped. Some foundries believe that exothermic sleeves are generally better than insulating sleeves at small riser sizes while others believe exothermic sleeves are better at larger riser sizes [1]. Because the FOSECO sleeve materials have a similar  $f$  value, one would expect a significant difference in achievable casting yield between the



insulating and exothermic sleeve materials if the exothermic effect had a special impact at a given casting size. Since this is not the case it is fair to conclude that whether a sleeve is exothermic or insulating is insufficiently descriptive of its performance compared to other sleeves at any casting size studied here. Rather the overall quality of the sleeve material, described by  $f$ , will determine its performance. This is supported by the results for the CFX 760 sleeve material which behaves similarly to the FOSECO sleeve materials, in that there is no abrupt increase or decrease in yield at smaller or larger sizes, but has an additional 5% yield. The coincidence of maximum yields for all three sleeves at small casting size is explained by sleeve thickness effects as they relate to the approximation used here.

In order to determine the impact of sleeve thickness on casting yield, the same procedure is employed using the cube and square plates of varying sizes. However rather than using a continuously varying sleeve thickness, the riser size is minimized for a set sleeve thickness. Simulations are performed for cubes of side length 3, 6, 12, and 24 inches and their volume equivalent square plates. Riser sleeve properties for the FOESCO Kalminex 2000 are used. These properties approximate a typical or average ( $f \sim 1.2$ ) riser sleeve.

The results of these simulations are shown in Figure 5.8. The results are presented as the absolute increase in yield for a sleeved riser casting over the same casting without sleeve for varying sleeve thickness. In the plot, the sleeve thickness is scaled by the riser diameter ( $t_{sleeve}/D$ ) because increasing the riser diameter should require a corresponding increase in sleeve thickness in order to maintain a given level of sleeve performance. This idea is validated as the results in Figure 5.8 collapse to well-defined curves for the chunky and rangy castings despite the highly variable casting sizes. The results in Figure 5.8 reinforce that riser sleeve induced increases in yield for rangy plates are minimal and that the use of riser sleeves for increasing the yield of rangy castings is likely unnecessary. Of course, there may be other reasons a foundry would wish to use a riser sleeve for a rangy casting. If a riser sleeve is used for a rangy casting, the scaled sleeve thickness does not need to be more than 0.1 for an average sleeve. For chunky castings such as cubes however, riser sleeves create large increases in yield, up to 40%. Figure 5.8 suggests that

an optimal sleeve thickness for chunky castings would be about 0.2 times the riser diameter. This coincides with the statement from Foseco that a sleeve thickness of 0.2 times the riser diameter is approximately infinite [10]. Additionally, decreasing the scaled thickness below 0.1 results in rapidly declining performance from a casting yield standpoint and should therefore be avoided. Note that for a sleeve of different quality, the optimum thickness may increase or decrease. The maximum achievable yield may also increase or decrease however Figure 5.7 suggests there may not be a large variation as the CFX 760 sleeve does not have a significantly different maximum yield, compared to the FOSECO sleeves, at small casting size where all three have optimum thickness.

Using the information in Figure 5.8, the plot of commercially available sleeve thickness from Figure 5.5 is transformed and approximate yield increases for chunky castings are given in Figure 5.9. The transformed plot shows that most commercially available riser sleeves, indicated by the black crosses, should give at least 25% increases in yield. Doubling the riser sleeve thickness at larger diameters could result in an additional 10% yield but whether the increased yield would offset the assumed increase in riser sleeve cost is unknown. Figure 5.8 suggests that sleeves for chunky castings not have a scaled thickness less than 0.1 however Figure 5.9 shows that most sleeves fall below this thickness at diameters greater than 6". The approximation of commercially available sleeve thicknesses (red line) shows that sleeve thickness is near optimum at very small riser diameters but quickly drops to sub-optimal levels ( $t_{sleeve}/D < 0.1$ ). This explains the coincidence of maximum achievable yields found in Figure 5.7 (a). All the sleeve materials have similar maximum yields at small casting sizes where the riser diameter is small enough to have optimum sleeve thickness. As casting size increases, the sleeve thickness prescribed by the approximation decreases from a scaled value near the optimum 0.2 at diameter 1" to a scaled value near 0.08 at diameters greater than 6". As the scaled thickness decreases below the optimum thickness, the differences in  $f$  values between the sleeve materials in Figure 5.7 (a) become apparent.

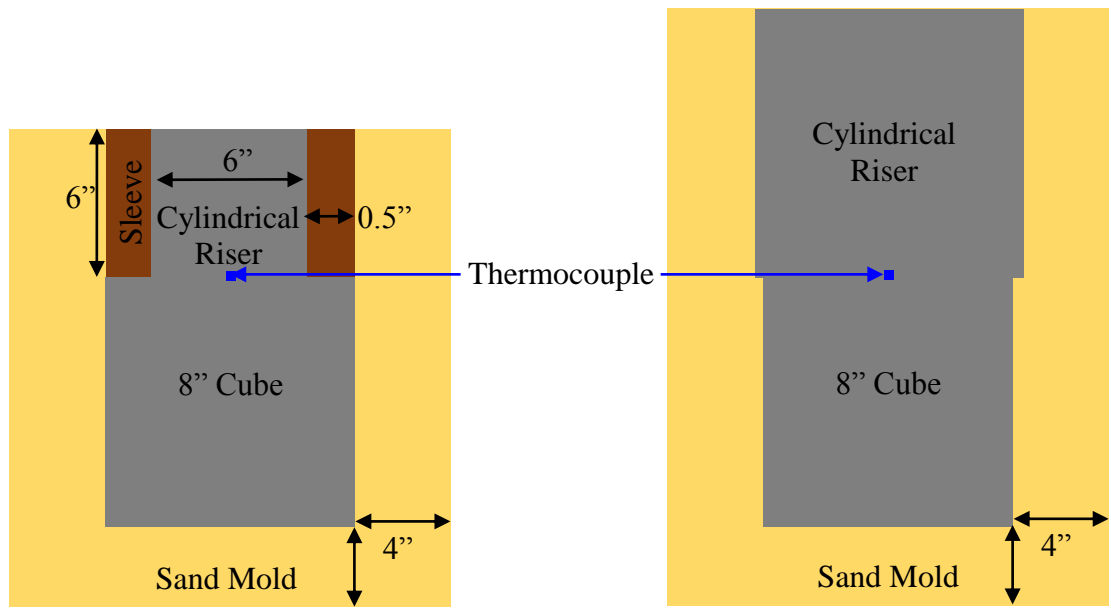


Figure 5.1. Simulation geometry used to determine the apparent modulus and modulus extension factor for a given riser sleeve. The riser without sleeve has a variable diameter. Riser aspect ratio is always 1.

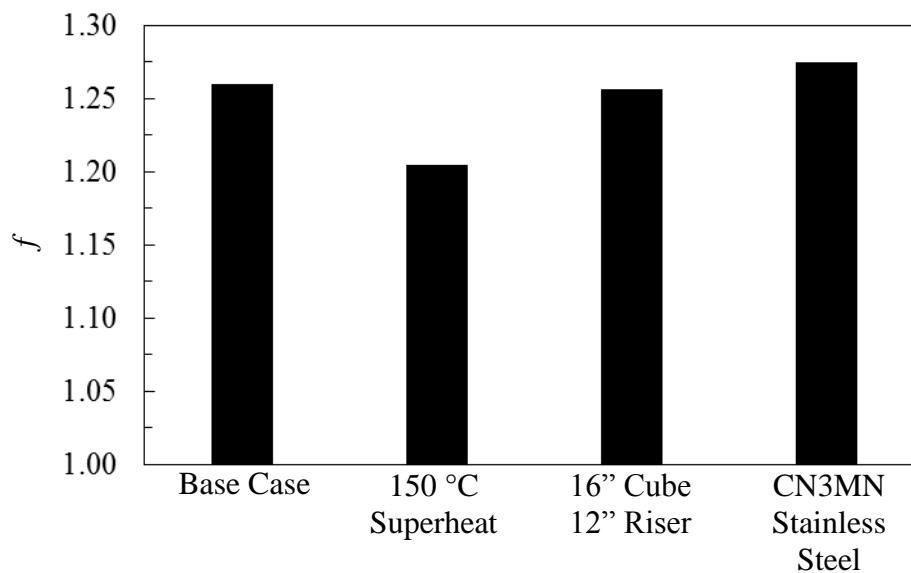


Figure 5.2. Sensitivity of the modulus extension factor  $f$  to three casting parameters; superheat, casting size and alloy. Base case is an 8'' cube casting with 6'' riser, 0.5'' sleeve, and WCB alloy steel with 30 °C superheat.

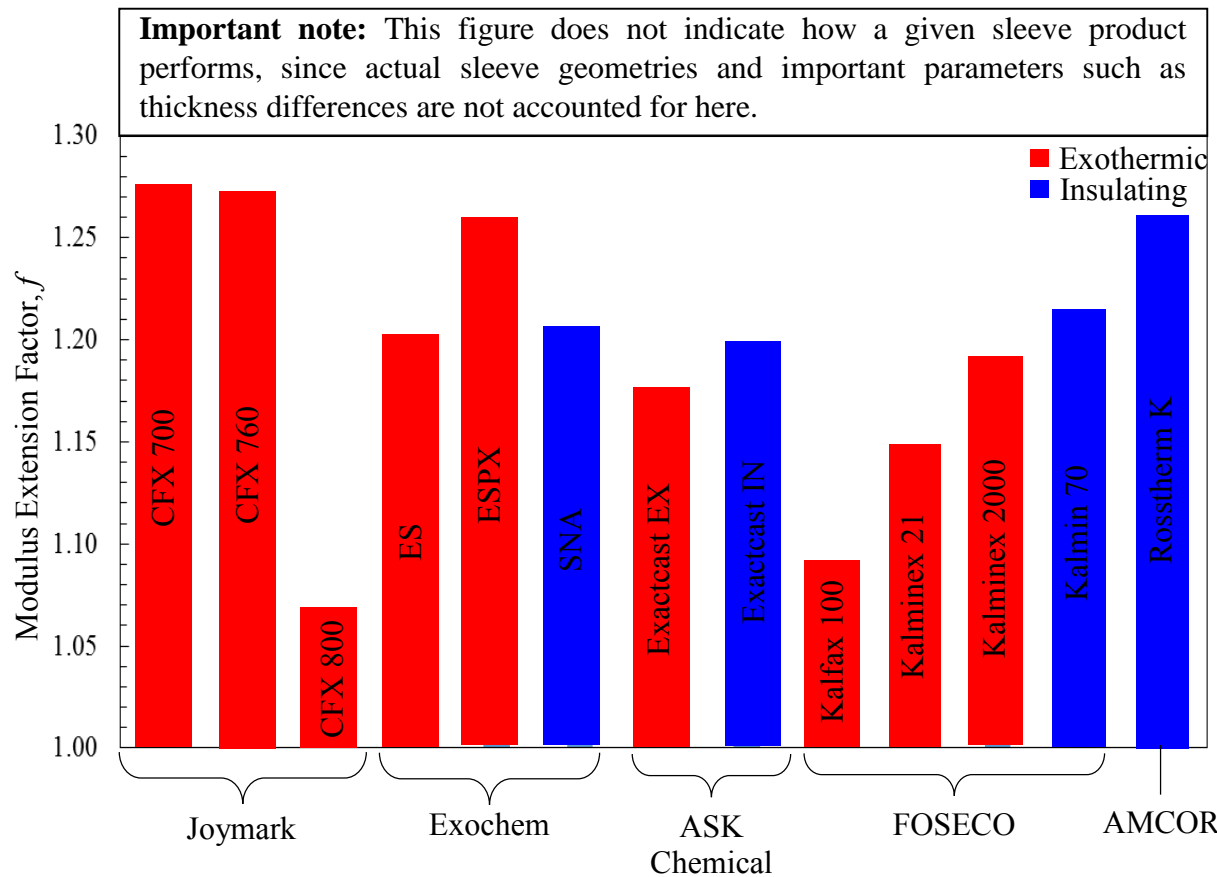
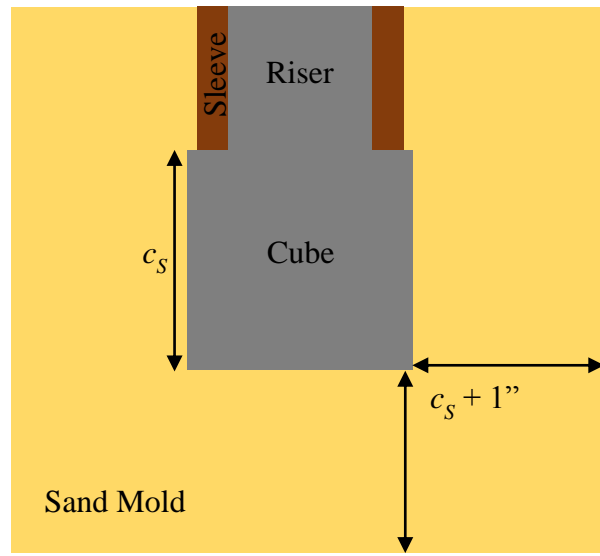
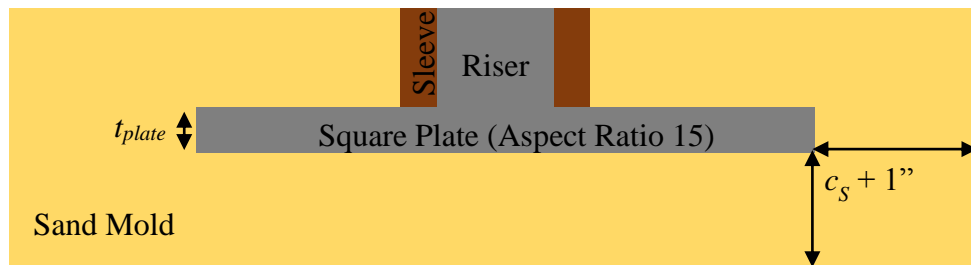


Figure 5.3. Modulus extension factors for the 13 sleeve materials investigated. Factors were determined via simulation for identical 0.5” thick sleeves insulating a 6” diameter x 6” tall cylindrical top riser on an 8” cube casting.



(a)



(b)

Figure 5.4. General schematics of the simulation geometries used to study achievable casting yield. (a) Schematic geometry for a cube of side length  $c_s$ . Side lengths of 3, 6, 9, 12, 18, and 24 inches were used. (b) Schematic geometry for a square plate of thickness  $t_{plate}$  and aspect ratio 15. The six plate castings studied have volumes equivalent to the six cube volumes.

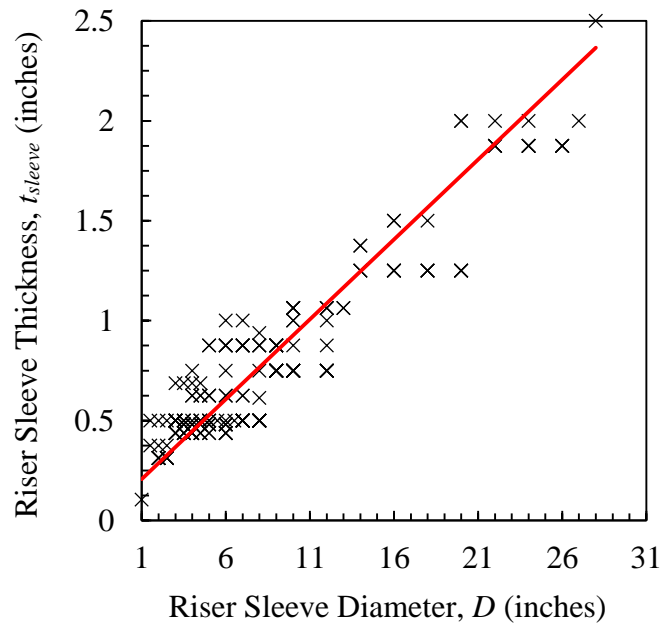


Figure 5.5. Plot of riser sleeve dimensions as listed in manufacturer's product data. The red line is a linear approximation of the data. The fit indicates that the riser sleeve thickness in inches,  $t_{sleeve}$ , increases with the riser sleeve inner diameter in inches,  $D$ , according to the equation  $t_{sleeve} = 0.08D + 0.126$ .

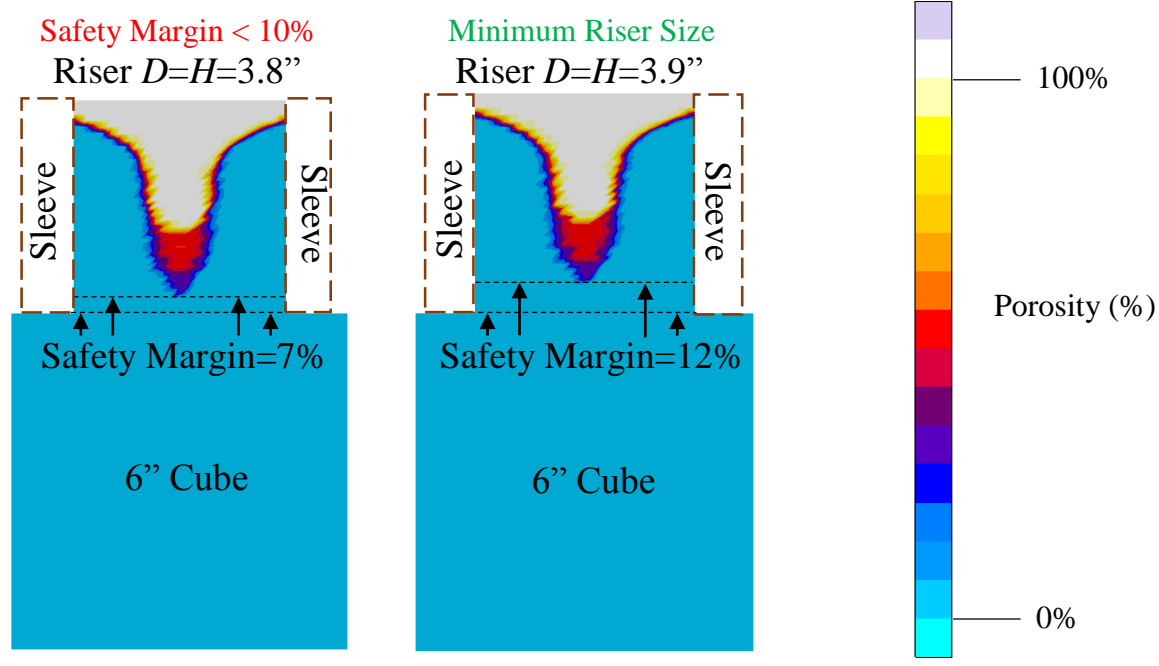


Figure 5.6. Examples of simulated shrinkage porosity used to determine maximum achievable casting yield. A 0.7% porosity threshold was used to determine the extent of the riser pipe. The minimum margin of safety goal was 10% of the riser height.



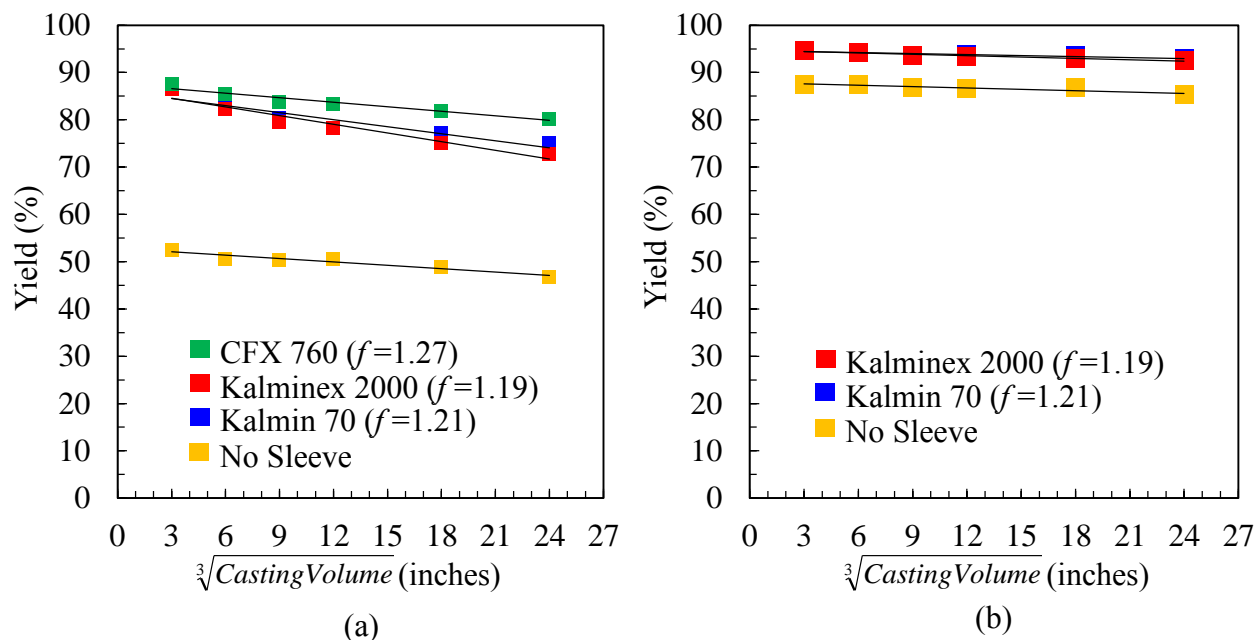


Figure 5.7. Maximum achievable casting yield for (a) cube castings and (b) square plate castings without sleeve, castings with insulating riser sleeves, and castings with exothermic sleeves. Insulating and exothermic sleeves behave similarly at all sizes.  $f$  values are those from Figure 5.3.

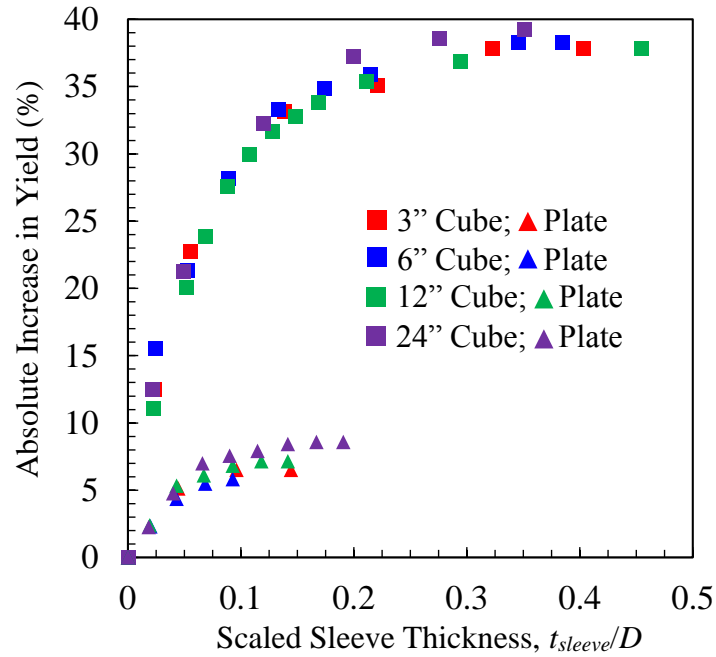


Figure 5.8. Absolute increase in maximum achievable casting yield for the exothermic riser sleeved casting over the casting with no sleeve case versus the scaled sleeve thickness ( $t_{sleeve}/D$ ) used. Results are shown for cube castings (squares) and square plate castings (triangles) with an aspect ratio 15 having volumes equal to those of the cube castings.

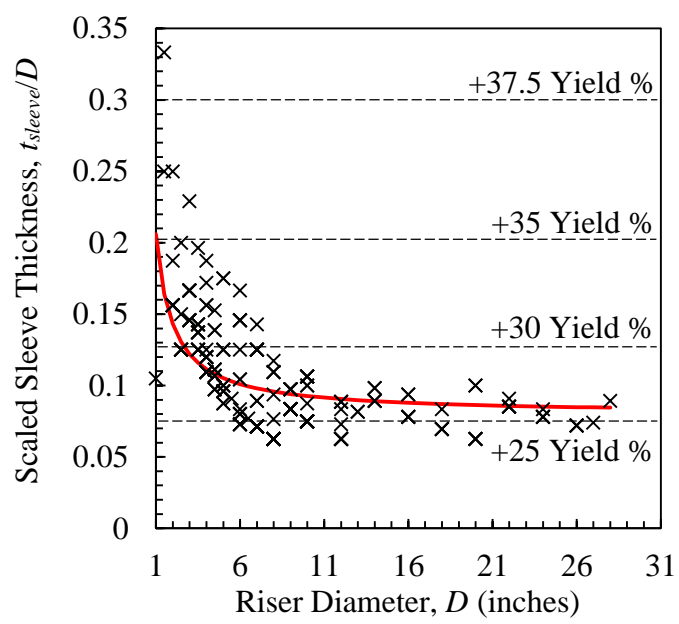


Figure 5.9. Scaled sleeve thickness of commercially available riser sleeves as determined from manufacturer product information and approximate predicted increases in casting yield for high moduli castings. Predicted increases in yield correspond to the absolute increase in yield over chunky castings with no sleeve. The red curve is the approximation of commercially available sleeve thicknesses derived from Figure 5.5

## CHAPTER 7: CONCLUSIONS AND RECOMMENDATIONS FOR FUTURE STUDIES

### 7.1 Conclusions

Effective thermophysical properties have been developed for thirteen popular riser sleeve materials by implementing an inverse modeling technique. An experimental design was devised to isolate the effects of a riser sleeve and casting experiments were performed to collect temperature data. Simulations of the casting experiments were created and riser sleeve thermophysical properties were iteratively modified until satisfactory agreement between the measured and simulated data was achieved. The finalized riser sleeve thermophysical properties have been made available for use in casting simulation. During the process of development, the thermal conductivity was identified as the most influential thermophysical property for riser sleeves.

The modulus extension factor (MEF) was identified as a quantity which succinctly describes the performance of a given riser sleeve and was also found to be independent of riser size. The MEF was calculated for all thirteen sleeves and found to range from 1.07 to 1.27 for a sleeve of 0.5" thickness surrounding a 6" diameter riser with 6" height.

Analyses of sleeve effects on casting yield were performed in order to optimize sleeve application. The application of riser sleeves to cylindrical risers feeding rangy castings was found to provide only an 8% gain in yield compared to using a riser without sleeve. Chunky castings were found to have up to a 40% gain in yield however. It was demonstrated that the exothermic effect has no independent benefit at different casting sizes and only a sleeve material's overall quality, which is described by its MEF, matters.

The achievable casting yield was found to be highly dependent on riser sleeve thickness. Investigation of sleeve thickness effects determined that the optimum thickness for a typical riser sleeve for a rangy casting is 0.1 times the riser diameter and 0.2 times the riser diameter for chunky castings. Sleeve thicknesses of less than 0.1 were shown to be undesirable from a casting yield

perspective. Yield gains for a given sleeve thickness were estimated using the properties for a typical riser sleeve. Manufacturer data for riser sleeve thickness was collected and presented. It was shown that most commercially available sleeves have sub-optimum thickness for achieving maximum casting yields.

## 7.2 Recommendations for Future Studies

During the course of this work several topics in need of additional investigation, but outside the scope of this work, became apparent. The sleeve properties developed here are effective properties designed to model interactions between the sleeve and a metal with a liquidus temperature around 1500 °C and a 100 °C freezing range. The properties should effectively model things such as the evolution of hot gas during binder burn off. Investigating the accuracy of these properties in simulating alloys with much lower liquidus temperatures, for example less than 1000 °C, and a different freezing range may reveal that different interactions need to be modeled in those alloys.

The importance of the exothermic effect may also be different in lower temperature alloys. Sleeves with heat releases of 850 kJ/kg only provided a small extension of the solidification time of the riser for steels. However a low temperature alloy such as an aluminum alloy, with liquidus temperature around 650 °C, an exothermic riser sleeve with 850 kJ/kg heat release may be able to reheat the metal, significantly lengthening the solidification time compared to an insulating material.

The riser sleeves studied in this work contained a maximum of 21% exothermic content. Private communications with foundries have discussed some very expensive riser sleeves said to have over 30% exothermic content. Developing properties and analyzing casting yield gains for this sleeve would be informative to see if higher amounts of exothermic material are sufficient for the exothermic effect to distinguish itself at a given casting size.

In the steel casting industry the use of hot topping on risers is common, however no hot topping was used in this work in order to isolate the effects of the sleeve. Determining the MEF

for different hot toppings and the MEF for combinations of riser sleeve and hot topping would prove highly useful to the casting industry. This may also warrant use of the apparent surface alteration factor (ASAF) as it is supposed to account for this combination.

A practical analysis would be to balance the predicted gains in casting yield in Figure 5.9 with the predicted cost increase of making a sleeve thicker. With this information cost balanced optimum thicknesses could be prescribed. This work would likely have to be carried out by an interested party with access to cost information as there is great upside for process efficiency but little additional scientific insight to gain.

## REFERENCES

1. Blair, M., "Riser Sleeves-Insulating or Exothermic," *Proceedings of the 64th SFSA Technical and Operating Conference*, Paper No. 3.3, Steel Founders' Society of America (SFSA), Chicago, IL, 2010.
2. Hardin, R.A., Williams, T.J., and Beckermann, C., "Riser Sleeve Properties for Steel Castings and the Effect of Sleeve Type on Casting Yield," *Proceedings of the 67th SFSA Technical and Operating Conference*, Paper No. 5.2, Steel Founders' Society of America (SFSA), Chicago, IL, 2013.
3. *MAGMA<sup>5</sup> Release Notes* (version 5.2), MAGMA GmbH, Aachen, Germany, 2014.
4. Mair, H., "A Survey of the Application of Exothermic and Insulating Materials in Steel and Iron Foundries" in the *Journal of Steel Castings Research*, no. 54, pp. 1-6, March 1971.
5. Brown, J.R., "Feeding of Castings," Chapter 19 in *Foseco Ferrous Foundryman's Handbook* 11<sup>th</sup> Ed., pp. 296-343, Butterworth-Heinemann, Oxford, United Kingdom, 2000.
6. Burns, T.A., "Application of Insulating and Exothermic Risers to Castings" Section IX in *Foseco Foundryman's Handbook* 9<sup>th</sup> Ed., pp. 378-416, Pergamon Press, New York, USA, 1986.
7. Wlodawer, R., "The Calculation of Exothermic Feeder Head Materials" Chapter 12 in *Directional Solidification of Steel Castings* 1<sup>st</sup> Ed., pp. 163-214, Pergamon Press, New York, USA, 1966.
8. Sully, L., Wren, J.E., and Bates, C.E., *Evaluation of Exothermic and Insulating Materials – A Literature Review*, SFSA Special Report No. 13, pp. 1-53, March 1977.
9. Bates, C.E., Scott, W.D., Sully, L., and Wren, J.E., *Evaluation of Riser Feeding Aids*, SFSA Research Report No. 83, pp. 1-21, June 1977.
10. Foseco, "Measuring the Thermal Efficiency of Feeding Aids," *Foundry Practice*, vol. 205, pp. 6-10, 1982.
11. Midea, A. C., Burns, M., Schneider, M., Wagner, I., "Advanced Thermo-Physical Data for Casting Process Simulation – The Importance of Accurate Riser Sleeve Properties," *International Foundry Research*, vol. 59, pp. 34-43, 2007.
12. Ignaszak, Z., Popielarski, P., and Ciura, J. "Heat Source Description of Iso-Exothermic Sleeves with the Use of Continuous Function," *Archives of Foundry*, Vol. 5, No. 15, pp. 157-163, 2005.
13. Ignaszak, Z., and Popielarski, P., "Contribution to Thermal Properties of Multi-Component Porous Ceramic Materials Used in High-Temperature Processes in the Foundry Industry," in *Heat and Mass Transfer in Porous Media*, (ed. J. Delgado), Advanced Structured Materials 13, Springer-Verlag, Berlin, Germany pp. 187-218, 2012.
14. DASyLab v8.0, National Instruments, 11500 N. Mopac Expwy, Austin, TX 78759
15. Miettinen, J., "Calculation of Solidification-Related Thermophysical Properties for Steels", *Metallurgical and Materials Transactions B*, vol. 28, no. 2, pp 281-297, 1997.

16. Dantzig, J. A., Tucker III, C. A., "Heat Conduction and Materials Processing" Chapter 4 in *Modeling in Materials Processing*, pp. 87-131, Cambridge University Press, New York, USA, 2001.
17. Kelter, P., Mosher, M., and Scott, A., *Chemistry: The Practical Science*, pp. 196-197, Houghton Mifflin, Boston, MA, 2009.